NORSAR Scientific Report No. 1-2007

Semiannual Technical Summary

1 July - 31 December 2006

Frode Ringdal (ed.)

Kjeller, February 2007

REPORT DOCUMENTATION PAGE

Form Approved
OMB No. 0704-0188

1. REPORT DATE *(DD-MM-YYYY)*	2. REPORT TYPE	3. DATES COVERED *(From - To)*
15-02-2007	Semiannual Technical Summary	1 July - 31 December 2006

4. TITLE AND SUBTITLE
Semiannual Technical Summary, 1 July - 31 December 2006

5a. CONTRACT NUMBER
FA2521-06-C-8003

5b. GRANT NUMBER

5c. PROGRAM ELEMENT NUMBER
NDC Support / R&D

6. AUTHOR(S)
Frode Ringdal (Ed.)

5d. PROJECT NUMBER
T/6110

5e. TASK NUMBER
SOW Task 4.2 & 4.3

5f. WORK UNIT NUMBER
CDRL sequence nos. A001-A004

7. PERFORMING ORGANIZATION NAME(S) AND ADDRESS(ES)
Stiftelsen NORSAR
Post Box 53
NO-2027 Kjeller
Norway

8. PERFORMING ORGANIZATION REPORT NUMBER
Scientific Report No. 1-2007

9. SPONSORING/MONITORING AGENCY NAME(S) AND ADDRESS(ES)
AFTAC/TTS, 1030 South Highway A1A MS 1000, Patrick AFB, FL 32925-3002

Army Space and Missile Defense Command , 1515 Wilson Blvd., Suite 720
Arlington, VA 22209

10. SPONSOR/MONITOR'S ACRONYM(S)
AFTAC/TTS & USASMDC

11. SPONSOR/MONITOR'S REPORT NUMBER(S)

12. DISTRIBUTION/AVAILABILITY STATEMENT
Approved for public release; distribution unlimited

13. SUPPLEMENTARY NOTES

14. ABSTRACT

This report describes the activities carried out at NORSAR under Contract No. FA2521-06-C-8003 (T/6110) for the period 1 July - 31 December 2006. In addition, this report provides summary information on operation and maintenance (O&M) activities at the Norwegian National Data Center (NDC) during the same period. Research activities described in this report are largely funded by the United States Government, and the United States also covers the cost of transmission of selected data to the US NDC. The O&M activities, including operation of transmission links within Norway and to Vienna, Austria, are being funded jointly by the CTBTO/PTS and the Norwegian Government, with the understanding that the funding of O&M activities for primary stations in the

(cont.)

15. SUBJECT TERMS
NORSAR, Norwegian Seismic Array

16. SECURITY CLASSIFICATION OF:			17. LIMITATION OF ABSTRACT	18. NUMBER OF PAGES	19a. NAME OF RESPONSIBLE PERSON
a. REPORT	b. ABSTRACT	c. THIS PAGE			Capt. Edward Talley, AFTAC/TTX
U	U	U	SAR	81	19b. TELEPHONE NUMBER *(Include area code)* (321) 494-9471

Reset

Standard Form 298 (Rev. 8/98)
Prescribed by ANSI Std. Z39.18

Abstract (cont.)

International Monitoring System (IMS) will gradually be transferred to the CTBTO/PTS. The O&M statistics presented in this report are included for the purpose of completeness, and in order to maintain consistency with earlier reporting practice.

The seismic arrays operated by the Norwegian NDC comprise the Norwegian Seismic Array (NOA), the Arctic Regional Seismic Array (ARCES) and the Spitsbergen Regional Array (SPITS). This report presents statistics for these three arrays as well as for additional seismic stations which through cooperative agreements with institutions in the host countries provide continuous data to the NORSAR Data Processing Center (NDPC). These additional stations include the Finnish Regional Seismic Array (FINES) and the Hagfors array in Sweden (HFS).

The NOA Detection Processing system has been operated throughout the period with an uptime of 100%. A total of 2,805 seismic events have been reported in the NOA monthly seismic bulletin during the reporting period. On-line detection processing and data recording at the NDC of data from ARCES, FINES, SPITS and HFS data have been conducted throughout the period. Processing statistics for the arrays for the reporting period are given.

A summary of the activities at the Norwegian NDC and relating to field installations during the reporting period is provided in Section 4. Norway is now contributing primary station data from two seismic arrays: NOA (PS27) and ARCES (PS28), one auxiliary seismic array SPITS (AS72), and one auxiliary three-component station (AS73). These data are being provided to the IDC via the global communications infrastructure (GCI). Continuous data from the three arrays are in addition being transmitted to the US NDC. The performance of the data transmission to the US NDC has been satisfactory during the reporting period.

So far among the Norwegian stations, the NOA and the ARCES array (PS27 and PS28 respectively), the radionuclide station at Spitsbergen (RN49) and the auxiliary seismic station on Jan Mayen (AS73) have been certified. Provided that adequate funding continues to be made available (from the PTS and the Norwegian Ministry of Foreign Affairs), we envisage continuing the provision of data from these and other Norwegian IMS-designated stations in accordance with current procedures. The IMS infrasound station at Karasjok (IS37) is expected to be built during 2007, provided that the local authorities grant the permissions required for the establishment of the station.

Summaries of three scientific and technical contributions are presented in Chapter 6 of this report.

Section 6.1 is a paper which was presented at the 28th Seismic Research Review and which contains a progress report of a project entitled “Basic research on seismic and infrasonic monitoring of the European Arctic”. This project represents a three-year research effort aimed at improving seismic and infrasonic monitoring tools at regional distances, with emphasis on the European Arctic region, which includes the former Novaya Zemlya test site. The project has two main components: a) to improve seismic processing in this region using the regional seismic arrays installed in northern Europe and b) to investigate the potential of using combined seismic/infrasonic processing to characterize events in this region. In the latter case, we plan on using the northern European seismic array network in combination with infrasonic stations either installed or scheduled for installation in the near future.

During this reporting period, we have implemented basic infrasonic processing software for the Apatity infrasonic array and for the ARCES seismic array. In the case of ARCES, there are

currently no infrasonic sensors available (the plans are to install an infrasound array in 2006/2007), but the seismic sensors have proved useful as an initial substitute for detecting and processing infrasonic signals from explosions at local and regional distances. We have developed an algorithm for associating detected infrasonic phases (either by ARCES or Apatity) with regional seismic events detected and located by the on-line Generalized Beamforming (GBF) process which is currently in experimental operation at NORSAR. We searched the GBF bulletin for approximately one full year of data for seismic events at local or near regional epicentral distances to ARCES or the Apatity infrasound array. We found that 944 infrasound signals could be associated with 651 different seismic events from the GBF bulletin. The large majority of these events were confirmed mining explosions, mainly on the Kola Peninsula.

We present results from an analysis of seismic and infrasonic signals from a set of 108 surface explosions in northern Finland, carried out for the purpose of destroying old ammunition. We have used waveform cross-correlation on ARCES seismic recordings to determine very accurate origin times for the explosions. The extremely high correlation coefficients observed for this data set indicate that these explosions are all very closely spaced, probably within an area of some hundreds of meters in diameter. We have used this database to study the stability of slowness estimates for both seismic and infrasonic phases, using ARCES and Apatity array recordings. By analyzing various subconfigurations of the ARCES array, we find that the scatter (standard deviation) in the azimuth estimates for the explosions is about inversely proportional to array aperture. When carrying out a similar analysis of infrasonic data, we find that, in contrast to the case for the seismic P-waves, the azimuth scatter using our f-k estimation process does not decrease when the array aperture increases. Furthermore, the average azimuth remains essentially unbiased both with varying array aperture and with varying filter bands. This is also in contrast to the situation for seismic P-waves, where we have found strong frequency dependent and configuration dependent azimuth anomalies.

The recent upgrade of the Spitsbergen seismic array, which has included installation of five new three-component seismometers, has resulted in a significant improvement of S-phase detection. We demonstrate this improvement by presenting analysis of recent small seismic events on Novaya Zemlya, where three events (of m_b=2.2, 2.3 and 2.7) were detected by the GBF process during March 2006.

Section 6.2 is entitled “The Capability for Seismic Monitoring of the North Korea Test Site”. On 9 October 2006 the Democratic People’s Republic of Korea (DPRK) conducted an underground nuclear explosion at a test site near Kimchaek. The explosion was detected by several seismic stations in the International Monitoring System (IMS), and the event magnitude as reported in the REB was 4.1. In this paper we analyze the recorded waveforms in order to investigate the capability of the IMS to monitor the DPRK test site for possible future explosions. Our analysis is based upon the so-called Site-Specific Threshold Monitoring (SSTM) approach. Using actual seismic data recorded by a given network, SSTM calculates a continuous “threshold trace”, which provides, at any instance in time, an upper magnitude bound on any seismic event that could have occurred at the target site at that time.

We find that the IMS primary network has a typical “threshold monitoring capability” of between mb 2.3 and 2.5 for the DPRK test site. Not unexpectedly, it turns out that the Korean array (KSRS) is of essential importance in obtaining such low thresholds. We have also experimentally investigated how the capability could be improved by adding non-IMS stations to the network. We find that by adding the nearby station MDJ in China, the threshold monitoring capability is improved to between magnitude 2.1 and 2.3.

A different perspective is to investigate the actual network detection capability for events at the test site, requiring at least 3 IMS stations to detect the event. This is the traditional way of looking at network capability, and the resulting threshold will always be considerably higher than that obtained by the SSTM approach. A global capability map, which is published by the IDC for each hour, shows that at the time of the event, the IMS 3-station detection capability was approximately 3.5. This is an order of magnitude higher than the threshold obtained by SSTM.

We conclude that the SSTM approach allows the analyst to identify times when there is a possibility of occurrence of events too small to be detected by the usual 3-primary station requirement, and to subject such occasions to extensive analysis in order to determine whether an event in fact occurred. Thus, the SSTM approach constitutes a valuable supplement to the traditional network processing carried out at the IDC.

Section 6.3 is entitled "A Case Study of Seismic Event Identification: Explosions in NW Russia using the ARCES seismic array". It contains a continued study of combining seismic and infrasonic recordings for detection and characterization of seismic events at local and regional distances. In a previous NORSAR Semiannual Technical Summary (NORSAR Sci. Rep. 2-2005) we presented results from an analysis of several surface explosions which occurred during March 2005 in Russia near the Norwegian border. At least two of the explosions were reported felt/heard over a large area in the Varanger peninsula, northern Norway, at an epicentral distance of more than 100 km. These explosions were presumably carried out for the purpose of destroying old ammunition, and have been of interest due to the generation of infrasound signals recorded both on the microbarograph mini-array at Apatity and on the ARCES seismic array. At the time, only six events of this category had been identified by us.

This paper describes the results from applying array-based waveform correlation to the ARCES array in order to detect additional such explosions which might have occurred inm recent years. All of the six events in the initial study appeared to have either a low SNR or a waveform suggesting a complicated source-time function. It was judged that the fifth of these events appeared to have the best combination of a relatively simple waveform envelope and a reasonable SNR. Using this event as a basis, an empirical matched filter detector using a 60.0 second long template of ARCES array data, filtered between 3.0 and 8.0 Hz, was initiated and run over three years of continuous data.

The filtered and normalized waveform template was correlated against incoming waveform data segments with a length of approximately 10 minutes. Prior to the main run, the statistics of single-channel and array correlation coefficient traces were examined in order to establish empirical criteria for declaring a detection. Every occurrence of a correlation detection satisfying these criteria was followed by an f-k analysis of the single-channel correlation coefficient traces with the slowness vector and the relative beam-gain being recorded.

Between January 1, 2002, and December 31, 2005, a total of 17485 detections were made based upon the value of the (scaled) array correlation coefficient beam alone. By applying four specific post-processing criteria (based on the value of the array correlation coefficient beam, the value of the scaled correlation coefficient, the size of the correlation coefficient slowness vector and the beam gain), we were able to reduce the number to 557 event candidates. Many of these were multiple detections in rapid succession, therefore clearly corresponding to the same event (or the same group of multiple explosions). By grouping these events, the number was reduced to 244 event candidates, 220 of which could be associated with GBF detections in the automatic NORSAR regional processing system. While the events located by the GBF sys-

tem were scattered over a large region (several hundred kilometers across), their detection by the correlation detector clearly indicates co-location to within a few kilometers, and therefore provides an reduced location uncertainty by orders of magnitude.

We have thus demonstrated in this study that the rank-1 waveform correlation detector on an array has proved to be a very effective tool for the detection and approximate location of events from a given source region despite the lack of similarity between signals from subsequent events. Of paramount importance is the alignment of the correlation coefficient traces which facilitates a powerful screening criterion. We do not yet have Ground Truth confirmation of these events and some unrelated events from a similar direction may have been included. However, this procedure has created a shortlist of events for analyst review which has far fewer possible false alarms than any other procedure currently available.

AFTAC Project Authorization	:	T/6110
Purchase Request No.	:	F3KTK85290A1
Name of Contractor	:	Stiftelsen NORSAR
Effective Date of Contract	:	1 March 2006
Contract Expiration Date	:	30 September 2011
Amount of Contract	:	$ 1,003,494.00
Project Manager	:	Frode Ringdal +47 63 80 59 00
Title of Work	:	The Norwegian Seismic Array (NORSAR) Phase 3
Period Covered by Report	:	1 July - 31 December 2006

The views and conclusions contained in this document are those of the authors and should not be interpreted as necessarily representing the official policies, either expressed or implied, of the U.S. Government.

Part of the research presented in this report was supported by the Army Space and Missile Defense Command, under contract no. W9113M-05-C-0224. Other activities were supported and monitored by AFTAC, Patrick AFB, FL32925, under contract no. FA2521-06-C-8003. Other sponsors are acknowledged where appropriate.

The operational activities of the seismic field systems and the Norwegian National Data Center (NDC) are currently jointly funded by the Norwegian Government and the CTBTO/PTS, with the understanding that the funding of IMS-related activities will gradually be transferred to the CTBTO/PTS.

Table of Contents

Page

1 Summary

This report describes the activities carried out at NORSAR under Contract No. FA2521-06-C-8003 for the period 1 July - 31 December 2006. In addition, it provides summary information on operation and maintenance (O&M) activities at the Norwegian National Data Center (NDC) during the same period. Research activities described in this report are largely funded by the United States Government, and the United States also covers the cost of transmission of selected data from the Norwegian NDC to the United States NDC. The O&M activities, including operation of transmission links within Norway and to Vienna, Austria are being funded jointly by the CTBTO/PTS and the Norwegian Government, with the understanding that the funding of O&M activities for primary stations in the International Monitoring System (IMS) will gradually be transferred to the CTBTO/PTS. The O&M statistics presented in this report are included for the purpose of completeness, and in order to maintain consistency with earlier reporting practice.

The seismic arrays operated by the Norwegian NDC comprise the Norwegian Seismic Array (NOA), the Arctic Regional Seismic Array (ARCES) and the Spitsbergen Regional Array (SPITS). This report presents statistics for these three arrays as well as for additional seismic stations which through cooperative agreements with institutions in the host countries provide continuous data to the NORSAR Data Processing Center (NDPC). These additional stations include the Finnish Regional Seismic Array (FINES) and the Hagfors array in Sweden (HFS).

The NOA Detection Processing system has been operated throughout the period with an uptime of 100%. A total of 2,805 seismic events have been reported in the NOA monthly seismic bulletin during the reporting period. On-line detection processing and data recording at the NDC of data from ARCES, FINES, SPITS and HFS data have been conducted throughout the period. Processing statistics for the arrays for the reporting period are given.

A summary of the activities at the Norwegian NDC and relating to field installations during the reporting period is provided in Section 4. Norway is now contributing primary station data from two seismic arrays: NOA (PS27) and ARCES (PS28), one auxiliary seismic array SPITS (AS72), and one auxiliary three-component station (AS73). These data are being provided to the IDC via the global communications infrastructure (GCI). Continuous data from the three arrays are in addition being transmitted to the US NDC. The performance of the data transmission to the US NDC has been satisfactory during the reporting period.

So far among the Norwegian stations, the NOA and the ARCES array (PS27 and PS28 respectively), the radionuclide station at Spitsbergen (RN49) and the auxiliary seismic station on Jan Mayen (AS73) have been certified. Provided that adequate funding continues to be made available (from the PTS and the Norwegian Ministry of Foreign Affairs), we envisage continuing the provision of data from these and other Norwegian IMS-designated stations in accordance with current procedures. The IMS infrasound station at Karasjok (IS37) is expected to be built during 2007, provided that the local authorities grant the permissions required for the establishment of the station.

Summaries of three scientific and technical contributions are presented in Chapter 6 of this report.

Section 6.1 is a paper which was presented at the 28th Seismic Research Review and which contains a progress report of a project entitled “Basic research on seismic and infrasonic monitoring of the European Arctic”. This project represents a three-year research effort aimed at

improving seismic and infrasonic monitoring tools at regional distances, with emphasis on the European Arctic region, which includes the former Novaya Zemlya test site. The project has two main components: a) to improve seismic processing in this region using the regional seismic arrays installed in northern Europe and b) to investigate the potential of using combined seismic/infrasonic processing to characterize events in this region. In the latter case, we plan on using the northern European seismic array network in combination with infrasonic stations either installed or scheduled for installation in the near future.

During this reporting period, we have implemented basic infrasonic processing software for the Apatity infrasonic array and for the ARCES seismic array. In the case of ARCES, there are currently no infrasonic sensors available (the plans are to install an infrasound array in 2006/2007), but the seismic sensors have proved useful as an initial substitute for detecting and processing infrasonic signals from explosions at local and regional distances. We have developed an algorithm for associating detected infrasonic phases (either by ARCES or Apatity) with regional seismic events detected and located by the on-line Generalized Beamforming (GBF) process which is currently in experimental operation at NORSAR. We searched the GBF bulletin for approximately one full year of data for seismic events at local or near regional epicentral distances to ARCES or the Apatity infrasound array. We found that 944 infrasound signals could be associated with 651 different seismic events from the GBF bulletin. The large majority of these events were confirmed mining explosions, mainly on the Kola Peninsula.

We present results from an analysis of seismic and infrasonic signals from a set of 108 surface explosions in northern Finland, carried out for the purpose of destroying old ammunition. We have used waveform cross-correlation on ARCES seismic recordings to determine very accurate origin times for the explosions. The extremely high correlation coefficients observed for this data set indicate that these explosions are all very closely spaced, probably within an area of some hundreds of meters in diameter. We have used this database to study the stability of slowness estimates for both seismic and infrasonic phases, using ARCES and Apatity array recordings. By analyzing various subconfigurations of the ARCES array, we find that the scatter (standard deviation) in the azimuth estimates for the explosions is about inversely proportional to array aperture. When carrying out a similar analysis of infrasonic data, we find that, in contrast to the case for the seismic P-waves, the azimuth scatter using our f-k estimation process does not decrease when the array aperture increases. Furthermore, the average azimuth remains essentially unbiased both with varying array aperture and with varying filter bands. This is also in contrast to the situation for seismic P-waves, where we have found strong frequency dependent and configuration dependent azimuth anomalies.

The recent upgrade of the Spitsbergen seismic array, which has included installation of five new three-component seismometers, has resulted in a significant improvement of S-phase detection. We demonstrate this improvement by presenting analysis of recent small seismic events on Novaya Zemlya, where three events (of m_b=2.2, 2.3 and 2.7) were detected by the GBF process during March 2006.

Section 6.2 is entitled “The Capability for Seismic Monitoring of the North Korea Test Site”. On 9 October 2006 the Democratic People’s Republic of Korea (DPRK) conducted an underground nuclear explosion at a test site near Kimchaek. The explosion was detected by several seismic stations in the International Monitoring System (IMS), and the event magnitude as reported in the REB was 4.1. In this paper we analyze the recorded waveforms in order to investigate the capability of the IMS to monitor the DPRK test site for possible future explosions. Our analysis is based upon the so-called Site-Specific Threshold Monitoring (SSTM)

approach. Using actual seismic data recorded by a given network, SSTM calculates a continuous "threshold trace", which provides, at any instance in time, an upper magnitude bound on any seismic event that could have occurred at the target site at that time.

We find that the IMS primary network has a typical "threshold monitoring capability" of between mb 2.3 and 2.5 for the DPRK test site. Not unexpectedly, it turns out that the Korean array (KSRS) is of essential importance in obtaining such low thresholds. We have also experimentally investigated how the capability could be improved by adding non-IMS stations to the network. We find that by adding the nearby station MDJ in China, the threshold monitoring capability is improved to between magnitude 2.1 and 2.3.

A different perspective is to investigate the actual network detection capability for events at the test site, requiring at least 3 IMS stations to detect the event. This is the traditional way of looking at network capability, and the resulting threshold will always be considerably higher than that obtained by the SSTM approach. A global capability map, which is published by the IDC for each hour, shows that at the time of the event, the IMS 3-station detection capability was approximately 3.5. This is an order of magnitude higher than the threshold obtained by SSTM.

We conclude that the SSTM approach allows the analyst to identify times when there is a possibility of occurrence of events too small to be detected by the usual 3-primary station requirement, and to subject such occasions to extensive analysis in order to determine whether an event in fact occurred. Thus, the SSTM approach constitutes a valuable supplement to the traditional network processing carried out at the IDC.

Section 6.3 is entitled "A Case Study of Seismic Event Identification: Explosions in NW Russia using the ARCES seismic array". It contains a continued study of combining seismic and infrasonic recordings for detection and characterization of seismic events at local and regional distances. In a previous NORSAR Semiannual Technical Summary (NORSAR Sci. Rep. 2-2005) we presented results from an analysis of several surface explosions which occurred during March 2005 in Russia near the Norwegian border. At least two of the explosions were reported felt/heard over a large area in the Varanger peninsula, northern Norway, at an epicentral distance of more than 100 km. These explosions were presumably carried out for the purpose of destroying old ammunition, and have been of interest due to the generation of infrasound signals recorded both on the microbarograph mini-array at Apatity and on the ARCES seismic array. At the time, only six events of this category had been identified by us.

This paper describes the results from applying array-based waveform correlation to the ARCES array in order to detect additional such explosions which might have occurred inm recent years. All of the six events in the initial study appeared to have either a low SNR or a waveform suggesting a complicated source-time function. It was judged that the fifth of these events appeared to have the best combination of a relatively simple waveform envelope and a reasonable SNR. Using this event as a basis, an empirical matched filter detector using a 60.0 second long template of ARCES array data, filtered between 3.0 and 8.0 Hz, was initiated and run over three years of continuous data.

The filtered and normalized waveform template was correlated against incoming waveform data segments with a length of approximately 10 minutes. Prior to the main run, the statistics of single-channel and array correlation coefficient traces were examined in order to establish empirical criteria for declaring a detection. Every occurrence of a correlation detection satisfying these criteria was followed by an f-k analysis of the single-channel correlation coefficient traces with the slowness vector and the relative beam-gain being recorded.

Between January 1, 2002, and December 31, 2005, a total of 17485 detections were made based upon the value of the (scaled) array correlation coefficient beam alone. By applying four specific post-processing criteria (based on the value of the array correlation coefficient beam, the value of the scaled correlation coefficient, the size of the correlation coefficient slowness vector and the beam gain), we were able to reduce the number to 557 event candidates. Many of these were multiple detections in rapid succession, therefore clearly corresponding to the same event (or the same group of multiple explosions). By grouping these events, the number was reduced to 244 event candidates, 220 of which could be associated with GBF detections in the automatic NORSAR regional processing system. While the events located by the GBF system were scattered over a large region (several hundred kilometers across), their detection by the correlation detector clearly indicates co-location to within a few kilometers, and therefore provides an reduced location uncertainty by orders of magnitude.

We have thus demonstrated in this study that the rank-1 waveform correlation detector on an array has proved to be a very effective tool for the detection and approximate location of events from a given source region despite the lack of similarity between signals from subsequent events. Of paramount importance is the alignment of the correlation coefficient traces which facilitates a powerful screening criterion. We do not yet have Ground Truth confirmation of these events and some unrelated events from a similar direction may have been included. However, this procedure has created a shortlist of events for analyst review which has far fewer possible false alarms than any other procedure currently available.

Frode Ringdal

2 Operation of International Monitoring System (IMS) Stations in Norway

2.1 PS27 — Primary Seismic Station NOA

The mission-capable data statistics were 100%, the same as for the previous reporting period. The net instrument availability was 97.919%.

There were no outages of all subarrays at the same time in the reporting period.

Monthly uptimes for the NORSAR on-line data recording task, taking into account all factors (field installations, transmissions line, data center operation) affecting this task were as follows:

2006		Mission Capable	Net instrument availability
July	:	100%	96.649%
August	:	100%	94.075%
September	:	100%	97.585%
October	:	100%	99.932%
November	:	100%	99.987%
December	:	100%	99.939%

B. Kr. Hokland

NOA Event Detection Operation

In Table 2.1.1 some monthly statistics of the Detection and Event Processor operation are given. The table lists the total number of detections (DPX) triggered by the on-line detector, the total number of detections processed by the automatic event processor (EPX) and the total number of events accepted after analyst review (teleseismic phases, core phases and total).

	Total DPX	Total EPX	Accepted Events		Sum	Daily
			P-phases	Core Phases		
Jul	7,991	1,003	328	67	395	12.7
Aug	6,644	838	290	66	356	11.5
Sep	8,160	916	300	67	367	12.2
Oct	9,918	924	380	60	440	14.2
Nov	12,985	1,409	830	66	896	29.9
Dec	11,642	862	307	44	351	11.3
	57,340	5,952	2,435	370	2,805	15.3

Table 2.1.1. *Detection and Event Processor statistics, 1 July - 31 December 2006.*

NOA detections

The number of detections (phases) reported by the NORSAR detector during day 182, 2006, through day 365, 2006, was 62,816, giving an average of 341 detections per processed day (184 days processed).

B. Paulsen

U. Baadshaug

2.2 PS28 — Primary Seismic Station ARCES

The mission-capable data statistics were 99.554%, as compared to 99.997% for the previous reporting period. The net instrument availability was 98.921%.

The main outages in the period are presented in Table 2.2.1.

Day	Period
Jul 12	00.04-00.09
Jul 12	00.10-00.19
Jul 12	00.20-00.29
Jul 22	06.41-06.49
Jul 22	06.51-06.59
Dec 26	16.24-24.00
Dec 27	00.00-10.11
Dec 27	20.18-21.31

Table 2.2.1. *The main interruptions in recording of ARCES data at NDPC, 1 July - 31 December 2006.*

Monthly uptimes for the ARCES on-line data recording task, taking into account all factors (field installations, transmission lines, data center operation) affecting this task were as follows:

2006		Mission Capable	Net instrument availability
July	:	99.912%	98.819%
August	:	100%	99.329%
September	:	100%	100%
October	:	100%	100%
November	:	100%	100%
December	:	97.442%	95.446%

B.Kr. Hokland

Event Detection Operation

ARCES detections

The number of detections (phases) reported during day 182, 2006, through day 365, 2006, was 216,728, giving an average of 1178 detections per processed day (184 days processed).

Events automatically located by ARCES

During days 182, 2006, through 365, 2006, 10,802 local and regional events were located by ARCES, based on automatic association of P- and S-type arrivals. This gives an average of

58.7 events per processed day (184 days processed). 57% of these events are within 300 km, and 83% of these events are within 1000 km.

U. Baadshaug

2.3 AS72 — Auxiliary Seismic Station Spitsbergen

The mission-capable data for the period were 96.259%, as compared to 100% for the previous reporting period. The net instrument availability was 96.063%.

The main outages in the period are presented in Table 2.3.1.

Day	Period
Dec 12	12.55-24.00
Dec 13	00.00-24.00
Dec 14	00.00-24.00
Dec 15	00.00-24.00
Dec 16	00.00-24.00
Dec 17	00.00-24.00
Dec 18	00.00-08.25
Dec 18	08.44-09.00
Dec 19	10.48-24.00
Dec 20	00.00-11.59
Dec 20	12.00-12.01
Dec 20	13.07-13.22

Table 2.3.1. *The main interruptions in recording of Spitsbergen data at NDPC, 1 July - 31 December 2006.*

Monthly uptimes for the Spitsbergen on-line data recording task, taking into account all factors (field installations, transmissions line, data center operation) affecting this task were as follows:

2006		Mission Capable	Net instrument availability
July	:	100%	99.816%
August	:	100%	99.987%
September	:	100%	99.775 %
October	:	100%	99.883%
November	:	100%	99.730%
December	:	77.797%	61.022%

B.Kr. Hokland

Event Detection Operation

Spitsbergen array detections

The number of detections (phases) reported from day 182, 2006, through day 365, 2006, was 533,689, giving an average of 2,982 detections per processed day (179 days processed).

Events automatically located by the Spitsbergen array

During days 182, 2006, through 365, 2006, 52,879 local and regional events were located by the Spitsbergen array, based on automatic association of P- and S-type arrivals. This gives an average of 295.4 events per processed day (184 days processed). 76% of these events are within 300 km, and 90% of these events are within 1000 km.

U. Baadshaug

2.4 AS73 — Auxiliary Seismic Station at Jan Mayen

The IMS auxiliary seismic network includes a three-component station on the Norwegian island of Jan Mayen. The station location given in the protocol to the Comprehensive Nuclear-Test-Ban Treaty is 70.9˚N, 8.7˚W.

The University of Bergen has operated a seismic station at this location since 1970. A so-called Parent Network Station Assessment for AS73 was completed in April 2002. A vault at a new location (71.0^{o}N, 8.5^{o}W) was prepared in early 2003, after its location had been approved by the PrepCom. New equipment was installed in this vault in October 2003, as a cooperative effort between NORSAR and the CTBTO/PTS. Continuous data from this station are being transmitted to the NDC at Kjeller via a satellite link installed in April 2000. Data are also made available to the University of Bergen.

The station was certified by the CTBTO/PTS on 12 June 2006.

J. Fyen

2.5 IS37 — Infrasound Station at Karasjok

The IMS infrasound network will include a station at Karasjok in northern Norway. The coordinates given for this station are 69.5˚N, 25.5˚E. These coordinates coincide with those of the primary seismic station PS28.

A site survey for this station was carried out during June/July 1998 as a cooperative effort between the CTBTO/PTS and NORSAR. The site survey led to a recommendation on the exact location of the infrasound station. There was, however, a strong local opposition against establishing the station at the recommended location, and two alternative sites have been identified. The appropriate applications have been sent to the local authorities to obtain the permissions needed to establish the station at one of these alternative locations. Station installation is expected to take place in the fall of 2007, provided that such permissions are granted by mid-June 2007 at the latest.

A site preparation contract has been signed with the PTS. Due to scarce vegetation, possible high winds and difficult arctic operating conditions, the PTS has accepted our proposal to build a station comprising 9 elements.

J. Fyen

2.6 RN49 — Radionuclide Station on Spitsbergen

The IMS radionuclide network includes a station on the island of Spitsbergen. This station is also among those IMS radionuclide stations that will have a capability of monitoring for the presence of relevant noble gases upon entry into force of the CTBT.

A site survey for this station was carried out in August of 1999 by NORSAR, in cooperation with the Norwegian Radiation Protection Authority. The site survey report to the PTS contained a recommendation to establish this station at Platåberget, near Longyearbyen. The infrastructure for housing the station equipment was established in early 2001, and a noble gas detection system, based on the Swedish “SAUNA” design, was installed at this site in May 2001, as part of PrepCom’s noble gas experiment. A particulate station (“ARAME” design) was installed at the same location in September 2001. A certification visit to the particulate sta-

tion took place in October 2002, and the particulate station was certified on 10 June 2003. Both systems underwent substantial upgrading in May/June 2006. The equipment at RN49 is being maintained and operated in accordance with a contract with the CTBTO/PTS.

S. Mykkeltveit

3 Contributing Regional Seismic Arrays

3.1 NORES

NORES has been out of operation since lightning destroyed the station electronics on 11 June 2002.

J. Torstveit

3.2 Hagfors (IMS Station AS101)

Data from the Hagfors array are made available continuously to NORSAR through a cooperative agreement with Swedish authorities.

The mission-capable data statistics were 99.996%, as compared to 100% for the previous reporting period. The net instrument availability was 99.996%.

The main outages in the period are presented in Table 3.2.1.

Day	Period
Sep 10	18.56-18.59
Dec 03	14.57-15.00
Dec 27	23.57-24.00
Dec 28	00.00-00.01

Table 3.2.1. *The main interruptions in recording of Hagfors data at NDPC, 1 July - 31 December 2006.*

Monthly uptimes for the Hagfors on-line data recording task, taking into account all factors (field installations, transmissions line, data center operation) affecting this task were as follows:

2006		Mission Capable	Net instrument availability
July	:	100%	100%
August	:	100%	100%
September	:	99.993%	99.993%
October	:	100%	100%
November	:	100%	100%
December	:	99.986%	99.985%

B.Kr. Hokland

Hagfors Event Detection Operation

Hagfors array detections

The number of detections (phases) reported from day 182, 2006, through day 365, 2006, was 165,775, giving an average of 901 detections per processed day (184 days processed).

Events automatically located by the Hagfors array

During days 182, 2006, through 365, 2006, 3655 local and regional events were located by the Hagfors array, based on automatic association of P- and S-type arrivals. This gives an average of 19.9 events per processed day (184 days processed). 74% of these events are within 300 km, and 93% of these events are within 1000 km.

U. Baadshaug

3.3 FINES (IMS station PS17)

Data from the FINES array are made available continuously to NORSAR through a cooperative agreement with Finnish authorities.

The mission-capable data statistics were 99.991%, as compared to 99.998% for the previous reporting period. The net instrument availability was 97.220%.

Many short outages (not more than 10 seconds) occurred from August 23 to August 31.

Monthly uptimes for the FINES on-line data recording task, taking into account all factors (field installations, transmissions line, data center operation) affecting this task were as follows:

2006		Mission Capable	Net instrument availability
July	:	100%	99.991%
August	:	99.949%	97.881%
September	:	100%	99.296%
October	:	99.999%	99.952%
November	:	100%	90.833%
December	:	100%	95.230%

B.Kr. Hokland

FINES Event Detection Operation

FINES detections

The number of detections (phases) reported during day 182, 2006, through day 365, 2006, was 50,427, giving an average of 274 detections per processed day (184 days processed).

Events automatically located by FINES

During days 182, 2006, through 365, 2006, 2812 local and regional events were located by FINES, based on automatic association of P- and S-type arrivals. This gives an average of 15.3 events per processed day (184 days processed). 81% of these events are within 300 km, and 91% of these events are within 1000 km.

U. Baadshaug

3.4 Regional Monitoring System Operation and Analysis

The Regional Monitoring System (RMS) was installed at NORSAR in December 1989 and has been operated at NORSAR from 1 January 1990 for automatic processing of data from ARCES and NORES. A second version of RMS that accepts data from an arbitrary number of arrays and single 3-component stations was installed at NORSAR in October 1991, and regular operation of the system comprising analysis of data from the 4 arrays ARCES, NORES, FINES and

GERES started on 15 October 1991. As opposed to the first version of RMS, the one in current operation also has the capability of locating events at teleseismic distances.

Data from the Apatity array was included on 14 December 1992, and from the Spitsbergen array on 12 January 1994. Detections from the Hagfors array were available to the analysts and could be added manually during analysis from 6 December 1994. After 2 February 1995, Hagfors detections were also used in the automatic phase association.

Since 24 April 1999, RMS has processed data from all the seven regional arrays ARCES, NORES, FINES, GERES (until January 2000), Apatity, Spitsbergen, and Hagfors. Starting 19 September 1999, waveforms and detections from the NORSAR array have also been available to the analyst.

Phase and event statistics

Table 3.5.1 gives a summary of phase detections and events declared by RMS. From top to bottom the table gives the total number of detections by the RMS, the number of detections that are associated with events automatically declared by the RMS, the number of detections that are not associated with any events, the number of events automatically declared by the RMS, and finally the total number of events worked on interactively (in accordance with criteria that vary over time; see below) and defined by the analyst.

New criteria for interactive event analysis were introduced from 1 January 1994. Since that date, only regional events in areas of special interest (e.g, Spitsbergen, since it is necessary to acquire new knowledge in this region) or other significant events (e.g, felt earthquakes and large industrial explosions) were thoroughly analyzed. Teleseismic events of special interest are also analyzed.

To further reduce the workload on the analysts and to focus on regional events in preparation for Gamma-data submission during GSETT-3, a new processing scheme was introduced on 2 February 1995. The GBF (Generalized Beamforming) program is used as a pre-processor to RMS, and only phases associated with selected events in northern Europe are considered in the automatic RMS phase association. All detections, however, are still available to the analysts and can be added manually during analysis.

	Jul 06	Aug 06	Sep 06	Oct 06	Nov 06	Dec 06	Total
Phase detections	172,997	213,818	238,213	234,247	155,896	138,222	1,153,393
- Associated phases	6,688	9,111	12,665	11,303	6,320	4,201	50,288
- Unassociated phases	166,309	204,707	225,548	222,944	149,576	134,021	1,103,105
Events automatically declared by RMS	1,337	1,965	2,645	2,472	1,380	872	10,671
No. of events defined by the analyst	63	68	130	71	41	39	412

Table 3.5.1. RMS phase detections and event summary 1 July - 31 December 2006.

U. Baadshaug

B. Paulsen

4 NDC and Field Activities

4.1 NDC Activitities

NORSAR functions as the Norwegian National Data Center (NDC) for CTBT verification. Six monitoring stations, comprising altogether 129 field sensors, will be located on Norwegian territory as part of the future IMS as described elsewhere in this report. The four seismic IMS stations are all in operation today, and all of them are currently providing data to the CTBTO on a regular basis. PS27, PS28, AS73 and RN49 are all certified. The infrasound station in northern Norway is planned to be established within next year. Data recorded by the Norwegian stations is being transmitted in real time to the Norwegian NDC, and provided to the IDC through the Global Communications Infrastructure (GCI). Norway is connected to the GCI with a frame relay link to Vienna.

Operating the Norwegian IMS stations continues to require increased resources and additional personnel both at the NDC and in the field. Strictly defined procedures as well as increased emphasis on regularity of data recording and timely data transmission to the IDC in Vienna have led to increased reporting activities and implementation of new procedures for the NDC. The NDC carries out all the technical tasks required in support of Norway's treaty obligations. NORSAR will also carry out assessments of events of special interest, and advise the Norwegian authorities in technical matters relating to treaty compliance.

Verification functions; information received from the IDC

After the CTBT enters into force, the IDC will provide data for a large number of events each day, but will not assess whether any of them are likely to be nuclear explosions. Such assessments will be the task of the States Parties, and it is important to develop the necessary national expertise in the participating countries. An important task for the Norwegian NDC will thus be to make independent assessments of events of particular interest to Norway, and to communicate the results of these analyses to the Norwegian Ministry of Foreign Affairs.

Monitoring the Arctic region

Norway will have monitoring stations of key importance for covering the Arctic, including Novaya Zemlya, and Norwegian experts have a unique competence in assessing events in this region. On several occasions in the past, seismic events near Novaya Zemlya have caused political concern, and NORSAR specialists have contributed to clarifying these issues.

International cooperation

After entry into force of the treaty, a number of countries are expected to establish national expertise to contribute to the treaty verification on a global basis. Norwegian experts have been in contact with experts from several countries with the aim of establishing bilateral or multilateral cooperation in this field. One interesting possibility for the future is to establish NORSAR as a regional center for European cooperation in the CTBT verification activities.

NORSAR event processing

The automatic routine processing of NORSAR events as described in NORSAR Sci. Rep. No. 2-93/94, has been running satisfactorily. The analyst tools for reviewing and updating the solu-

tions have been continually modified to simplify operations and improve results. NORSAR is currently applying teleseismic detection and event processing using the large-aperture NOA array as well as regional monitoring using the network of small-aperture arrays in Fennoscandia and adjacent areas.

Communication topology

Norway has implemented an independent subnetwork, which connects the IMS stations AS72, AS73, PS28, and RN49 operated by NORSAR to the GCI at NOR_NDC. A contract has been concluded and VSAT antennas have been installed at each station in the network. Under the same contract, VSAT antennas for 6 of the PS27 subarrays have been installed for intra-array communication. The seventh subarray is connected to the central recording facility via a leased land line. The central recording facility for PS27 is connected directly to the GCI (Basic Topology). All the VSAT communication is functioning satisfactorily. As of 10 June 2005, AS72 and RN49 are connected to NOR_NDC through a VPN link.

Jan Fyen

4.2 Status Report: Provision of data from Norwegian seismic IMS stations to the IDC

Introduction

This contribution is a report for the period July - December 2006 on activities associated with provision of data from Norwegian seismic IMS stations to the International Data Centre (IDC) in Vienna. This report represents an update of contributions that can be found in previous editions of NORSAR's Semiannual Technical Summary. It is noted that as of 30 June 2006, three of the four Norwegian seismic stations providing data to the IDC have been formally certified.

Norwegian IMS stations and communications arrangements

During the reporting interval 1 July - 31 December 2006, Norway has provided data to the IDC from the four seismic stations shown in Fig. 4.2.1. PS27 —NOA is a 60 km aperture teleseismic array, comprised of 7 subarrays, each containing six vertical short period sensors and a three-component broadband instrument. PS28 — ARCES is a 25-element regional array with an aperture of 3 km, whereas AS72 — Spitsbergen array (station code SPITS) has 9 elements within a 1-km aperture. AS73 — JMIC has a single three-component broadband instrument.

The intra-array communication for NOA utilizes a land line for subarray NC6 and VSAT links based on TDMA technology for the other 6 subarrays. The central recording facility for NOA is located at the Norwegian National Data Center (NOR_NDC).

Continuous ARCES data are transmitted from the ARCES site to NOR_NDC using a 64 kbits/s VSAT satellite link, based on BOD technology.

Continuous SPITS data were transmitted to NOR_NDC via a VSAT terminal located at Platåberget in Longyearbyen (which is the site of the IMS radionuclide monitoring station RN49 installed during 2001) up to 10 June 2005. The central recording facility (CRF) for the SPITS array has been moved to the University of Spitsbergen (UNIS). A 512 bps SHDSL link has been established between UNIS and NOR_NDC. Data from the array elements to the CRF

are transmitted via a 2.4 Ghz radio link (Wilan VIP-110). Both AS72 and RN49 data are now transmitted to NOR_NDC over this link using VPN technology.

A minimum of seven-day station buffers have been established at the ARCES and SPITS sites and at all NOA subarray sites, as well as at the NOR_NDC for ARCES, SPITS and NOA.

The NOA and ARCES arrays are primary stations in the IMS network, which implies that data from these stations is transmitted continuously to the receiving international data center. Since October 1999, this data has been transmitted (from NOR_NDC) via the Global Communications Infrastructure (GCI) to the IDC in Vienna. Data from the auxiliary array station SPITS — AS72 have been sent in continuous mode to the IDC during the reporting period. AS73 — JMIC is an auxiliary station in the IMS, and the JMIC data have been available to the IDC throughout the reporting period on a request basis via use of the AutoDRM protocol (Kradolfer, 1993; Kradolfer, 1996). In addition, continuous data from all three arrays is transmitted to the US_NDC.

Uptimes and data availability

Figs. 4.2.2 and 4.2.3 show the monthly uptimes for the Norwegian IMS primary stations ARCES and NOA, respectively, for the period 1 July - 31 December 2006, given as the hatched (taller) bars in these figures. These barplots reflect the percentage of the waveform data that is available in the NOR_NDC data archives for these two arrays. The downtimes inferred from these figures thus represent the cumulative effect of field equipment outages, station site to NOR_NDC communication outage, and NOR_NDC data acquisition outages.

Figs. 4.2.2 and 4.2.3 also give the data availability for these two stations as reported by the IDC in the IDC Station Status reports. The main reason for the discrepancies between the NOR_NDC and IDC data availabilities as observed from these figures is the difference in the ways the two data centers report data availability for arrays: Whereas NOR_NDC reports an array station to be up and available if at least one channel produces useful data, the IDC uses weights where the reported availability (capability) is based on the number of actually operating channels.

Use of the AutoDRM protocol

NOR_NDC's AutoDRM has been operational since November 1995 (Mykkeltveit & Baadshaug, 1996). The monthly number of requests by the IDC for JMIC data for the period July - December 2006 is shown in Fig. 4.2.4.

NDC automatic processing and data analysis

These tasks have proceeded in accordance with the descriptions given in Mykkeltveit and Baadshaug (1996). For the period July - December 2006, NOR_NDC derived information on 425 supplementary events in northern Europe and submitted this information to the Finnish NDC as the NOR_NDC contribution to the joint Nordic Supplementary (Gamma) Bulletin, which in turn is forwarded to the IDC. These events are plotted in Fig. 4.2.5.

Data access for the station NIL at Nilore, Pakistan

NOR_NDC continued to provide access to the seismic station NIL at Nilore, Pakistan, through a VSAT satellite link between NOR_NDC and Pakistan's NDC in Nilore. On 10 December

2006, the VSAT ground station in Nilore was damaged by lightning. It was brought back into operation on 14 December through use of spare units stored on-site.

Current developments and future plans

NOR_NDC is continuing the efforts towards improving and hardening all critical data acquisition and data forwarding hardware and software components, so as to meet the requirements related to operation of IMS stations.

The NOA array was formally certified by the PTS on 28 July 2000, and a contract with the PTS in Vienna currently provides partial funding for operation and maintenance of this station. The ARCES array was formally certified by the PTS on 8 November 2001, and a contract with the PTS is in place which also provides for partial funding of the operation and maintenance of this station. Provided that adequate funding continues to be made available (from the PTS and the Norwegian Ministry of Foreign Affairs), we envisage continuing the provision of data from all Norwegian seismic IMS stations without interruption to the IDC in Vienna.

U. Baadshaug
S. Mykkeltveit
J. Fyen

References

Kradolfer, U. (1993): Automating the exchange of earthquake information. *EOS, Trans., AGU*, 74, 442.

Kradolfer, U. (1996): AutoDRM — The first five years, *Seism. Res. Lett.*, 67, 4, 30-33.

Mykkeltveit, S. & U. Baadshaug (1996): Norway's NDC: Experience from the first eighteen months of the full-scale phase of GSETT-3. *Semiann. Tech. Summ., 1 October 1995 - 31 March 1996*, NORSAR Sci. Rep. No. 2-95/96, Kjeller, Norway.

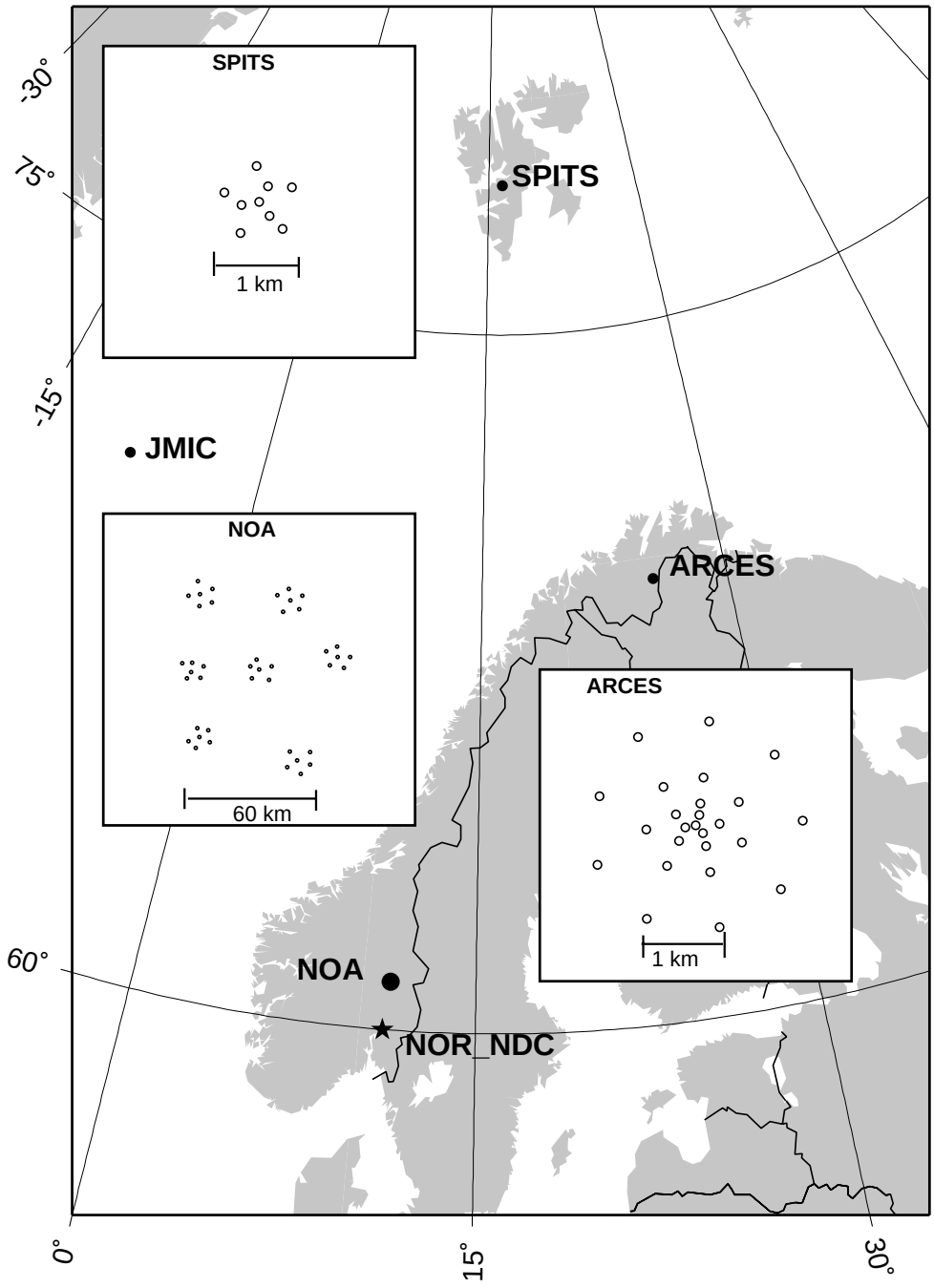

Fig. 4.2.1. The figure shows the locations and configurations of the three Norwegian seismic IMS array stations that provided data to the IDC during the period July - December 2006. The data from these stations and the JMIC three-component station are transmitted continuously and in real time to the Norwegian NDC (NOR_NDC). The stations NOA and ARCES are primary IMS stations, whereas SPITS and JMIC are auxiliary IMS stations.

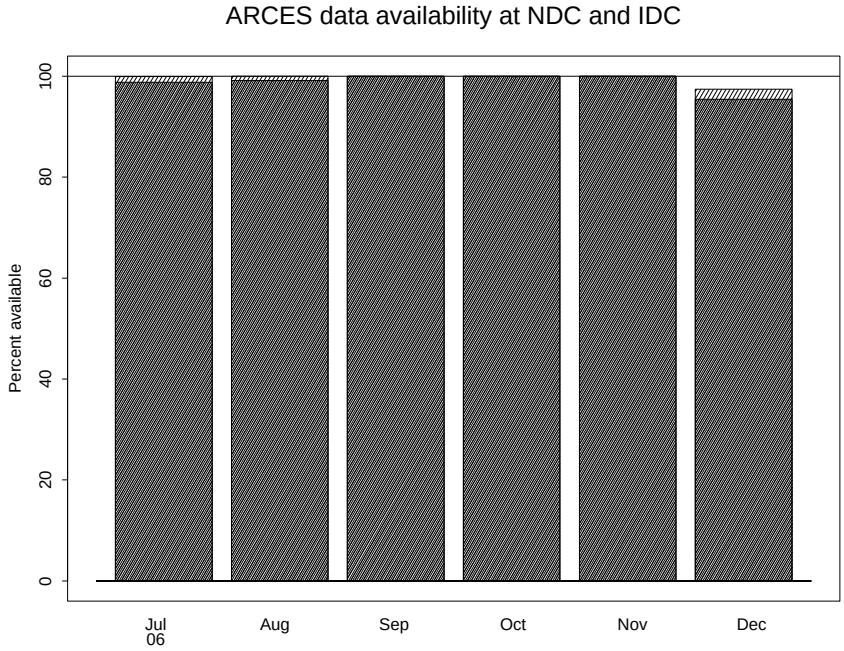

Fig. 4.2.2. The figure shows the monthly availability of ARCES array data for the period July - December 2006 at NOR_NDC and the IDC. See the text for explanation of differences in definition of the term "data availability" between the two centers. The higher values (hatched bars) represent the NOR_NDC data availability.

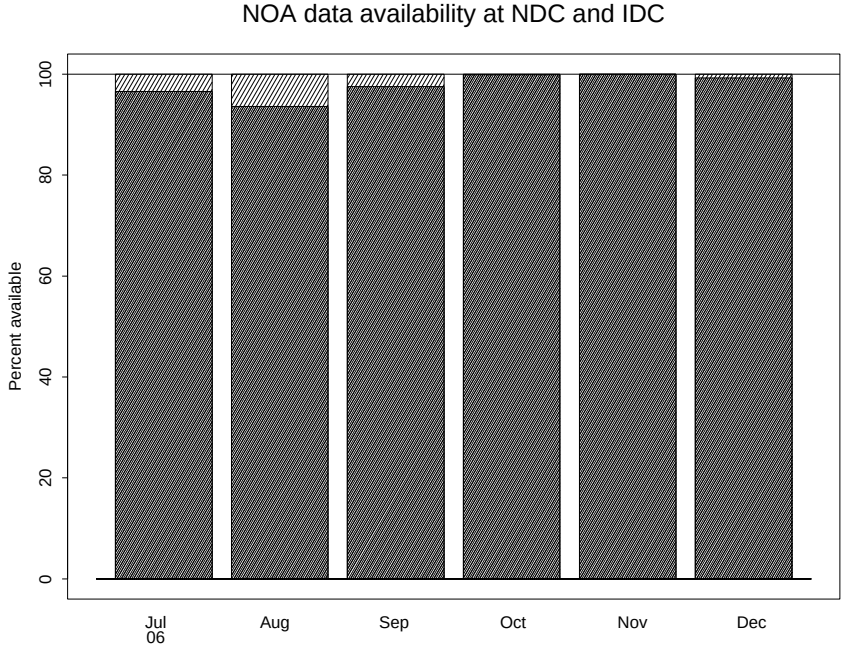

Fig. 4.2.3. The figure shows the monthly availability of NORSAR array data for the period July - December 2006 at NOR_NDC and the IDC. See the text for explanation of differences in definition of the term "data availability" between the two centers. The higher values (hatched bars) represent the NOR_NDC data availability.

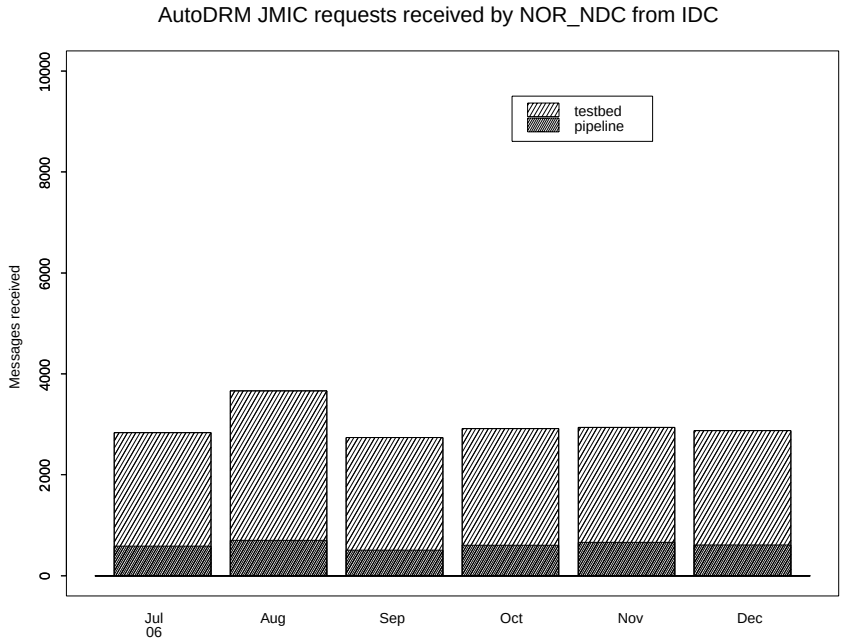

Fig. 4.2.4. The figure shows the monthly number of requests received by NOR_NDC from the IDC for JMIC waveform segments during July - December 2006.

Reviewed Supplementary events

Fig. 4.2.5. The map shows the 445 events in and around Norway contributed by NOR_NDC during July - December 2006 as supplementary (Gamma) events to the IDC, as part of the Nordic supplementary data compiled by the Finnish NDC. The map also shows the main seismic stations used in the data analysis to define these events.

4.3 Field Activities

The activities at the NORSAR Maintenance Center (NMC) at Hamar currently include work related to operation and maintenance of the following IMS seismic stations: the NOA teleseismic array (PS27), the ARCES array (PS28) and the Spitsbergen array (AS72). Some work has also been carried out in connection with the seismic station on Jan Mayen (AS73), the radionuclide station at Spitsbergen (RN49), and preparations for the infrasound station at Karasjok (IS37). NORSAR also acts as a consultant for the operation and maintenance of the Hagfors array in Sweden (AS101).

NORSAR carries out the field activities relating to IMS stations in a manner generally consistent with the requirements specified in the appropriate IMS Operational Manuals, which are currently being developed by Working Group B of the Preparatory Commission. For seismic stations these specifications are contained in the Operational Manual for Seismological Monitoring and the International Exchange of Seismological Data (CTBT/WGB/TL-11/2), currently available in a draft version.

All regular maintenance on the NORSAR field systems is conducted on a one-shift-per-day, five-day-per-week basis. The maintenance tasks include:

- Operating and maintaining the seismic sensors and the associated digitizers, authentication devices and other electronics components.
- Maintaining the power supply to the field sites as well as backup power supplies.
- Operating and maintaining the VSATs, the data acquisition systems and the intra-array data transmission systems.
- Assisting the NDC in evaluating the data quality and making the necessary changes in gain settings, frequency response and other operating characteristics as required.
- Carrying out preventive, routine and emergency maintenance to ensure that all field systems operate properly.
- Maintaining a computerized record of the utilization, status, and maintenance history of all site equipment.
- Providing appropriate security measures to protect against incidents such as intrusion, theft and vandalism at the field installations.

Details of the daily maintenance activities are kept locally. As part of its contract with CTBTO/PTS NORSAR submits, when applicable, problem reports, outage notification reports and equipment status reports. The contents of these reports and the circumstances under which they will be submitted are specified in the draft Operational Manual.

P.W. Larsen
K.A. Løken

5 Documentation Developed

Bungum, H., T. Kværna, S. Mykkeltveit, N. Maercklin, M. Roth, K. Åstebøl, D.B. Harris & S. Larsen (2006): Energy partitioning for seismic events in Fennoscandia and NW Russia. Proceedings, 28th Seismic Research Review, Orlando, Fl., 19-21 September 2006.

Gibbons, S.J. & F. Ringdal (2006): A case study of seismic event identification: Explosions in NW Russia using the ARCES seismic array. **In:** Semiannual Technical Summary, 1 July - 31 December 2006, NORSAR Sci. Rep. 1-2007, Kjeller, Norway.

Kværna, T., S. Larsen, M. Roth, H. Bungum & D.B. Harris: P- and S-wave eneryg partitioning from seismic events in underground mines, Bull. Seism. Soc. Am., submitted.

Kværna, T., S.J. Gibbons, F. Ringdal & D.B. Harris (2006): Integrated seismic event detection and location by advanced array processing. Proceedings, 28th Seismic Research Review, Orlando, Fl., 19-21 September 2006.

Kværna, T., F. Ringdal & U. Baadshaug (2006): The capability for seismic monitoring of the North Korean test site. **In:** Semiannual Technical Summary, 1 July - 31 December 2006, NORSAR Sci. Rep. 1-2007, Kjeller, Norway.

Maercklin, N., O. Ritzmann, H. Bungum & J.I. Faleide: A 3-D seismic velocity model for the greater Barents Sea region: Reference events and travel time modeling. Geophys. J. Int., submitted.

Oye, V., H. Bungum & M Roth (2006): Source parameters from microearthquakes in an underground ore mine. In: Radiated Energy and the Physics of Earthquake Faulting, Geophysical Monograph Series, vol. 170.

Ringdal, F., S.J. Gibbons & D.B. Harris (2006): Adaptive waveform correlation detectors for arrays: Algorithms for autonomoous calibration. In: Proceedings 28th Seismic Research Review, Orlando, Fl., 19-21 September 2006.

Ringdal, F., T. Kværna, S. Mykkeltveit, S.J. Gibbons & J. Schweitzer (2006): Basic research on seismic and infrasonic monitoring of the European Arctic. In: Proceedings 28th Seismic Research Review, Orlando, Fl., 19-21 September 2006.

Ringdal, F. (2006): Semiannual Technical Summary, 1 January - 30 June 2006. NORSAR Sci. Rep. 2-2006, Kjeller, Norway, August 2006.

Ringdal, F., T. Kværna, S. Mykkeltveit, S.J. Gibbons & J. Schweitzer (2006): Basic research on seismic and infrasonic monitoring of the European Arctic. **In:** Semiannual Technical Summary, 1 July - 31 December 2006, NORSAR Sci. Rep. 1-2007, Kjeller, Norway.

Ritzman, O., N. Maercklin, J.I. Faleide, H. Bungum, W.D. Mooney & S.T. Detweiler (2006): A 3D geophysical model of the crust in the Barents Sea Region: Model construction and basement characterization. Geophys. J. Int., in press.

Ritzman, O., N. Maercklin, H. Bungum, W.D. Mooney & S.T. Detweiler (2006): A 3D geophysical model of the crust in the Barents Sea Region. In: Proceedings 28th Seismic Research Review, Orlando, Fl., 19-21 September 2006.

Schweitzer, J. (2006): How can the ISC location procedures be improved) Phys. Earth Planet. Inter., 158, 19-26.

Schweitzer, J. & D. Storchak (2006): Modernizing the ISC location procedures (editorial) (2006): Phys. Earth Planet. Inter., 158, 1-3.

Weidle, Ch., A. Levshin, J. Schweitzer, N. Maercklin, N. Shapiro & M. Ritzwoller (2006): Surface wave tomograpy of the European Arctic. Geophys. res. abstract, 8.

6 Summary of Technical Reports / Papers Published

6.1 Basic research on seismic and infrasonic monitoring of the European Arctic

(Paper presented at the 28th Seismic Research Review)

ABSTRACT

This project represents a three-year research effort aimed at improving seismic and infrasonic monitoring tools at regional distances, with emphasis on the European Arctic region, which includes the former Novaya Zemlya test site. The project has two main components: a) to improve seismic processing in this region using the regional seismic arrays installed in northern Europe and b) to investigate the potential of using combined seismic/infrasonic processing to characterize events in this region. In the latter case, we plan on using the northern European seismic array network in combination with infrasonic stations either installed or scheduled for installation in the near future.

During this reporting period, we have implemented basic infrasonic processing software for the Apatity infrasonic array and for the ARCES seismic array. In the case of ARCES, there are currently no infrasonic sensors available (the plans are to install an infrasound array in 2006/2007), but the seismic sensors have proved useful as an initial substitute for detecting and processing infrasonic signals from explosions at local and regional distances. We have developed an algorithm for associating detected infrasonic phases (either by ARCES or Apatity) with regional seismic events detected and located by the on-line Generalized Beamforming (GBF) process which is currently in experimental operation at NORSAR. We searched the GBF bulletin for approximately one full year of data for seismic events at local or near regional epicentral distances to ARCES or the Apatity infrasound array. We found that 944 infrasound signals could be associated with 651 different seismic events from the GBF bulletin. The large majority of these events were confirmed mining explosions, mainly on the Kola Peninsula.

We present results from an analysis of seismic and infrasonic signals from a set of 108 surface explosions in northern Finland, carried out for the purpose of destroying old ammunition. We have used waveform cross-correlation on ARCES seismic recordings to determine very accurate origin times for the explosions. The extremely high correlation coefficients observed for this data set indicate that these explosions are all very closely spaced, probably within an area of some hundreds of meters in diameter. We have used this database to study the stability of slowness estimates for both seismic and infrasonic phases, using ARCES and Apatity array recordings. By analyzing various subconfigurations of the ARCES array, we find that the scatter (standard deviation) in the azimuth estimates for the explosions is about inversely proportional to array aperture. When carrying out a similar analysis of infrasonic data, we find that, in contrast to the case for the seismic P-waves, the azimuth scatter using our f-k estimation process does not decrease when the array aperture increases. Furthermore, the average azimuth remains essentially unbiased both with varying array aperture and with varying filter bands. This is also in contrast to the situation for seismic P-waves, where we have found strong frequency dependent and configuration dependent azimuth anomalies.

The recent upgrade of the Spitsbergen seismic array, which has included installation of five new three-component seismometers, has resulted in a significant improvement of S-phase

detection. We demonstrate this improvement by presenting analysis of recent small seismic events on Novaya Zemlya, where three events (of m_b=2.2, 2.3 and 2.7) were detected by the GBF process during March 2006.

6.1.1 Objective

The objective of the project is to carry out reseach to improve the current capabilities for monitoring small seismic events in the European Arctic, which includes the former Russian test site at Novaya Zemlya. The project has two main components: a) to improve seismic processing in this region using the regional seismic arrays installed in northern Europe and b) to investigate the potential of using combined seismic/infrasonic processing to characterize events in this region. In the latter case, we plan on using the northern European seismic array network in combination with infrasonic arrays either installed or scheduled for installation in the near future

6.1.2 Research Accomplished

Infrasound data processing using Apatity and ARCES array data

The Apatity infrasound array is a three-element array co-located with the nine-element Apatity short-period regional seismic array, which was installed in 1992 on the Kola Peninsula, Russia by the Kola Regional Seismological Centre (KRSC). For further details see Baryshnikov (2004).

The 25 element ARCES array is a short-period regional seismic array, located in northern Norway. ARCES has no infrasound sensors, but because of special near surface installation conditions, many of its seismic sensors are also sensitive to infrasound signals. The seismic sensors have therefore proved useful as an initial substitute for detecting and processing infrasonic signals from explosions at local and regional distances (see e.g., Ringdal & Schweitzer, 2005). Current plans are to install an infrasound array near the ARCES site in 2006/2007.

In this study, we have developed an initial STA/LTA-based infrasonic processing system for the Apatity infrasound array and for the ARCES seismic array. We have also developed an algorithm for associating detected infrasonic phases (either by ARCES or Apatity) to regional seismic events generated in the on-line Generalized Beamforming process which is currently in experimental operation at NORSAR. Some preliminary results are summarized in the following (for details, see Schweitzer et. al., 2006).

On the average, 23.4 infrasound signals per day were observed with the Apatity infrasound array and 7.6 signals per day with the ARCES array. These numbers of observations result from applying only an initial set of infrasound signal processing rules. We want to determine how many of these infrasonic signals can be associated to sources already known from their seismic signals. To investigate this question in more detail the following test was performed:

The Generalized Beamforming (GBF) algorithm (Ringdal and Kværna, 1989) integrates automatically all observations of local and regional phases from all seismic arrays analyzed at the NORSAR data center in one common bulletin, associates these observations to their common sources, and locates these seismic sources. It can be assumed that this bulletin is quite complete and that it is representative for local and regional seismic events in Fennoscandia and the European Arctic with local magnitudes above 1.5 in on-shore regions and above 2.5 overall. At large distances from the arrays, the threshold could be higher. We searched the GBF bulletin

for the first 351 days of the year 2005 (until the 17th of December) for seismic events at local or near regional epicentral distances to ARCES or the Apatity infrasound array. The following association criteria were used to correlate seismic events with presumed, corresponding infrasound signals:

- The epicentral distance of the event must be within 500 km from the array.
- The possible onset time of the infrasound signals was set to be within the time window spanned by group velocities between 0.2 and 0.7 km/s.
- The difference between the event backazimuth and the backazimuth observed for the infrasound signal should not be larger than 20 degrees.

BALTIC STATES-BELARUS-NW RUSSIA REGION

Origin time	Lat	Lon	Azres	Timres	Wres	Nphase	Ntot	Nsta	Netmag
2005-074:14.49.38.0	67.70	34.84	5.36	0.62	1.96	6	13	3	1.28

Sta	Dist	Az	Ph	Time	Tres	Azim	Ares	Vel	Snr	Amp	Freq	Fkq	Pol	Arid	Mag
APA	79.0	81.5	Pg	14.49.50.2	-0.5	87.3	5.8	7.3	31.0	494.1	4.32	1	1	743613	
APA	79.0	81.5	Lg	14.50.00.1	-0.5	81.4	-0.1	4.2	11.7	1577.1	3.67	1		743619	0.74
APA	79.0	81.5	s	14.50.03.0		83.2	1.7	3.4	6.4	1414.3	2.51	1		743620	0.87
APA	79.0	81.5	Ix	14.51.24.3		78.6	-2.9	0.325	14.2	5676.4	1.08	4		16005	
APA	79.0	81.5	Ix	14.54.24.6		73.3	-8.2	0.329	21.5	8792.5	9.88	6		16010	
APA	79.0	81.5	Ix	14.55.24.6		73.8	-7.7	0.338	116.5	66643.0	4.90	3		16015	
ARC	431.5	114.0	Pn	14.50.40.5	2.0	123.6	9.6	7.8	47.9	210.7	4.92	1		744345	
ARC	431.5	114.0	p	14.50.44.9		119.4	5.4	7.9	4.9	29.0	5.07	1		744348	
ARC	431.5	114.0	p	14.50.50.0		119.4	5.4	7.0	7.6	93.6	3.36	1	1	744349	
ARC	431.5	114.0	Sn	14.51.23.0	0.2	124.0	10.0	4.7	6.0	147.3	4.16	2	1	744357	1.25
ARC	431.5	114.0	s	14.51.27.2		116.4	2.4	3.7	3.5	80.1	4.28	3		744362	
ARC	431.5	114.0	s	14.51.33.6		111.3	-2.7	3.5	11.5	307.3	2.66	1	-3	744363	
ARC	431.5	114.0	s	14.51.38.1		129.2	15.2	4.6	11.3	378.2	3.90	1	-3	744369	1.69
ARC	431.5	114.0	Lg	14.51.41.5	0.3	117.9	3.9	5.1	4.7	216.0	2.74	1		744374	1.51
ARC	431.5	114.0	Ix	15.12.01.0		104.7	-9.3	0.319	10.7	130.4	4.17	2		97910	
ARC	431.5	114.0	Ix	15.12.52.6		104.0	-10.0	0.320	4.9	42.9	3.73	3		97915	
ARC	431.5	114.0	Ix	15.12.58.3		104.4	-9.6	0.319	4.3	59.1	3.45	3		97920	
ARC	431.5	114.0	Ix	15.13.54.4		102.3	-11.7	0.325	11.2	256.5	2.69	3		97925	
SPI	1304.8	143.5	p	14.52.21.8		163.0	19.5	5.6	6.4	72.3	5.89	2		743922	
SPI	1304.8	143.5	Pn	14.52.24.8	0.3	146.2	2.7	7.8	5.1	62.2	5.92	1		743925	

Fig. 6.1.1. GBF bulletin of an event in the Khibiny Massif, Kola Peninsula with associated infrasound signals (marked as Ix) observed at the Apatity infrasound array and at ARCES.

.

Applying these rules, 944 infrasound signals could be associated to 651 different events of the GBF bulletin. For these 651 events we obtained the following statistics:

- 333 events could be associated only with infrasound signals observed at the Apatity infrasound array.
- 250 events could be associated only with infrasound signals observed at the ARCES seismic array.
- 68 events could be associated with infrasound signals at both arrays, the ARCES seismic array and the Apatity infrasound array.

Figure 6.1.1 shows the GBF bulletin entry for an event in the Khibiny Massif, Kola Peninsula, for which infrasound signals were observed at both arrays. The source area is known to have numerous large explosions in open pit mines. The associated infrasound signals show quite small backazimuth residuals, the SNR of the observed infrasound signals at both arrays is of the same order as for the seismic signals, and at both arrays, the infrasound waves are arriving in different onset groups within a time window of 1 to 2 minutes.

Figures 6.1.2 and 6.1.3 show the results of the associations described above. We note that the seismic events with associated infrasound observations are concentrated around known mining areas. We further note that all of these associations are automatic, and have not been reviewed by an analyst. Nevertheless, we are confident that the vast majority of these associations are in fact real. Further work will include detailed review and statistical analysis of results from this association process.

Case study of explosions in northern Finland

Each year between mid-August and mid-September, a series of explosions in the north of Finland is recorded by the stations of the Finnish national seismograph network and also by the seismic arrays in northern Fennoscandia and NW Russia. Based upon event locations given in the seismic bulletin of the University of Helsinki, the geographical coordinates of the explosion site are assumed to be approximately 68.00°N and 25.96°E. The explosions are carried out by the Finnish military in order to destroy outdated ammunition and are easily identified from the automatic seismic bulletins at NORSAR for several reasons. Firstly, they are always detected with a high SNR on the ARCES array, secondly they register very stable azimuth estimates on the detection lists, and thirdly they take place at very characteristic times of day (the origin time indicated by the seismic observations almost invariably falls within a few seconds of a full hour, or half-hour in the middle of the day). A preliminary list of candidate events was obtained by scanning the GBF automatic detection lists for events which appeared to come from the correct region at appropriate times of day.

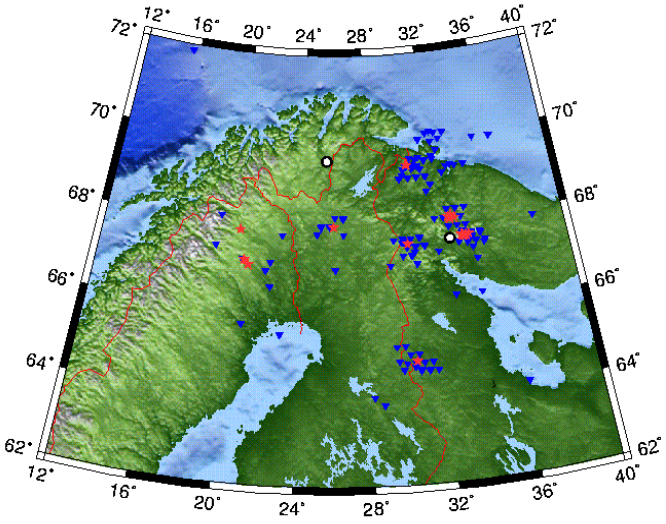

Fig. 6.1.2. The map shows the 651 automatically located events (GBF) for which either the ARCES seismic array or the Apatity infrasound array observed infrasound signals. The blue triangles show the GBF event locations and the red stars show the location of known sites with explosions either at the Earth's surface or in the atmosphere. Note that the automatic GBF locations usually scatter over a larger area around these source regions. Also note that the GBF locations employ a fixed grid, and that many of the grid points shown on the map have a large number of corrsponding events.

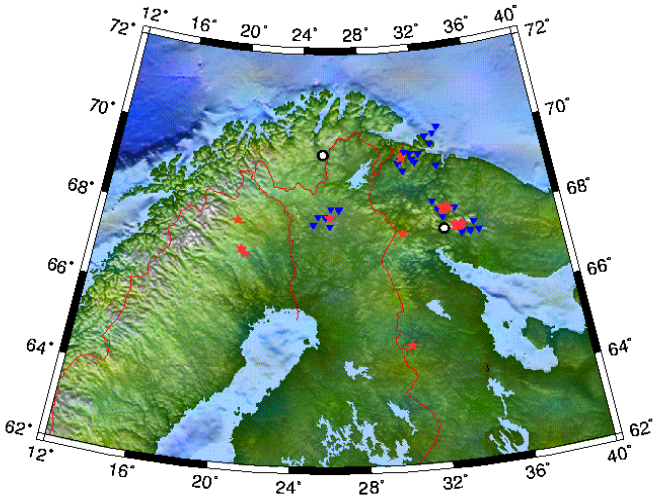

Fig. 6.1.3. This map is similar to Figure 6.1.2, and shows the 68 automatically located events (GBF) for which both the ARCES seismic array and the Apatity infrasound array observed infrasound signals. The blue triangles show the GBF event locations and the red stars show the location of known sites with explosions either at the Earth's surface or in the atmosphere.

Between 2001 and 2005, a total of 108 events were found which appeared to fit the general attributes of explosions from this site; the GBF location estimates for these events are displayed in Figure 6.1.6.1.4. These fully automatic estimates display a somewhat surprisingly large geographical spread and, assuming that these events are in fact essentially co-located, the origin times will be correspondingly spurious. Before we proceed in attempting to detect and analyse infrasound signals produced from these explosions, we must first confirm that all of our candidate events are in fact from essentially the same location and then obtain the best possible origin time for each event. To this end, we applied a waveform correlation procedure, which confirmed that the explosions were indeed closely spaced, probably within an area of some hundred meters in diameter (for details, see Ringdal and Gibbons, 2006).

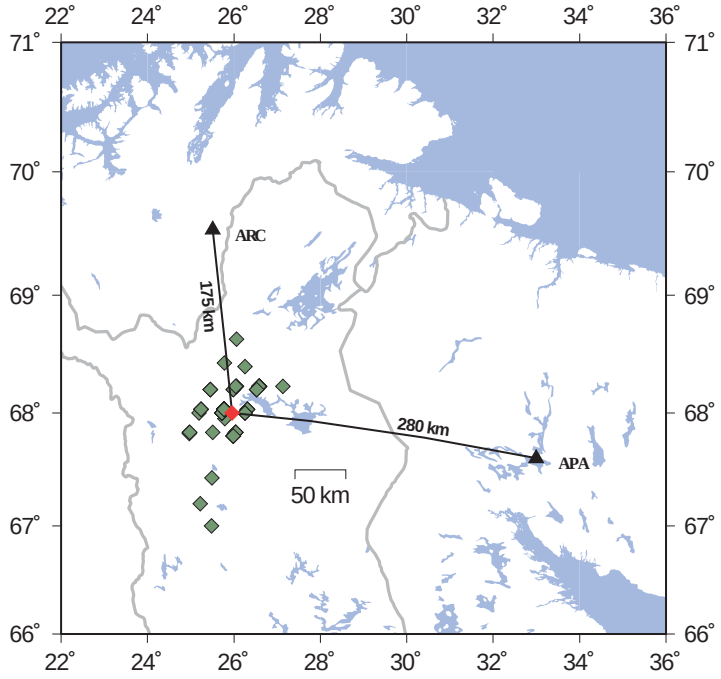

Fig. 6.1.4. Estimated location of the explosion site in northern Finland (orange diamond) in relation to the seismic arrays ARCES and Apatity together with the GBF fully automatic location estimates for 108 candidate events between August 2001 and September 2005 (green diamonds). The regular pattern of event location estimates is due to the fixed-grid trial epicenter procedure employed by the GBF.

Thus, this data set of more than 100 surface explosions in almost exactly the same place recorded by the ARCES and Apatity arrays provides an excellent opportunity to investigate the stability of slowness estimates, both for the seismic and infrasonic recordings. The paper by Ringdal and Gibbons (2006) presents results on the effects of filter frequency band, array aperture and number of sensors at both the Apatity and ARCES arrays. In this paper we will focus on using various sub-configurations of ARCES to simulate array configurations of various diameters and number of sensors.

Figure 6.1.5 shows the ARCES slowness estimates for the event set as a function of various sub-configuration of vertical-component seismometers. These are, in increasing sizes:

- The 4-element A-ring configuration (seismometers A0, A1, A2, A3)
- The 9-element A,B-ring configuration (by adding the seismometers B1-B5)
- The 16-element A,B,C-ring configuration (by adding the seismometers C1-C7)
- The 25-element A,B,C,D-ring configuration (comprising the full ARCES vertical-component array)

As expected, the scatter of the estimates decreases as the array size and number of seismometers increases, and the amount of decrease in the standard deviations is about proportional to the increase in array diameter. We note that the mean azimuth estimates show significant differences among the array configurations, even if we are applying the same bandpass filter (3-5 Hz) throughout.

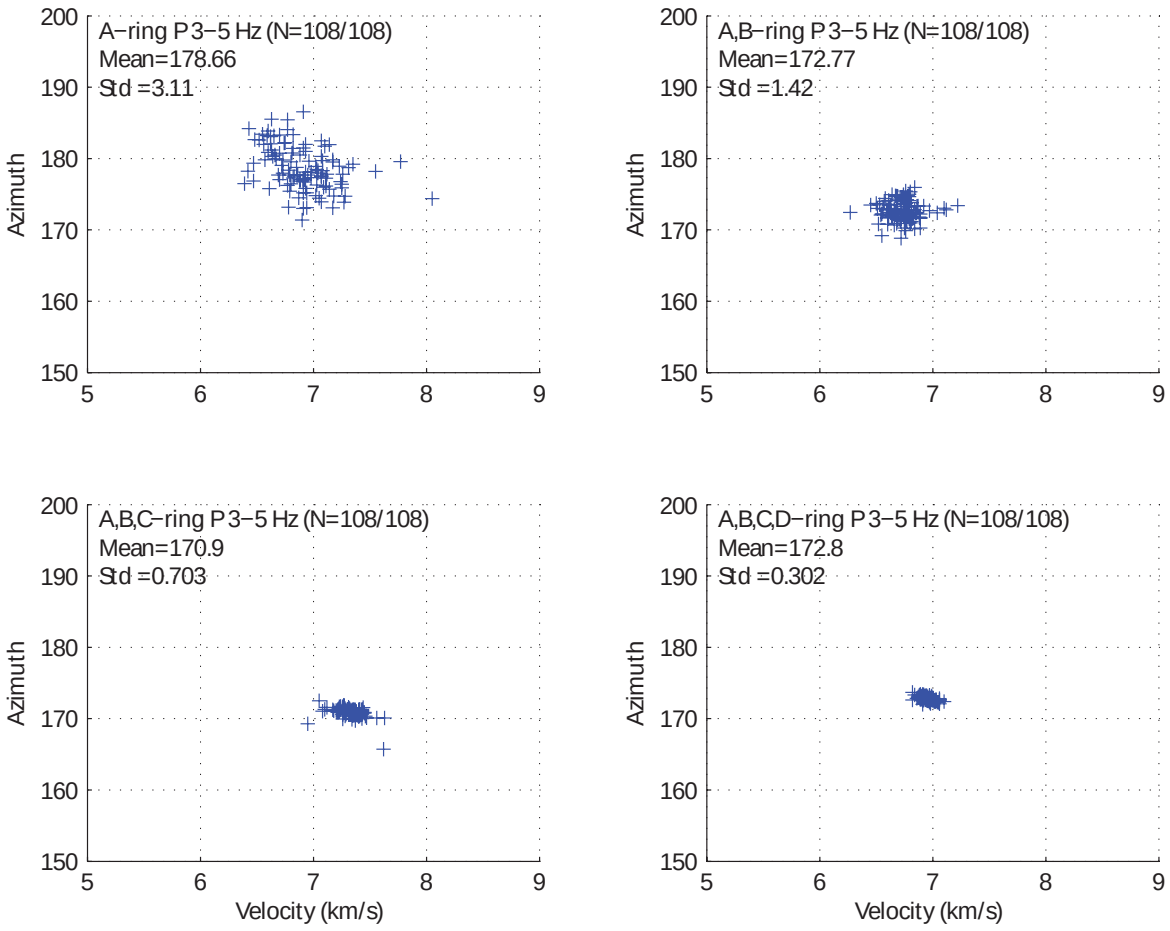

Fig. 6.1.5. Seismic slowness estimates of the 108 events in the data base. The figure corresponds to estimates for the seismic P-phase (25-35 seconds after the event origin time), in the filter band 3-5 Hz. The four subconfigurations are as described in the text. For each subconfiguration, the mean and standard deviation of the azimuth estimates are indicated.

We carried out a similar study of slowness estimates for infrasonic waves recorded at the ARCES seismic array. In this case, we used throughout a 60 second window beginning 620 seconds after the event origin time. Figure 6.1.6 shows the ARCES slowness estimates for the infrasonic phases (named Ix) as a function of the same sub-configuration of vertical-component seismometers as used in our studies of P-waves described above.

In contrast to the P-wave analysis, we were not able to make reliable slowness estimates for the infrasonic phases of all the events. This is mainly due to low infrasonic SNR for a number of the events in the database. This makes a comparison between the performances of different filters and subconfigurations more complicated, and we need to consider both the number of successful estimates and the variance reduction when evaluating the results.

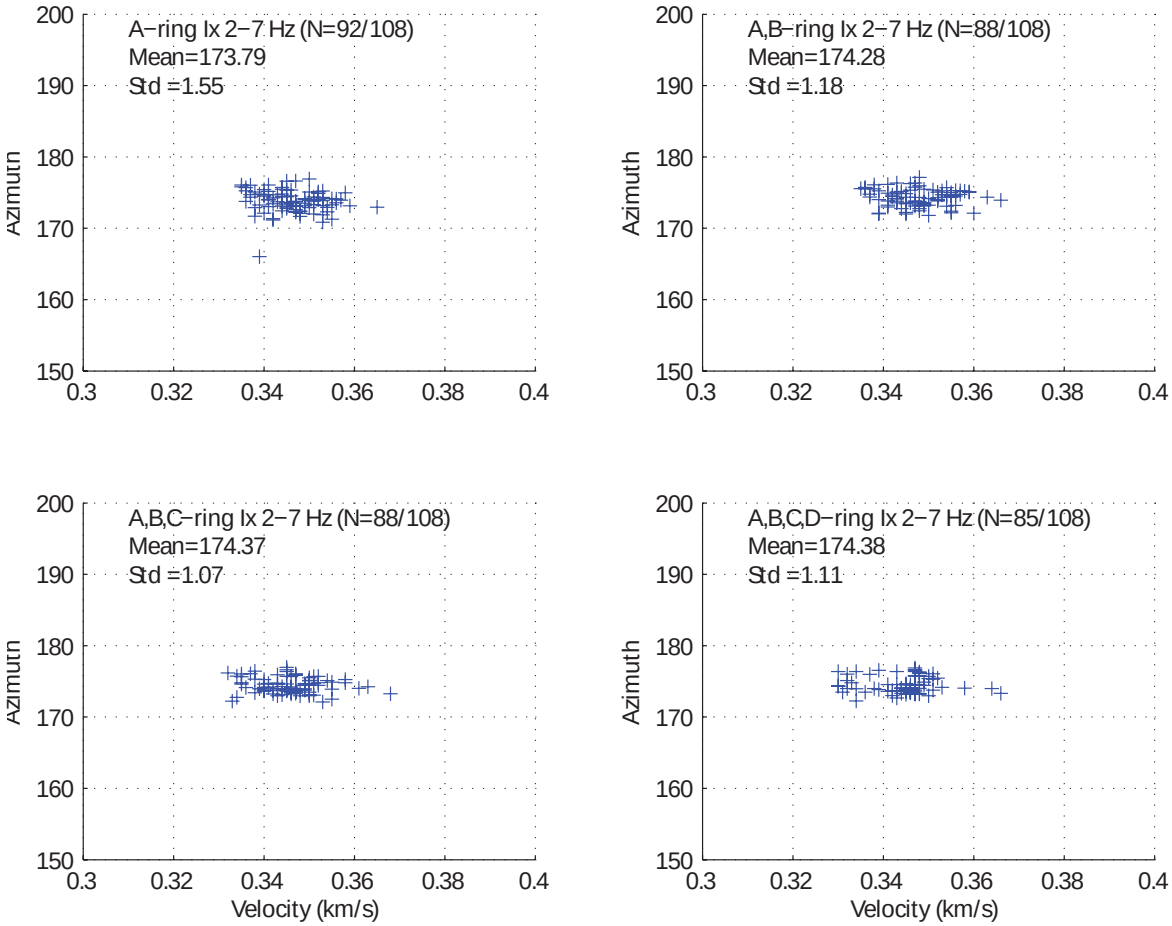

Fig. 6.1.6. Infrasonic slowness estimates of the 108 events in the data base. The figure corresponds to estimates for the infrasonic phase (620-680 seconds after the event origin time), in the filter band 2-7 Hz. The number of events for which reliable estimates could be made is indicated on each plot. The four subconfigurations are as described in the text. For each subconfiguration, the mean and standard deviation of the azimuth estimates are indicated.

When comparing the infrasonic results to those obtained for seismic P-waves, we see some interesting differences. For example, we see no significant variance reduction as the array aperture and number of sensors increases. Although there appears to be a slight reduction in the standard deviations, the largest number of successful estimates were in fact made using the smallest configuration. Therefore we consider that there is essentially no difference in the stability of the slowness estimates for these four configurations. It is of course possible that other estimation techniques could show such improvements, but it may also be that the variance in estimates is dominated by factors such as varying atmospheric conditions over the 5 years covered by this study. Another important observation is that the average azimuth values are essentially independent of the subconfiguration chosen. This also contrasts to our observations from seismic P-waves.

Detection of small seismic events near Novaya Zemlya

The recent upgrade of the Spitsbergen seismic array (Figure 6.1.7), which has included installation of five new three-component seismometers as well as an upgrading of the sampling rate from 40 to 80 Hz, has resulted in a significant improvement of S-phase detection. We demonstrate this improvement by presenting analysis of recent small seismic events near Novaya Zemlya, where three events (of m_b=2.2, 2.3 and 2.7) were detected by the GBF process during March 2006 (Table 6.1.1 and Figure 6.1.8).

Table 6.1.1 Seismic events near Novaya Zemlya detected during March 2006

Date	Origin time	Latitude (N)	Longitude (E)	Magnitude (mb)
05/03/2006	23.17.35.7	76.80	66.04	2.65
14/03/2006	20.57.02.4	75.07	53.05	2.23
30/03/2006	10.46.02.8	70.79	51.50	2.30

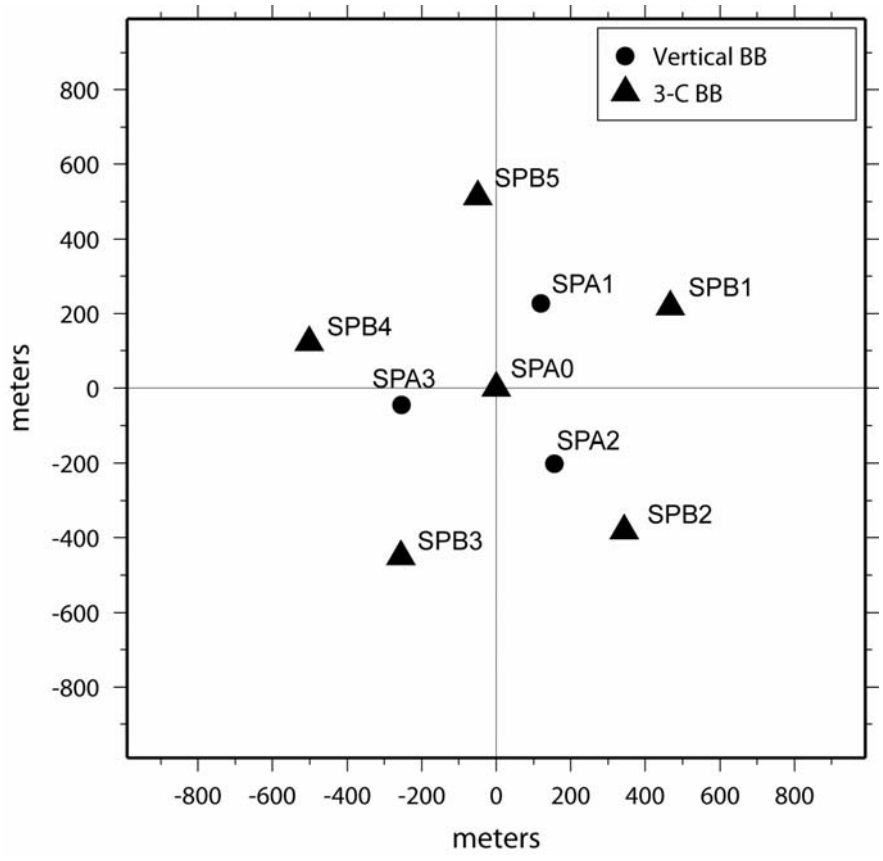

Fig. 6.1.7. Configuration of the upgraded Spitsbergen seismic array.

Figure 6.1.9 shows spectrograms of the Spitsbergen B1 seismometer (vertical, radial and transverse components) for the Novaya Zemlya event on 5 March 2006. The most noticeable feature is the high SNR of the P-phase for this small (m_b=2.65) event. In fact, the SNR on the array beam is above 100, indicating that even an event at this site more than an order of magnitude

smaller could have been detected. This should not, however, be extrapolated to a general statement about detection thresholds for the Spitsbergen array, since the SNR to a large extent depends upon path-specific focussing effects. Nevertheless, the amount of high-frequency energy is remarkable, taking into account the large epicentral distance (more than 1000 km). We note that the vertical and radial components have significant P-wave energy even above 20 Hz. The transverse component shows (not unexpectedly) a small P-wave and a much larger S-wave, indicating that the use of transverse components could be useful in detecting S-phases.

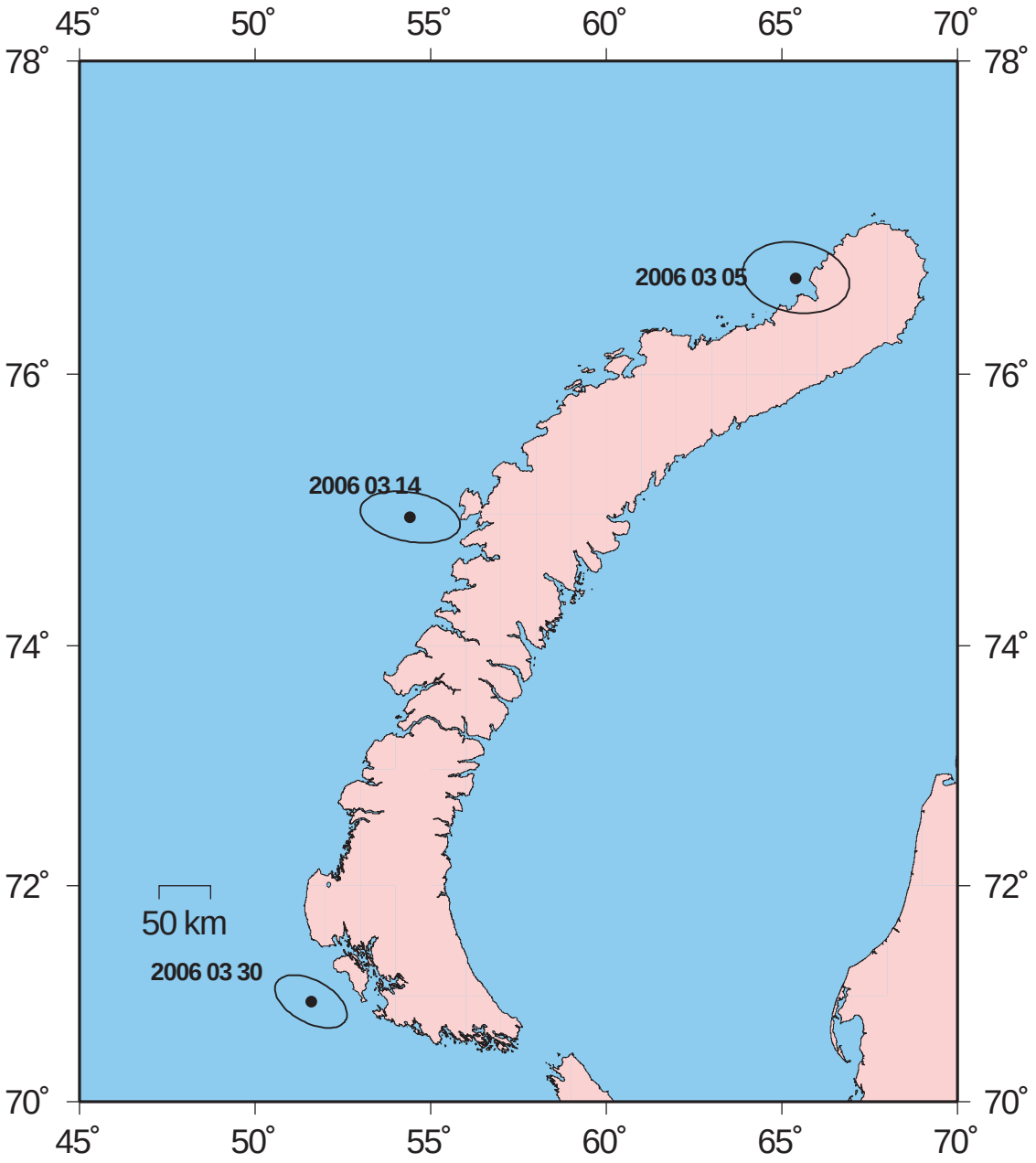

Fig. 6.1.8. Location of three low-magnitude seismic events which occurred near Novaya Zemlya during March 2006..

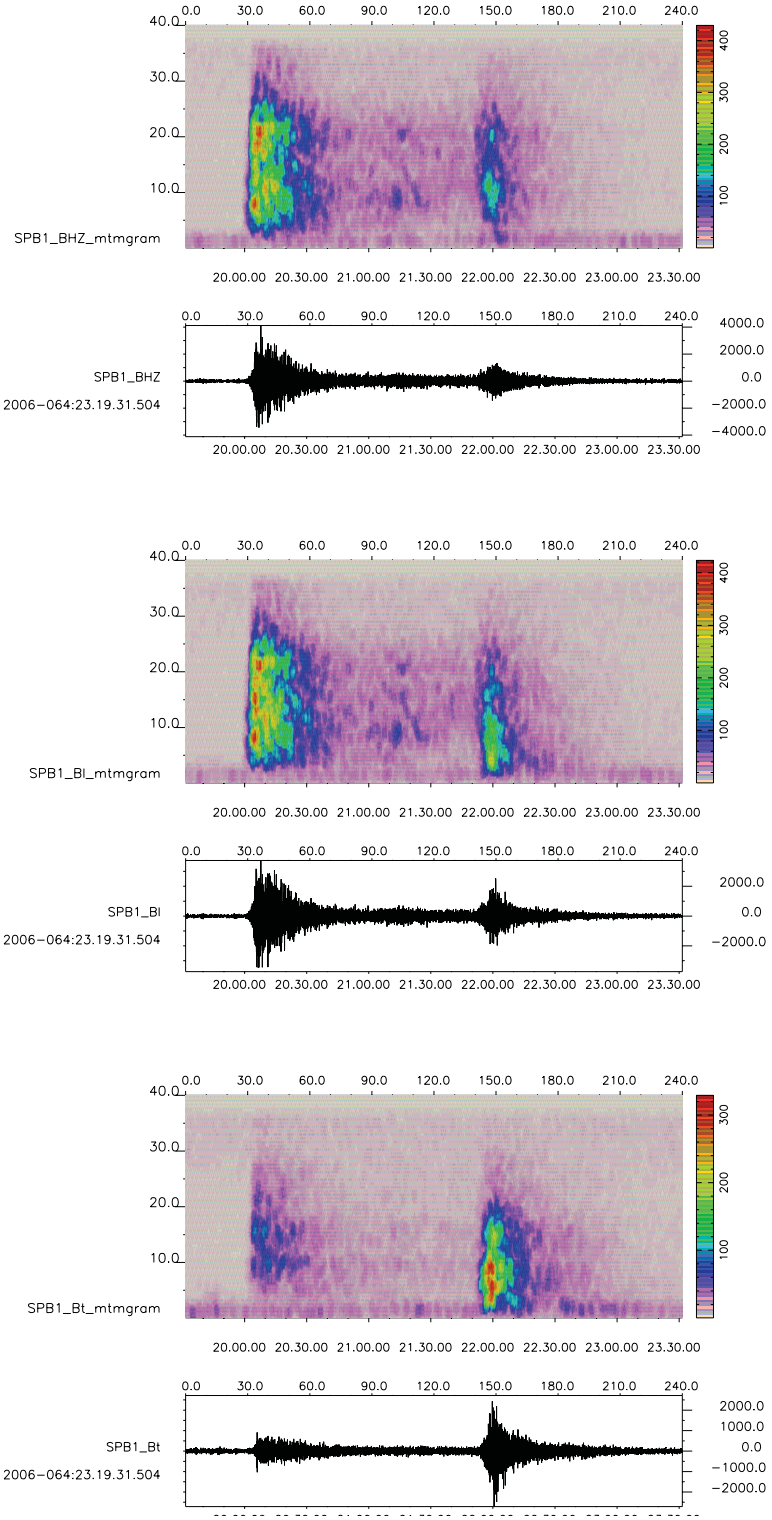

Fig. 6.1.9. Spectrograms for the Spitsbergen B1 seismometer (vertical, radial and transverse components) for the Novaya Zemlya event on 5 March 2006.

This is further illustrated in Figure 6.1.10, which shows selected Spitsbergen array beams for the 5 March 2006 Novaya Zemlya event. The top trace is a beam steered to the epicenter with a P-wave velocity, and using a typical detection filter (3-16 Hz). Note that the S-wave on this trace is fairly small, and would give a fairly marginal detection by the automatic process. The middle trace is an "optimum" beam designed to detect the S-wave. It represents the beams of the transverse components of the six three-component seismometers in the array, filtered in the band 2-4 Hz and steered to the epicenter with an S-phase velocity. Note the greatly improved SNR gain on this trace. The bottom trace shows, for comparison, a P-beam of vertical sensors using the same (2-4 Hz) filter. Clearly, the detection of S-phases could be greatly improved by augmenting the beam deployment with several steered beams , rotated so as to provide transverse components, toward the grid points in the beam deployment system.

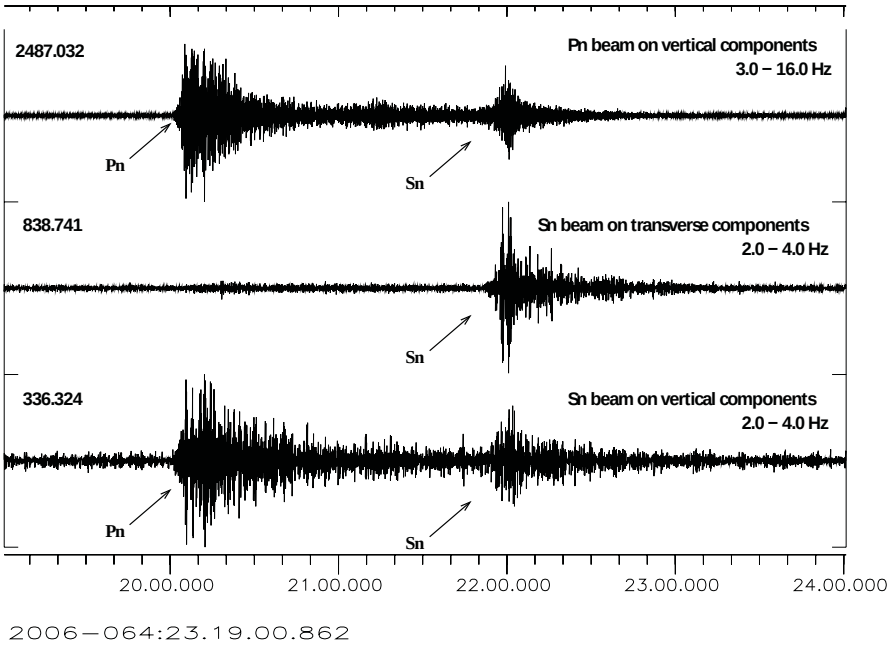

Fig. 6.1.10. Spitsbergen array waveforms for the 5 March 2006 Novaya Zemlya event. Note the greatly improved SNR gain for the Sn phase shown in middle trace, which represents the beams of the transverse components of the six three-component seismometers in the array.

Conclusions and Recommendations

The initial results from associating infrasonic observations to seismic events are promising. We plan in the future to compare in more detail the infrasound observations with analyst reviewed event locations. This will require a review by an analyst of each infrasound signal, in order to confirm their validity and to identify possible misassociations if appropriate. Furthermore, we will implement ant test additional infrasonic array detectors, such as the PMCC detector (Cansi, 1995).

The data set of more than 100 surface explosions in northern Finland in almost exactly the same place recorded by the ARCES and Apatity arrays has provided an excellent opportunity to investigate the stability of slowness estimates for seismic and infrasonic recordings as a function of array geometry, number of sensors and filter frequency band. Future work will focus using this database as well as the ground truth data base of mining explosions in the Kola Peninsula to assess the detectability of infrasonic phases under various atmospheric conditions.

The new Spitsbergen array configuration has shown excellent recordings of high-frequency data from Novaya Zemlya events. The new three-component instrumentation provides a great potential for improving S-phase detection at this array, and an enhanced S-phase detector will be implemented in the near future.

Acknowledgements

This research has been supported by the US Army SMDC under contract W9113M-05-C-0224.

Frode Ringdal
Tormod Kværna
Svein Mykkeltveit
Steven J. Gibbons
Johannes Schweitzer

References

Baryshnikov, A.K. (2004). Research of infrasound background characteristics for estimation of threshold sensitivity of infrasound method for nuclear test monitoring. Final Technical Report ISTC 1341-01 (Part 1 of total 2), International Science and Technology Center (ISTC), Moscow, 255 pp.

Cansi, Y. (1995). An automatic seismic event processing for detection and location: The P.M.C./C. method, *Geophys. Res. Lett.*, **22**, 1021-1024.

Ringdal, F. and S.J. Gibbons (2006). Seismic/Infrasonic Processing: Case study of explosions in north Finland. Semiannual Technical Summary, 1 July – 31 December 2005, NORSAR Sci. Rep. **1-2006**, 54-68.

Ringdal, F., and T. Kværna (1989). A multi-channel processing approach to real time network detection, phase association, and threshold monitoring, *Bull. seism. Soc. Am.*, **79**, pp. 1927-1940.

Ringdal, F. & J. Schweitzer (2005). Combined seismic/infrasonic processing: a case study of explosions in NW Russia. Semiannual Technical Summary, 1 January – 30 June 2005, NORSAR Sci. Rep. **2-2005**, 49-60.

Schweitzer, J., F. Ringdal, T. Kværna, V. Asming and Yu. Vinogradov (2006). Infrasound data processing using Apatity and ARCES array data. Semiannual Technical Summary, 1 July – 31 December 2005, NORSAR Sci. Rep. **1-2006**, 42-53.

6.2 The Capability for Seismic Monitoring of the North Korean Test Site

6.2.1 Abstract

On 9 October 2006 the Democratic People's Republic of Korea (DPRK) conducted an underground nuclear explosion at a test site near Kimchaek. The explosion was detected by several seismic stations in the International Monitoring System (IMS), and the event magnitude as reported in the REB was 4.1. In this paper we analyze the recorded waveforms in order to investigate the capability of the IMS to monitor the DPRK test site for possible future explosions. Our analysis is based upon the so-called Site-Specific Threshold Monitoring (SSTM) approach. Using actual seismic data recorded by a given network, SSTM calculates a continuous "threshold trace", which provides, at any instance in time, an upper magnitude bound on any seismic event that could have occurred at the target site at that time.

We find that the IMS primary network has a typical "threshold monitoring capability" of between mb 2.3 and 2.5 for the DPRK test site. Not unexpectedly, it turns out that the Korean array (KSRS) is of essential importance in obtaining such low thresholds. We have also experimentally investigated how the capability could be improved by adding non-IMS stations to the network. We find that by adding the nearby station MDJ in China, the threshold monitoring capability is improved to between magnitude 2.1 and 2.3.

A different perspective is to investigate the actual network detection capability for events at the test site, requiring at least 3 IMS stations to detect the event. This is the traditional way of looking at network capability, and the resulting threshold will always be considerably higher than that obtained by the SSTM approach. A global capability map, which is published by the IDC for each hour, shows that at the time of the event, the IMS 3-station detection capability was approximately 3.5. This is an order of magnitude higher than the threshold obtained by SSTM.

We conclude that the SSTM approach allows the analyst to identify times when there is a possibility of occurrence of events too small to be detected by the usual 3-primary station requirement, and to subject such occasions to extensive analysis in order to determine whether an event in fact occurred. Thus, the SSTM approach constitutes a valuable supplement to the traditional network processing.

6.2.2 Introduction

Traditionally, assessments of seismic network detection capabilities are based upon assuming statistical models for the noise and signal distributions. These models include station corrections for signal attenuation and a combinational procedure to determine the detection threshold as a function of the number of phase detections required for reliable location (Sykes and Evernden 1982; Harjes, 1985; Hannon 1985; Ringdal 1986; Sereno and Bratt, 1989).

In general, it is implicitly understood that any network will have a detection threshold that varies with time. It is important to retain such information along with the information on the average capability. However, the methods used in practical operation today make no attempt at specifying the time-dependency of the calculated threshold. For example, the noise models used in these capability assessments are not able to accommodate the effect of interfering signals, such as the coda of large earthquakes, which may cause the estimated thresholds to be significantly degraded at times. Furthermore, only a statistical capability assessment is achieved, with no time-dependent evaluation of when the possibility of undetected seismic events is par-

ticularly high, for example during unusual background noise conditions or outages of key stations.

The continuous threshold monitoring technique has been developed to address these issues. The basic principles were described by Ringdal and Kværna (1989, 1992) and by Kværna and Ringdal (1999), who showed that this method could be useful as a supplement to event detection analysis. Basically, the difference between the threshold monitoring approach and traditional detection threshold estimation can be described as follows (assuming a statistical model with a given confidence level):

- The *detection threshold* is an estimate of the *smallest* hypothetical seismic event at a given site or in a given region that could possibly be *detected* (e.g. by 3 stations)
- *Threshold monitoring* provides an estimate of the *largest* hypothetical seismic event at a given site or in a given region that could possibly have *occurred*.

The two approaches are therefore complementary, and each provides useful information in the context of seismic monitoring. The threshold monitoring approach could be especially useful to identify time intervals when the possibility of significant "hidden" seismic events is particularly high, thus enabling the analyst to concentrate on such time intervals for extensive analysis. Furthermore, the method provides an upper limit of the magnitude of non-detected events, which could be useful e.g. to assess the maximum M_S value for events for which no surface waves are detected.

The capability achieved by the threshold monitoring method is in general dependent upon the size of the target area, and it is convenient to consider three basic approaches:

- **Site-specific threshold monitoring**: A seismic network is focused on a small area, such as a known test site. This narrow focusing enables a high degree of optimization, using site-station specific calibration parameters and sharply focused array beams.
- **Regional threshold monitoring**: Using a dense geographical grid, and applying site-specific monitoring to each grid point, threshold contours for an extended region are computed through interpolation. In contrast to the site-specific approach, it is usually necessary to apply regionally averaged attenuation relations, and the monitoring capability will therefore not be quite as optimized.
- **Global threshold monitoring**: This is a natural extension of the regional monitoring approach, but requires a somewhat different strategy for effective implementation. Using a global network, and taking into account that phase propagation time is up to several tens of minutes, it is necessary to apply global travel-time and attenuation tables, possibly with regional corrections, and to use a much coarser geographical grid than in the regional approach.

The regional and global monitoring techniques provide geographical threshold maps that have several advantages over standard network capability maps. They are far more accurate during time intervals when interfering seismic events occur. They can also more easily reflect special conditions such as particularly favorable source-station propagation paths, and have the advantage of not being tied to specific event detection criteria. In principle, the threshold monitoring approach can be applied to geographical target points at any depth. In practice, for the initial version of the system, we limit the processing to shallow seismic events, by setting the depth parameter of each target point to zero.

In this paper, we will focus on the site-specific monitoring technique. We will develop a site-specific threshold monitoring setup for the North Korea nuclear test site, using as calibration information the data recorded by the IMS network and IRIS stations for the North Korea nuclear explosion on 9 October 2006.

6.2.3 Basic parameters of the North Korean nuclear test

Both the United States Geological Survey (USGS) and the International Data Centre (IDC) of the CTBT Organization in Vienna, Austria reported the nuclear test within hours of its occurrence. Figure 6.2.1 shows the geographical location of the test as reported by the USGS. This figure as well as Figure 6.2.2 are from the Web pages of the European-Mediterranean Seismological Centre (EMSC). Table 6.2.1 shows the event location estimates as provided by the IDC and by the USGS. We note that the epicentral solutions are quite consistent and that the estimated magnitudes are also quite similar (4.1 and 4.2).

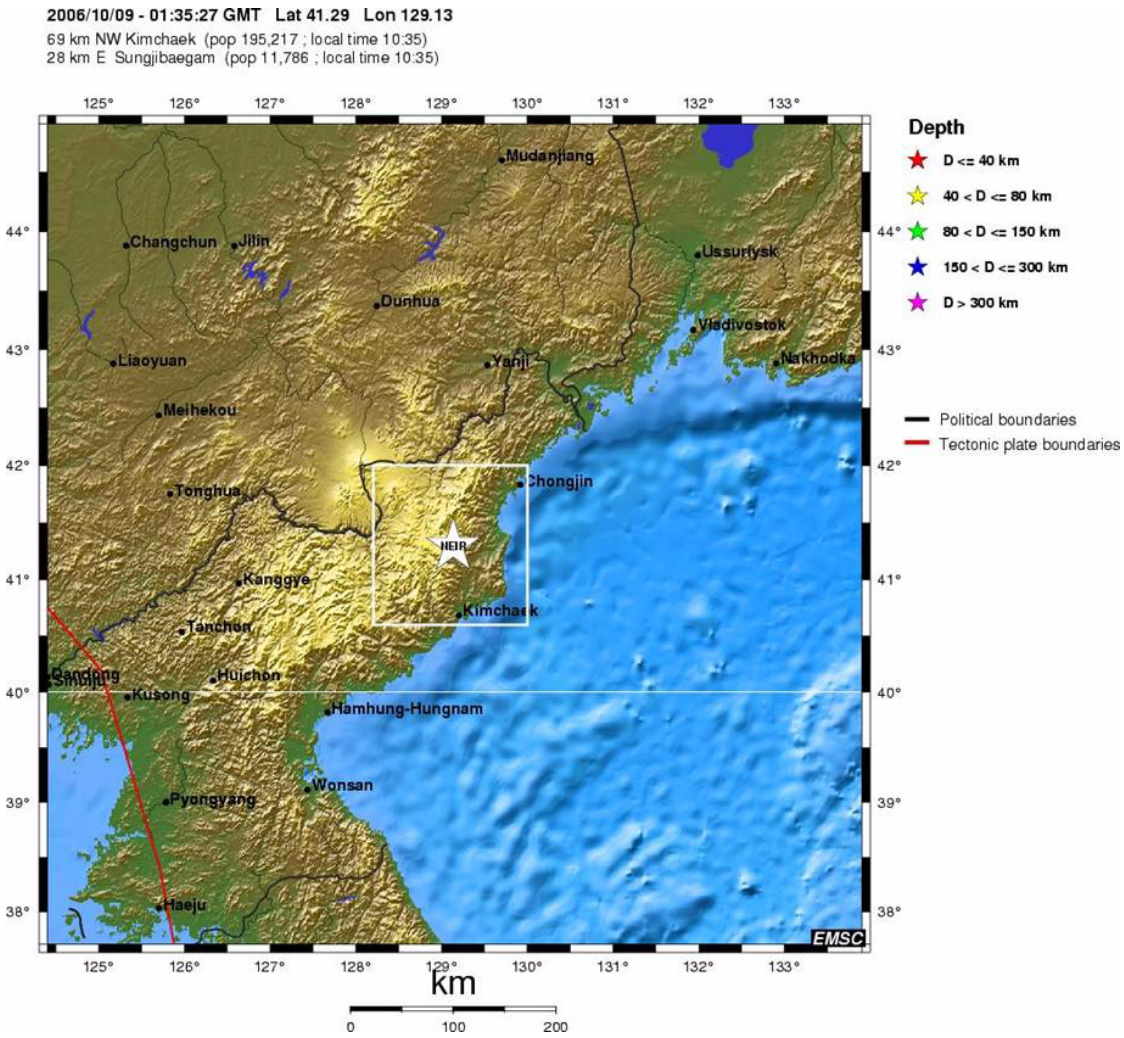

Fig. 6.2.1. Location of the reported North Korea underground nuclear explosion on 9 October 2006. Source of map: EMSC Web pages.

Figure 6.2.2 shows the regional seismicity from 1964 to 2006. There is some scattered seismicity near the test site, and it is interesting to compare the recordings of these earthquakes to the nuclear explosion (see e.g. Richards and Kim, 2007). One observation of interest in our context is that the P/S ratio is quite different for the explosion and the earthquakes in the nearby area. Since our task is to develop a site-specific threshold monitoring system to detect nuclear explosions, it is important that we calibrate the P and S-phases against an actual explosion, and not an earthquake.

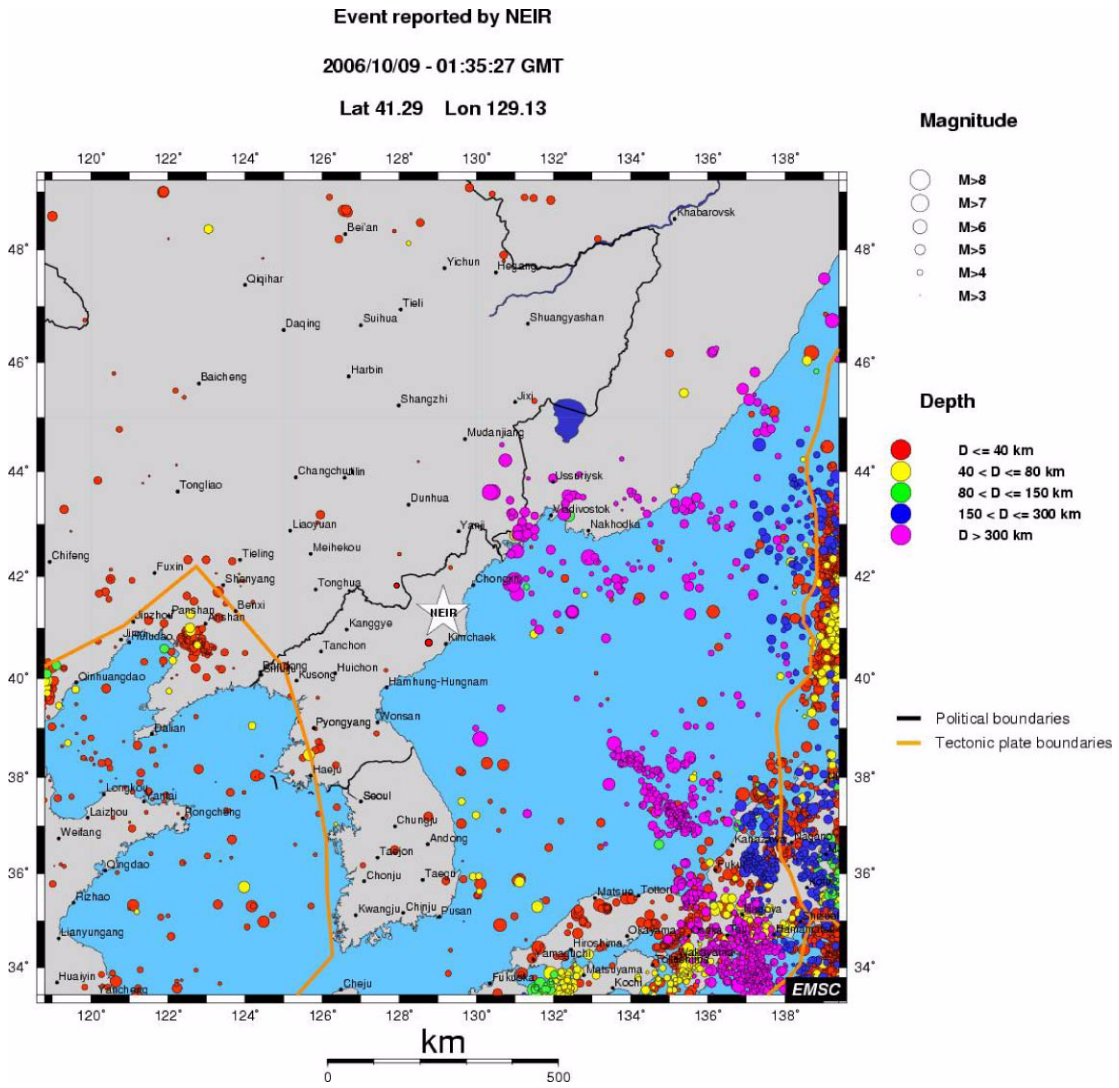

Fig. 6.2.2. Regional seismicity (1964-2006) in the region surrounding the North Korea nuclear test site. Data until 2002 are from the ISC bulletin, while two additional events in 2002 and 2004 reported by the USGS have been added.
Source of map: EMSC Web pages.

The USGS and IDC reported parameters for the North Korea nuclear test are given in Table 6.2.1, and m_b's of 4.2 and 4.1, respectively are reported. There has been much discussion about the actual yield (Y, in kiloton) of the explosion. A standard magnitude-yield relation for fully coupled explosions in hard rock at the former Soviet test site in Kazakhstan (Shagan River or Balapan) is (see Ringdal et. al., 1992):

$$m_b=4.45+0.75 \log(Y) \quad (1)$$

This would give an estimated yield of about 0.5 kt for m_b=4.2, and slightly lower for m_b=4.1. If we instead apply a formula appropriate to the Novaya Zemlya test site (see National Academy of Sciences, 2002):

$$m_b=4.25+0.75 \log(Y) \quad (2)$$

we obtain a somewhat higher yield estimate (about 1 kiloton for m_b=4.2 and again slightly lower for m_b=4.1). In the calculations later in this paper, we have adopted an m_b of 4.1 for the explosion.

Table 6.2.1. Reported parameters for the North Korea nuclear test 9 October 2006.

Data Source	Origin time	Latitude (N)	Longitude (E)	Magnitude (mb)
IDC	2006-282:01.35.27.6	41.3119	129.0189	4.1
USGS	2006-282:01.35.27.8	41.294	129.134	4.2

6.2.4 Seismic stations used for the site-specific threshold monitoring

Figure 6.2.3 shows the network selected for this study. This network comprises in general those IMS stations which had the best signal-to-noise ratio (SNR) for the 9 October explosion plus the Chinese station at Mudanjiang (MDJ), about 370 km north of the test site. MDJ data is openly available through the IRIS data management center. We note that data from the Korean Seismic array (KSRS) in South Korea was not operationally available from the IDC for the time period of the test. We are grateful to KIGAM for providing us with the KSRS data for our analysis.

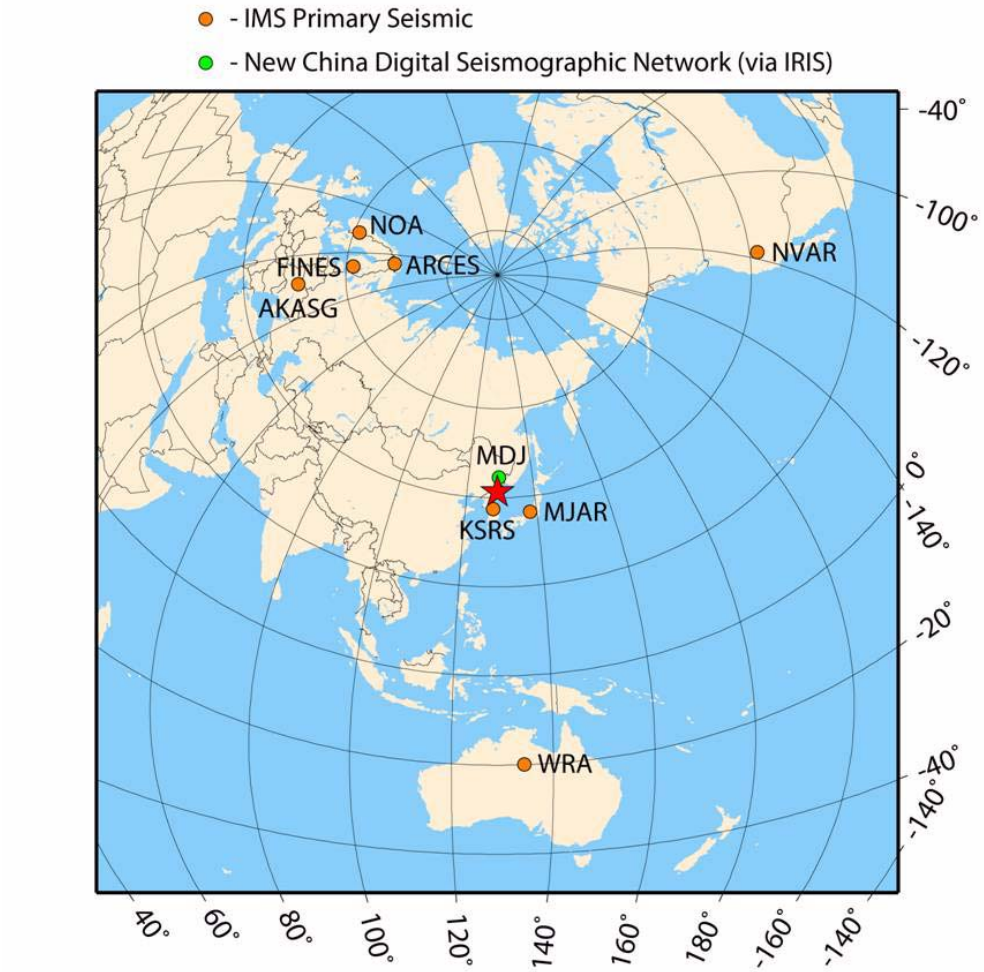

Fig. 6.2.3. Seismic network used for this study. The star marks the location of the target site.

Table 6.2.2 shows the primary seismic stations with P-phases in the Reviewed Event Bulletin (REB) for the 9 October explosion as well as three additional stations. For comparison, we also show the SNR obtained through our re-analysis of the data for selected stations (marked in red), which we will discuss further in the next section. In general, our results are consistent with those of the IDC, and we should emphasize that the SNR values obtained in this study are specifically directed towards optimizing the capability for detecting events at the test site, and therefore would normally be higher than those obtained in the routine general processing.

Table 6.2.2. Stations with P-phases in the REG and additional stations used in this study. Stations in red are used in the site-specific threshold monitoring calculations.

Station	Delta	Phase	IDC SNR	NEW SNR	Comment
MJAR	8.63	Pn	15.0	46.1	Single channel MJA3 (4-8 Hz)
SONM	17.36	Pn	3.4		
MKAR	33.63	P	4.4		
FINES	60.30	P	25.4	26.7	
WRA	61.14	P	10.6	46.9	
YKA	64.74	P	4.8		
AKASG	64.78	P	9.5	12.3	
ASAR	64.80	P	9.8		
NOA	66.20	P	4.6	7.6	
GERES	73.69	P	7.5		
STKA	73.74	P	4.6		
NVAR	79.69	P	14.5	19.6	Removed 3 channels with erroneous timing
PDAR	81.04	P	8.0		
LPAZ	151.00	PKPbc	5.0		
Stations used in this study which were not used for the REB solution:					
MDJ	3.33	Pn		142.8	IRIS station
KSRS	3.93	Pn		194.8	Not in IDC Operations
ARCES	61.60	P		5.4	A0, C-ring, D-ring

6.2.5 Tuning procedure

Once the monitoring network has been selected, each station needs to be tuned to the target site. This must be done separately for each phase that is to be included in the network processing. The tuning procedure generally comprises the following steps:

- For each location-station-phase combination, we estimate continuously the seismic amplitude levels. If the station is an array, we use short-term averages (STAs) of filtered beams to represent the amplitude levels. The steering parameters of the beams will then correspond to the apparent velocity and azimuth of the actual phase. The filter bands are chosen such that good signal-to-noise ratio (SNR) is ensured. If the observation unit is a three- or single-component station, the STA values are computed from a filtered single channel.
- When considering a potential event at a given time and location, we measure the seismic amplitude levels at the expected arrival times for the relevant seismic phases. For site-specific monitoring, the travel times of each phase are usually measured from the observed calibration event(s), but can also for each phase can be taken from standard travel time tables.
- In order to relate the STA observations to actual magnitude estimates, we apply the formula $m = log(STA) + b(d,h)$, where m is the estimated magnitude, STA is the representation of the seismic amplitude level and b is a distance-depth correction factor for each location-station-phase combination. The correction factors can be obtained by processing events with known magnitudes, or by using standard attenuation values.
- For assessing the significance of these magnitude estimates, we assume that they are sampled from a normal distribution with an assumed standard deviation. Experience with signal amplitude variation across the NORSAR array indicates that a standard deviation of 0.2 is a good value for a small epicentral area. A standard deviation of 0.3 has been used for the North Korean test site, as only one event has been used for calibration
- The magnitude limits computed by this algorithm are tied to a given confidence level, initially set to 0.9. This means that the estimated limits represent the largest magnitude of a possible hidden event, in the sense that there is at least a 90 per cent probability that one or more of the observed amplitude values would be exceeded by the signals from an event with magnitude above these limits.
- The method also allows for continuously estimating the network n-station detection capability, by using standard combinatorial formulas for the detection probabilities. Alternatively, we can also use a simplified scheme whereby we order the individual station thresholds in increasing sequence, and select the n^{th} smallest value as representing this capability at any point in time.

In the following figures, we summarize results from tuning of the stations that we have selected for our network processing. Additional details on the tuning parameters and on the considerations involved for the various stations are presented in Appendix 6.2.1.

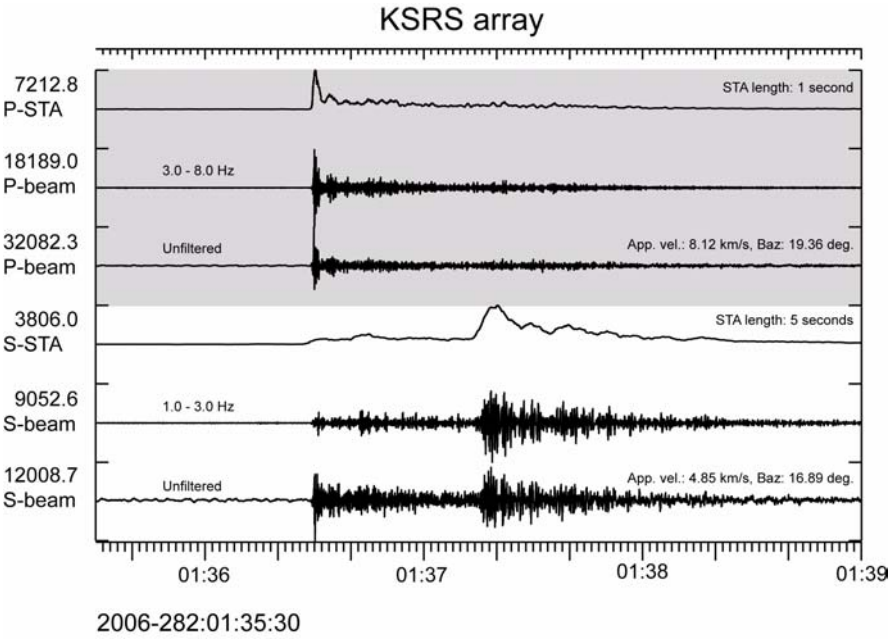

Fig. 6.2.4. The upper trace shows the short-term-average (STA) of the optimally filtered (3-8 Hz) P-beam at the KSRS array for the North-Korean underground nuclear test of 9 October 2006 (NK event). The filtered and unfiltered P-beams are shown in traces nos. 2 and 3. Trace no. 4 shows the short-term-average (STA) of the optimally filtered S-beam (1-3 Hz) for the same event. The filtered and unfiltered S-beams are shown in traces nos. 5 and 6.

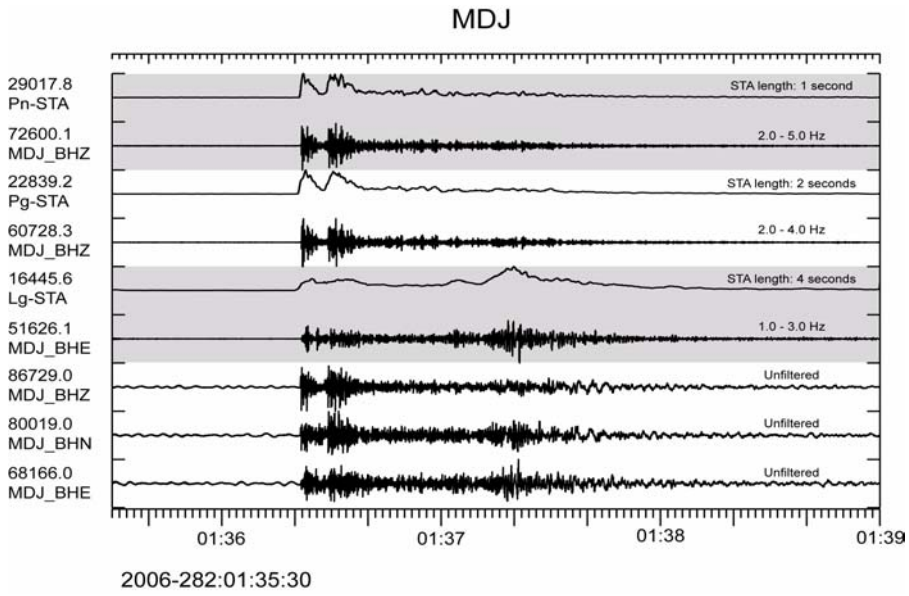

Fig. 6.2.5. The upper trace shows the short-term-average (STA) of the vertical component of station MDJ, filtered in the optimum frequency band for Pn (2-5 Hz) from the NK event. Trace no. 2 shows data filtered in the Pn band.
Trace no. 3 shows the short-term-average (STA) of the vertical component of station MDJ, filtered in the optimum frequency band for Pg (2-4 Hz). Trace no. 4 shows data filtered in the Pg band.
Trace no. 5 shows the short-term-average (STA) of the east-west component of station MDJ, filtered in the optimum frequency band for Lg (1-3 Hz). Trace no. 6 shows data filtered in the Lg band. The lower three traces show the MDJ unfiltered three-component recordings of the NK event.

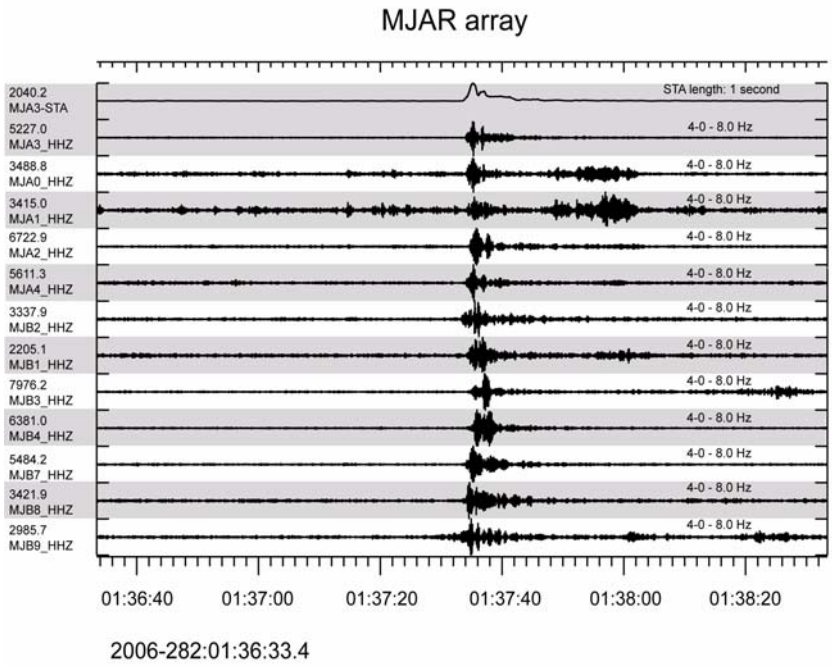

Fig. 6.2.6. The upper trace shows the short-term-average (STA) of the vertical component sensor MJA3 of the MJAR array, filtered in the optimum frequency band for the P phase (4-8 Hz) from the NK event. The traces below show all MJAR array sensors filtered in the 4-8 Hz band.
Due to the high frequencies and the low coherency between the array sensors, beamforming does not produce any SNR gain for this event. Consequently, data from the single sensor MJA3 will be used for threshold monitoring of the NK test site.

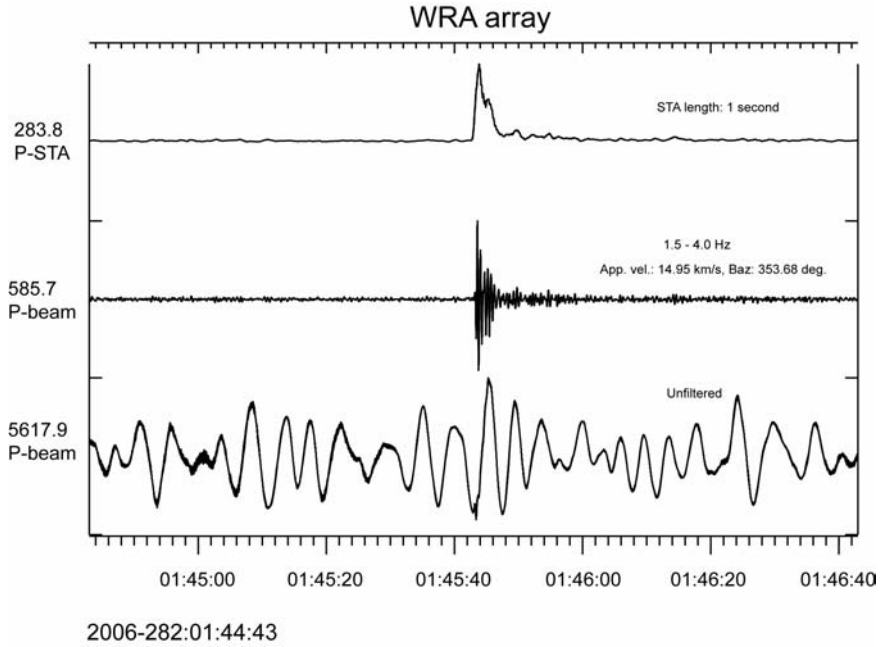

Fig. 6.2.7.The upper trace shows the short-term-average (STA) of the optimally filtered (1.5-4.0 Hz) P-beam at the WRA array for the North-Korean underground nuclear test of 9 October 2006 (NK event). The filtered and unfiltered P-beams are shown in traces nos. 2 and 3

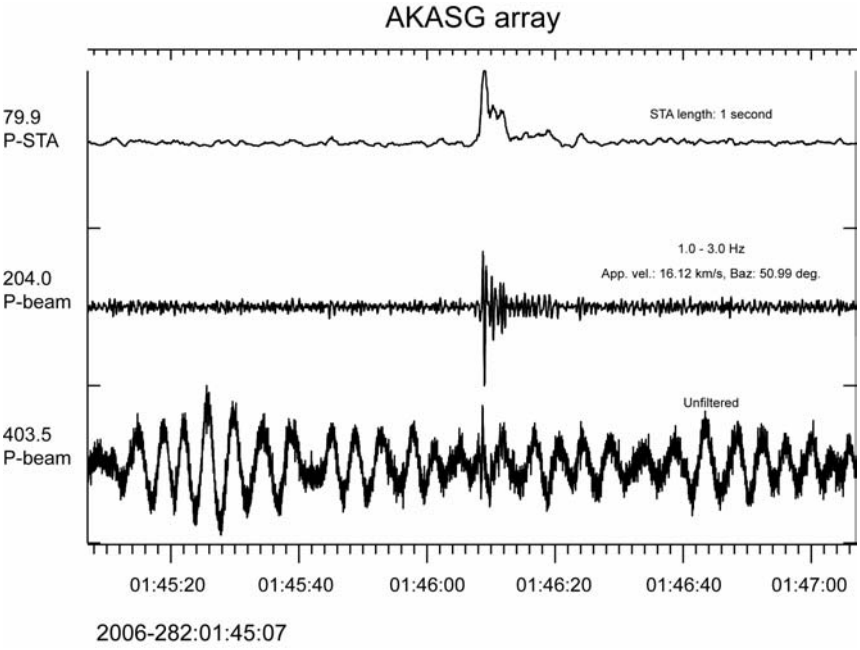

Fig. 6.2.8. The upper trace shows the short-term-average (STA) of the optimally filtered (2-4 Hz) P-beam at the AKASG array for the NK event. The filtered and unfiltered P-beams are shown in traces nos. 2 and 3.

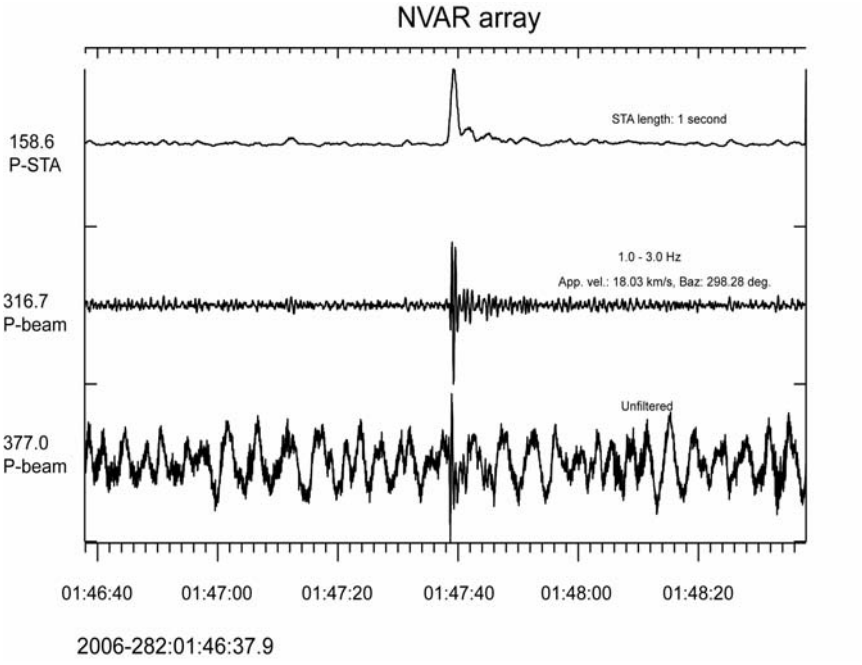

Fig. 6.2.9. The upper trace shows the short-term-average (STA) of the optimally filtered (1-3 Hz) P-beam at the NVAR array for the NK event. The filtered and unfiltered P-beams are shown in traces nos. 2 and 3.

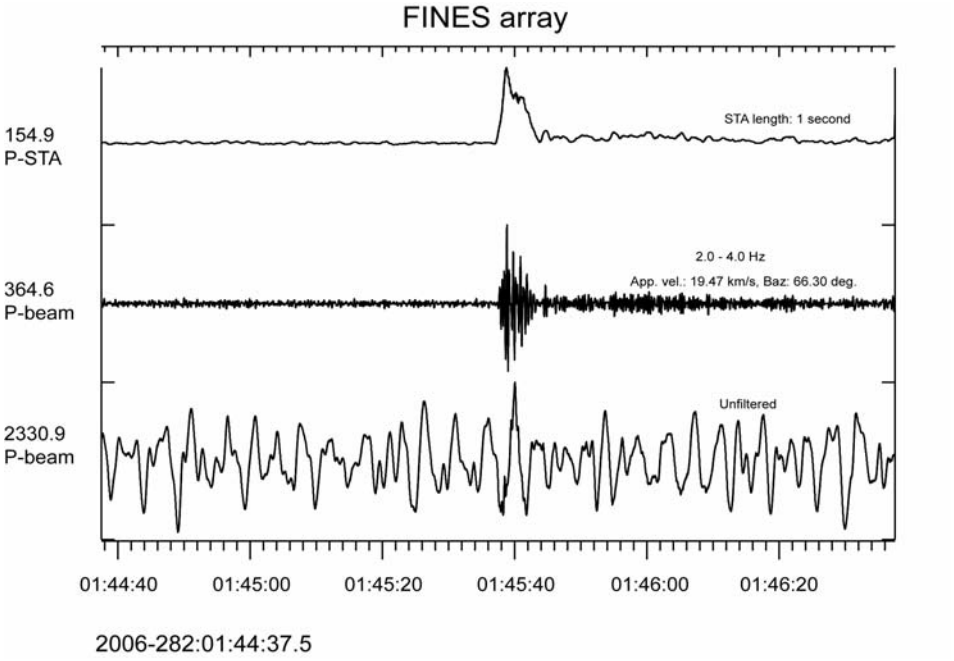

Fig. 6.2.10. The upper trace shows the short-term-average (STA) of the optimally filtered (2-4 Hz) P-beam at the FINES array for the NK event. The filtered and unfiltered P-beams are shown in traces nos. 2 and 3.

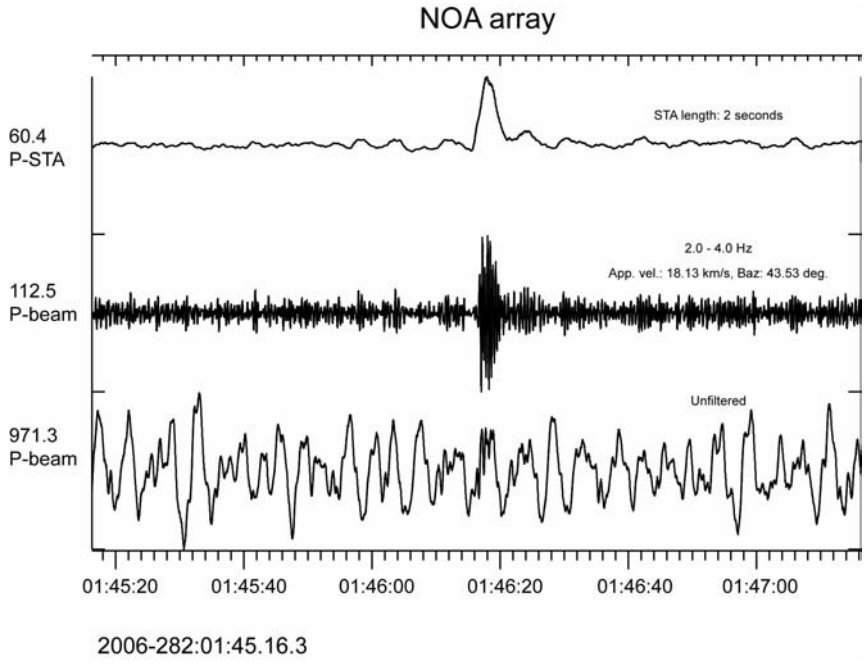

Fig. 6.2.11. The upper trace shows the short-term-average (STA) of the optimally filtered (2-4 Hz) P-beam at the NOA array for the NK event. The filtered and unfiltered P-beams are shown in traces nos. 2 and 3.

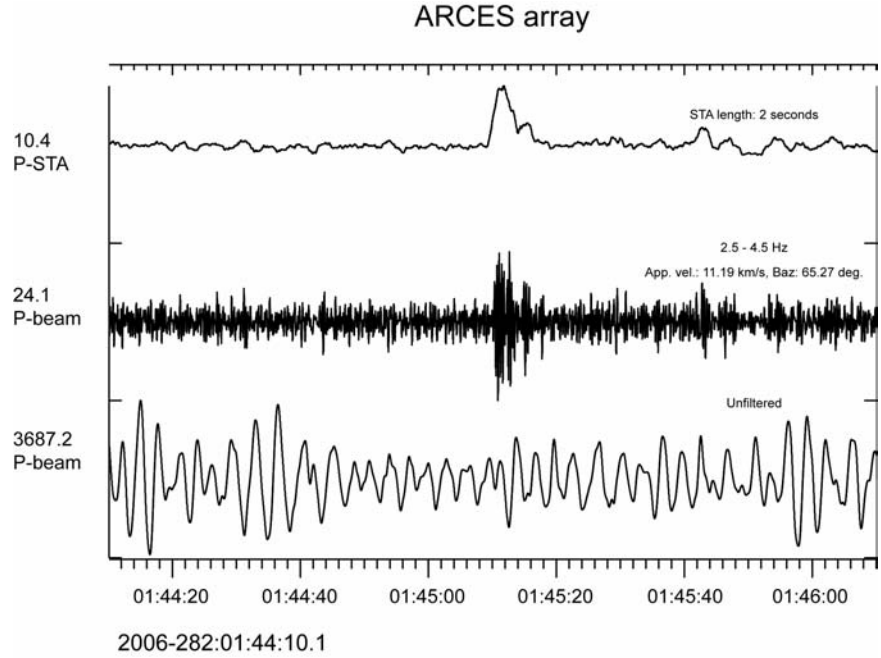

Fig. 6.2.12. The upper trace shows the short-term-average (STA) of the optimally filtered (2.5-4.5 Hz) P-beam at the ARCES array for the NK event. The filtered and unfiltered P-beams are shown in traces nos. 2 and 3.

6.2.6 Threshold processing results

We are now in a position to apply the network formulas to obtain the threshold processing results. We will show two different types of threshold traces for the North Korea nuclear test site:

- The *detection threshold traces*, which estimate, (at the 90% probability level) the smallest seismic event that can be detected by 3 or more stations in the network (SNR>4).
- The *monitoring threshold traces,* which estimate (at the 90% probability level) the largest seismic event that could possibly have occurred.

In each figure, the *detection threshold traces* are marked in red, the *monitoring threshold traces* are marked in blue.

Figure 6.2.13 shows the results for the day of the nuclear test (9 October 2006), using only those stations that were operational at the IDC during that day. We note that the detection threshold is typically around 4.0 or slightly below. At the time of the test, the detection threshold is around 3.75. The monitoring threshold averages about one magnitude unit lower than the detection threshold, i.e. close to magnitude 3.0.

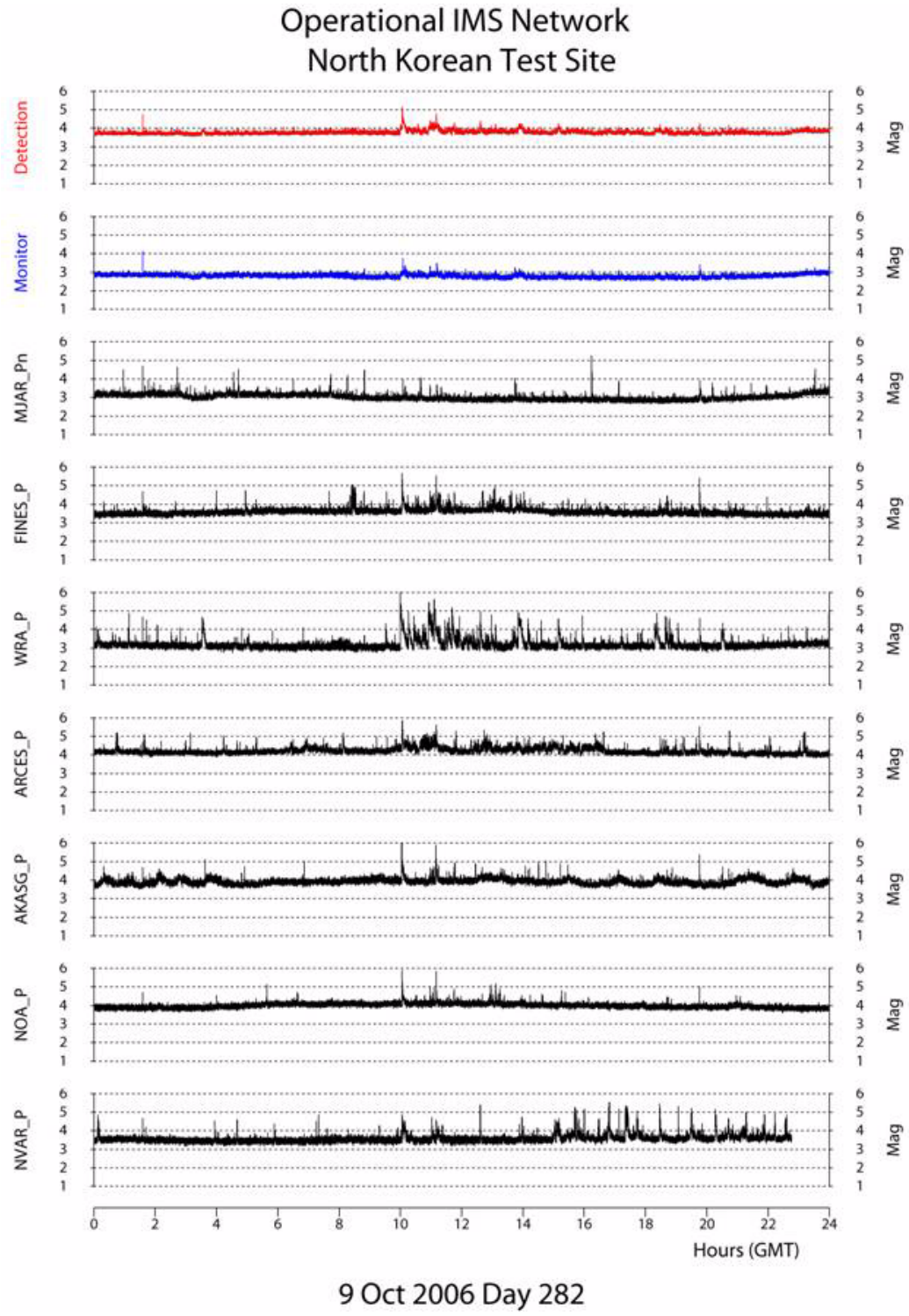

Fig. 6.2.13. Threshold monitoring results for the day of the nuclear test (9 October 2006). In this figure we have used only those of our selected stations that were operational at the IDC during that day. Detection thresholds (red) are close to magnitude 4.0 or slightly below, except for occasional increases during the nuclear test (at 01.35) and during some interfering events later in the day. The monitoring thresholds (blue) average about magnitude 3.0. The individual station P-thresholds (black) are also shown.

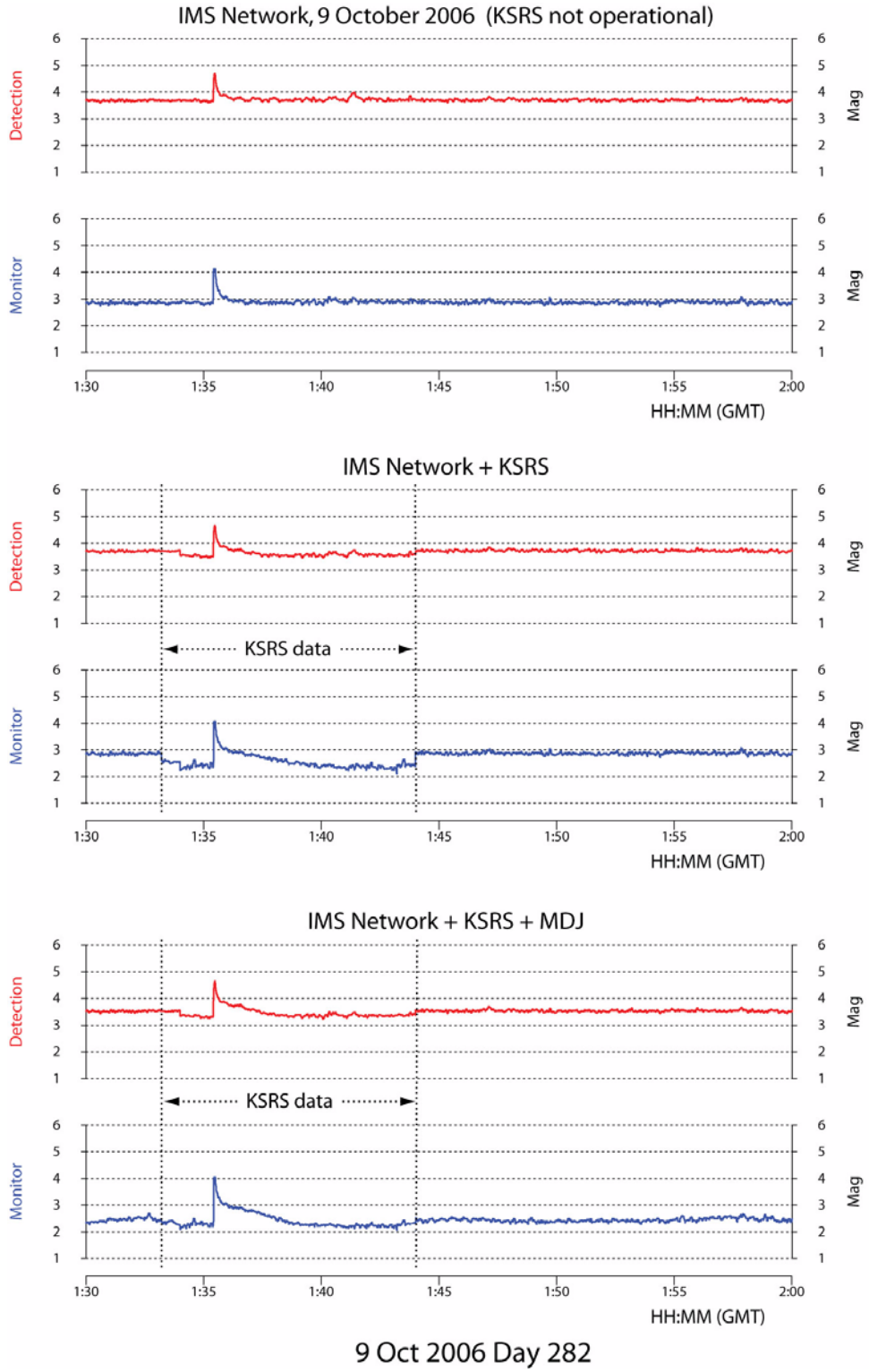

Fig. 6.2.14. Threshold monitoring results for a 30 minute period around the time of the nuclear test on 9 October 2006. The figure illustrate the effect of successively adding KSRS (middle panel) and MDJ (bottom panel) to the network which was operational during that day (top panel). We have only 10 minutes of KSRS data for this day. The monitoring thresholds (blue) decrease from magnitude 3.0 to close to magnitude 2.0. The detection thresholds (red) also decrease, but not as much as the monitoring thresholds.

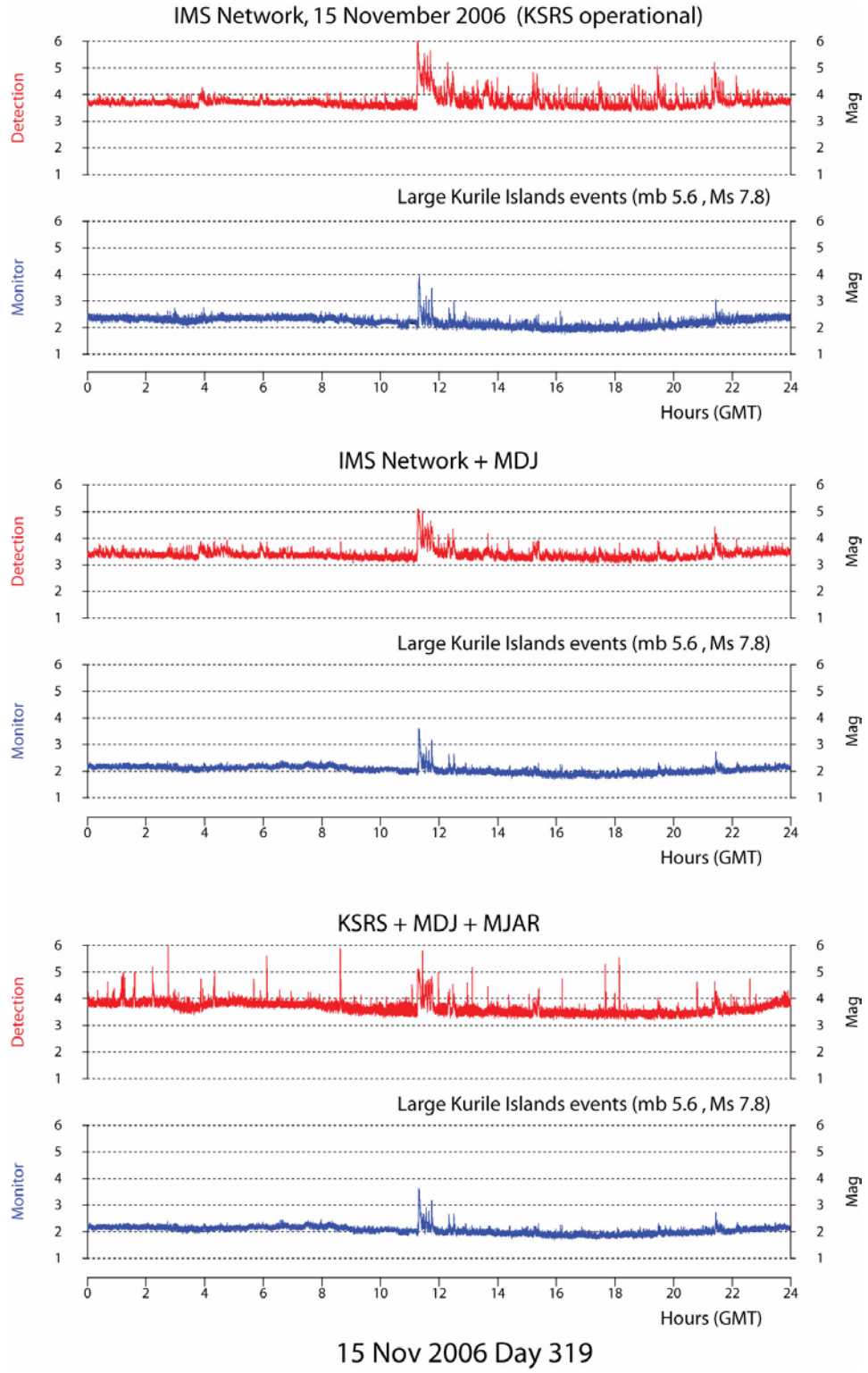

Fig. 6.2.15. This figure shows a one-day plot of detection traces (red) and monitoring traces (blue) for 15 November 2006. By that time, the KSRS array was operational in the IDC, and we also extracted a full day's data from the MDJ station in China. The top panel uses the IMS network (including KSRS); the middle panel shows the effect of adding the MDJ station and the bottom panel shows results from using only the three stations KSRS, MDJ and MJAR.

Figure 6.2.15 shows a one-day plot of detection traces (red) and monitoring traces (blue) for 15 November 2006. By that time, the KSRS array was operational in the IDC, and we also extracted a full day's data from the MDJ station in China. The top panel uses the IMS network (including KSRS); the middle panel shows the effect of adding the MDJ station and the bottom panel shows results from using only the three stations KSRS, MDJ and MJAR.

Figure 6.2.14 shows three threshold plots for a 30 minute interval including the time of the nuclear test. Each plot corresponds to a different station configuration. The top plot uses the IMS network as it was in operation during 9 October 2006. The middle plot shows the traces after adding data from KSRS (note that only about 10 minutes of data for this station was available to us). The bottom plot shows the results when also adding the MDJ station. We note that the monitoring thresholds (blue) decrease significantly as these sensitive stations are added. The detection thresholds (red) also decrease, but not as much as the monitoring thresholds.This illustrates one of the differences between using threshold monitoring and using the conventional 3-station requirement for estimating detection capability: The inclusion of one or two extremely sensitive stations at regional distances (with both P and S phases available) will obviously greatly improve the network detection capability. However, this may not necessarily be reflected in a significantly improved 3-station capability, since it is the P-wave at the 3rd best station that generally determines this capability.

Our final examples (Figure 6.2.15) show data for a full day (15 November 2006), during which a large earthquake in the Kurile Islands occurred. We note that from the end of October 2006, the KSRS array was operationally available, and we therefore have data for the entire day also for that array. We can make the following observations:

- The operational IMS network (now with KSRS available) shown in red on the top panel has a detection threshold of about magnitude 3.8, which is almost unchanged from the threshold observed in Figure 6.2.13 when KSRS was not available.
- In contrast, the monitoring trace (blue) on the top panel is lower by more than half a magnitude unit compared with the corresponding trace in Figure 6.2.13 where KSRS was not available.
- When adding MDJ to the IMS network (middle panel) we obtain a modest decrease (to about 3.5) for the detection trace (red), whereas the monitoring trace (blue) is now as low as 2.0 on the average. (Here we assume that detection processing is carried out for MDJ)

Finally Figure 6.2.15 gives an indication of how a regional network, comprising only the best stations, would perform compared with to a global network. This is illustrated in the bottom panel of the figure, which shows that using the network of MJAR, KSRS and MDJ appears to perform just about as well as the "full" network. However, this does not mean that the remaining stations are unimportant. In fact, during interfering events these additional (teleseismic) stations may help lower the thresholds. This is particularly evident for the detection traces (red). Also, if one of these three stations should have abnormally high noise conditions, or (worse) being out of operation, it is important to have additional stations that can contribute to reducing the resulting decline in capabilities.

6.2.7 Discussion

As shown in this paper, the "detection capability" of a global seismic network can be viewed from a number of different angles. The traditional global 3-station capability maps provide thresholds that are (for obvious reasons) considerably higher than those calculated by the site-specific threshold monitoring.

We note that both types of detection capability estimation are very valuable. The benefits of the traditional approach are well known, and will not be repeated here. The main benefit of the threshold monitoring approach is that (in practice) it is more representative of what can be detected in a situation where all the available resources are applied.

For example, the capability to monitor the Novaya Zemlya test site has been documented in a number of NORSAR Semiannual Technical Summaries. It has been demonstrated that in practice the Fennoscandian network is able to monitor the Novaya Zemlya test site down to magnitudes 2.0-2.5, while the corresponding level for 3-station detection using the global capability map is between 3.5 and 4.0 during normal noise conditions. Part of this large difference is due to the sensitive SPITS array not being a primary IMS station (and therefore not included in the detection process), but the main point is that the threshold monitoring approach gives a truer picture than the detection threshold approach as far as the real capability is concerned.

We see the same situation in the study of the North Korea test site. The inclusion of the two sensitive stations KSRS and MDJ clearly lead to a vast improvement in capability, and this is duly reflected in the threshold monitoring estimates, but not in the 3-station detection estimate.

We note, however, that if the threshold monitoring maps are to be compared with standard detection capability maps, it is necessary to introduce a threshold to make the comparison meaningful. Thus, if the threshold monitoring indicates a level of 2.0, it would be prudent to add e.g. 0.5 magnitude units to obtain a capability map for detecting events at the site.

It is also important to be aware that the main purpose of the threshold monitoring method is to call attention to any time instance when a given threshold is exceeded. This will enable the analyst to focus efforts on those events that are truly of interest in a monitoring situation. The analyst will then apply other, traditional analysis tools in detecting, locating and characterizing the source of the disturbance. Thus, the threshold monitoring method is a supplement to, and not a replacement of, traditional methods.

We finally provide some comments on the estimated monitoring capabilities for the North Korea test site in terms of explosion yields. According to the formulas (1) and (2) a magnitude of 2.0 would correspond to about 1 ton of explosives. Even taking into account the uncertainties involved when extrapolating over several orders of magnitude, and the need to add a detection threshold, it is clear that an explosion of several tons (fully coupled) would be unlikely to be missed by the available monitoring network. We note, however, that we do not know whether there are significant decoupling possibilities in the test site area, and any yield thresholds must therefore be treated with caution.

Tormod Kværna
Frode Ringdal
Ulf Baadshaug

Acknowledgement

We are grateful to Dr. Heon Cheol Chi of Korea Institute of Geoscience and Mineral Resources (KIGAM) for providing us with data from the KSRS seismic array.

This paper is a summary of a quarterly report previously submitted to USASMDC under contract W9113M-05-C-0224.

References

Hannon, W. (1985): Seismic verification of a comprehensive test ban, *Science*, 227, 251-257.

Harjes. H.-P. (1985): Global seismic network assessment for teleseismic detection of underground nuclear explosions, *J. Geophys., 57, 1-13.*

Kværna, T. and F. Ringdal (1999): Seismic Threshold Monitoring for Continuous Assessment of Global Detection Capability, *Bull. Seism. Soc. Am*., 89, 946-959.

Lilwall, R.C. and P.D. Marshall (1986): Body wave magnitudes and locations of Soviet underground explosions at the Novaya Zemlya test site, *AWRE Rep. NO 017/86*, Blacknest, U.K.

National Academy of Sciences (2002): Technical issues related to the Comprehensive Nuclear-Test-Ban Treaty, ISBN 0-309-08506-3, National Academy Press, Washington, D.C.

Richards, P.G. and Won-Young Kim (2007): Seismic Signature, *Nature physics*, Vol3, January 2007.

Ringdal, F. (1986): Study of magnitudes, seismicity and earthquake detectability using a global network, *Bull. Seism. Soc. Am*., 76, 1641-1659.

Ringdal, F. and T. Kværna (1989): A multichannel processing approach to real time network detection, phase association and threshold monitoring, *Bull. Seism. Soc. Am*., 79, 1927-1940.

Ringdal, F. and T. Kværna (1992): Continuous seismic threshold monitoring, *Geophys. J. Int*., 111, 505-514.

Ringdal, F., P.D. Marshall and R.W. Alewine (1992): Seismic yield determination of Soviet underground nuclear explosions at the Shagan River test site *Geophys. J. Int*., 109, 65-77.

Sereno, T.J. and S.R. Bratt (1989): Seismic detection capability at NORESS and implications for the detection threshold of a hypothetical network in the Soviet Union, *J. Geophys. Res*., 94, 10397-10414.

Sykes, L. and J. Evernden (1982): The verification of a comprehensive nuclear test ban, *Sci. Am*., 247, 47-55.

Appendix 6.2.1

Station Processing Parameters for Site-Specific Threshold Monitoring of the North Korean Nuclear Test Site

The tables of this appendix include the details about the site-specific threshold monitoring processing parameters obtained for the different stations.

1. KSRS, South Korea

Channel Name	Latitude	Longitude	Distance to NK	Baz to NK
KS01	37.4766 N	127.8940 E	3.928 deg 436.68 km	12.468 deg.

Phase	Arr.-time (th)	Tr.-time (th)	Slow. (th)	Slow. (obs)	Baz (obs)	R. pwr
Pn	01.36.29.12	61.52 s	13.75 s/deg. 8.09 km/s	8.12 km/s	19.36 deg.	0.23
Sn	01.37.15.90	108.30 s	24.67 s/deg. 4.51 km/s	4.85 km/s	16.89 deg	0.42

Phase	Arr.time (STA_{max})	Tr.-time (STA_{max})	STA len. (s)	STA_{max}	Filter	Channels	Correction m_b - log(STA_{max})
Pn	01.36.29.23	61.63	1.0 s	7212.79	3.0-8.0 Hz	All Z	0.2419
Sn	01.37.20.19	112.59	5.0 s	3805.97	1.0-3.0 Hz	All Z	0.5195

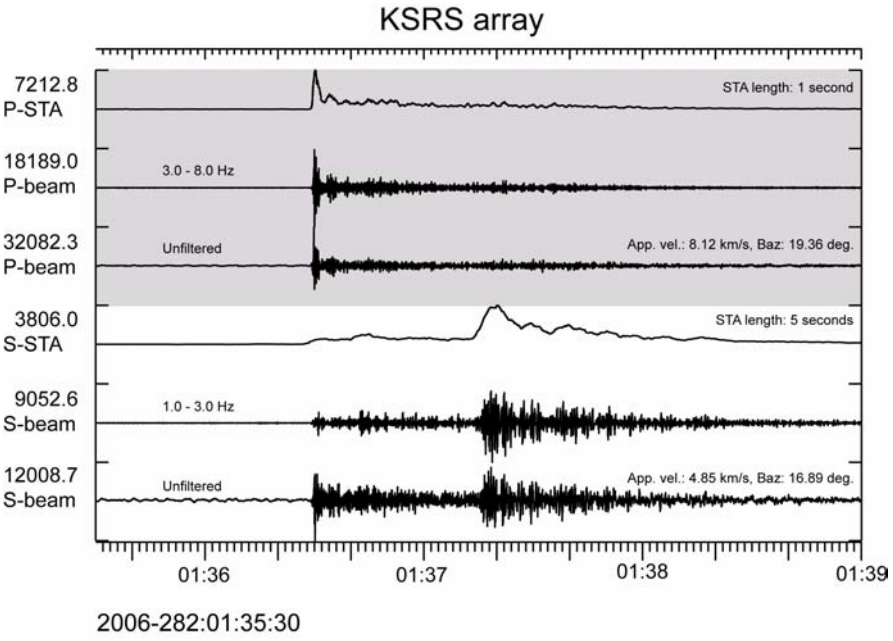

Fig. A6.2.1. The upper trace shows the short-term-average (STA) of the optimally filtered (3-8 Hz) P-beam at the KSRS array for the North-Korean underground nuclear test of 9 October 2006 (NK event). The filtered and unfiltered P-beams are shown in traces nos. 2 and 3. Trace no. 4 shows the short-term-average (STA) of the optimally filtered S-beam (1-3 Hz) for the same event. The filtered and unfiltered S-beams are shown in traces nos. 5 and 6.

2. MDJ (Mudajiang), China

Channel Name	Latitude	Longitude	Distance to NK	Baz to NK
MDJ	44.616 N	129.592 E	3.329 deg 370.06 km	187.454 deg.

Phase	Arr.-time (th)	Tr.-time (th)	Slow. (th)	Slow. (obs)	Baz (obs)	R. pwr
Pn	01.36.20.89	53.29 s	13.75 s/deg. 8.09 km/s	-	-	-
Pg	01.36.31.40	63.80 s	19.16 s/deg. 5.80 km/s	-	-	-
Sn	01.37.01.13	93.53 s	24.67 s/deg. 4.51 km/s	-	-	-
Lg	01.37.14.55	106.95	32.12 s/deg 3.46 km/s	-	-	-

Phase	Arr.time (STA_{max})	Tr.-time (STA_{max})	STA len. (s)	STA_{max}	Filter	Channels	Correction m_b - log(STA_{max})
Pn	01.36.22.35	54.75	1.0 s	29017.82	2.0-5.0 Hz	MDJ_BHZ	-0.3627
Pg	01.36.30.50	62.90	2.0 s	21546.42	2.0-4.0 Hz	MDJ_BHZ	-0.2334
Lg	01.37.19.91	112.31	4.0 s	16445.57	1.0-3.0 Hz	MDJ_BHE	-0.1160

Only the phases Pn and Lg are used in the threshold monitoring calculations.

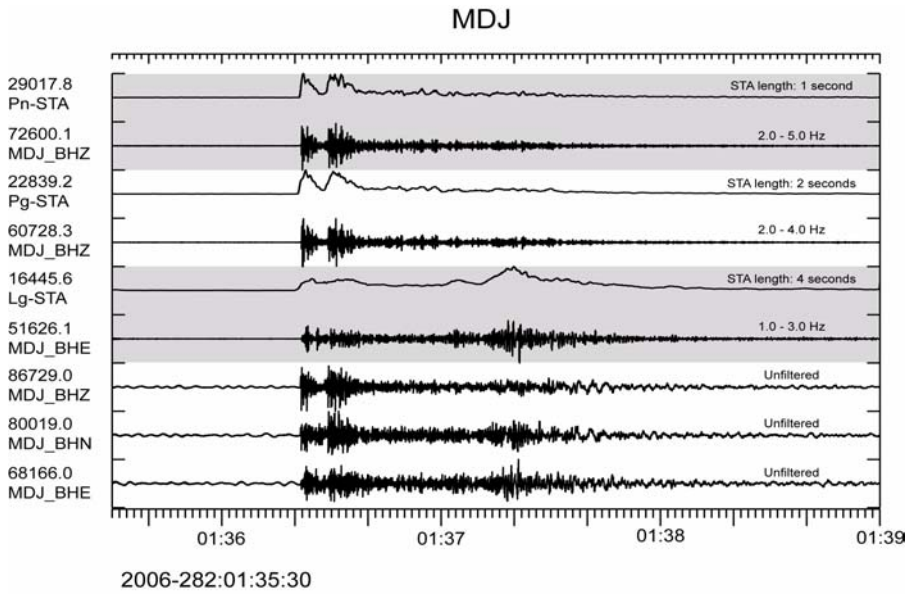

Fig. A6.2.2. The upper trace shows the short-term-average (STA) of the vertical component of station MDJ, filtered in the optimum frequency band for Pn (2-5 Hz) from the NK event. Trace no. 2 shows data filtered in the Pn band.
Trace no. 3 shows the short-term-average (STA) of the vertical component of station MDJ, filtered in the optimum frequency band for Pg (2-4 Hz). Trace no. 4 shows data filtered in the Pg band.
Trace no. 5 shows the short-term-average (STA) of the east-west component of station MDJ, filtered in the optimum frequency band for Lg (1-3 Hz). Trace no. 6 shows data filtered in the Lg band. The lower three traces show the MDJ unfiltered three-component recordings of the NK event.

3. MJAR, Japan

Channel Name	Latitude	Longitude	Distance to NK	Baz to NK
MJA3	36.4956 N	138.2467 E	8.651 deg 961.73 km	306.569 deg.

Phase	Arr.-time (th)	Tr.-time (th)	Slow. (th)	Slow. (obs)	Baz (obs)	R. pwr
Pn	01.37.33.98	126.38	13.72 s/deg. 8.10 km/s	-	.-	-

Phase	Arr.time (STA_{max})	Tr.-time (STA_{max})	STA len. (s)	STA_{max}	Filter	Channels	Correction m_b - log(STA_{max})
Pn	01.37.35.23	127.55	1.0 s	2040.19	4.0-8.0Hz	MJA3	0.7901

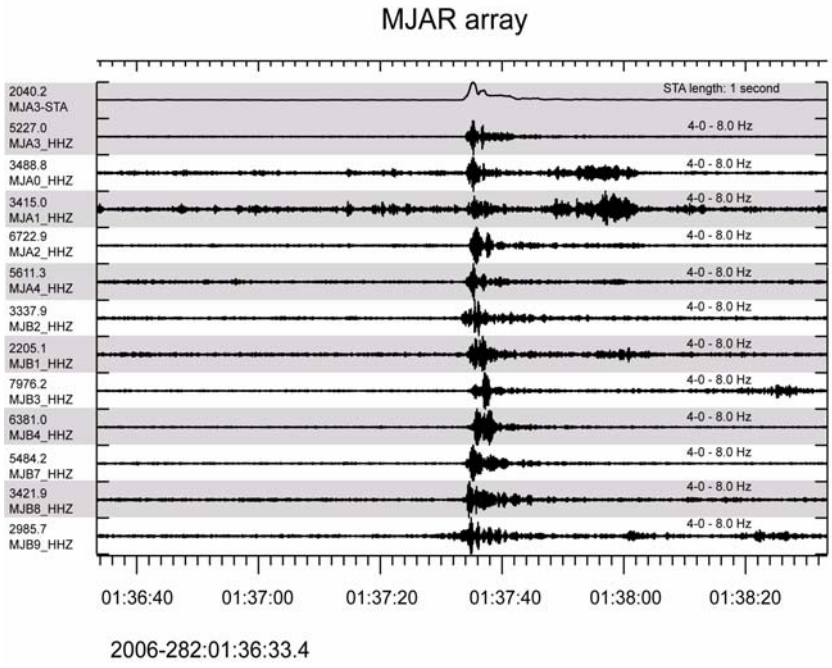

Fig. A6.2.3. The upper trace shows the short-term-average (STA) of the vertical component sensor MJA3 of the MJAR array, filtered in the optimum frequency band for the P phase (4-8 Hz) from the NK event. The traces below show all MJAR array sensors filtered in the 4-8 Hz band.
Due to the high frequencies and the low coherency between the array sensors, beamforming does not produce any SNR gain for this event. Consequently, data from the single sensor MJA3 is used for threshold monitoring of the NK test site.

4. WRA, Australia

Channel Name	Latitude	Longitude	Distance to NK	Baz to NK
MJA3	19.9426 S	134.3395 E	61.141 deg 6803.41 km	355.425 deg.

Phase	Arr.-time (th)	Tr.-time (th)	Slow. (th)	Slow. (obs)	Baz (obs)	R. pwr
P	01.45.43.67	616.07	6.78 s/deg. 16.40 km/s	14.94 km/s-	353.19 deg.	0.694

Phase	Arr.time (STA_{max})	Tr.-time (STA_{max})	STA len. (s)	STA_{max}	Filter	Channels	Correction m_b - log(STA_{max})
P	01.45.43.88	616.28	1.0 s	283.81	1.5-4.0Hz	All BHZ	1.6470

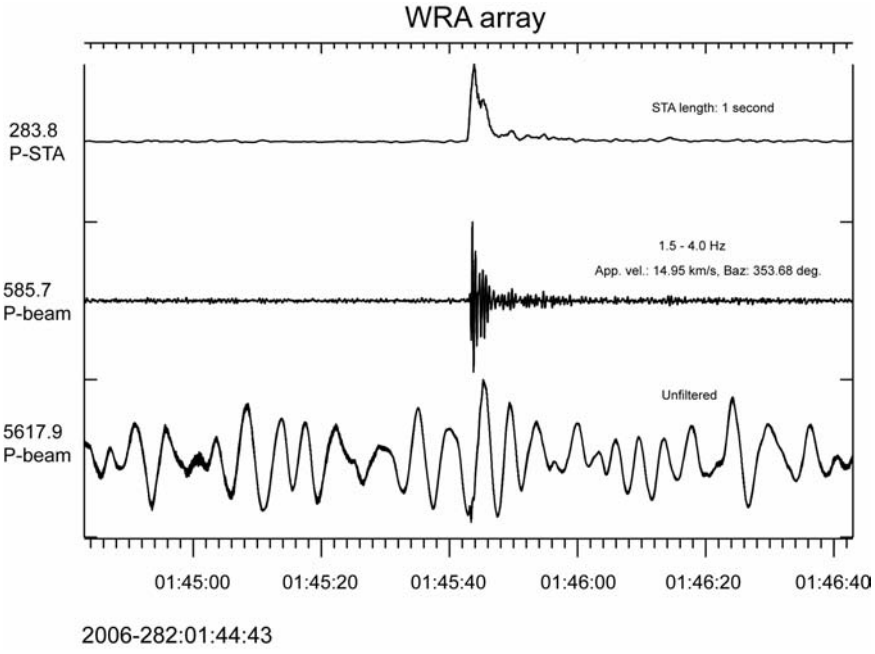

Fig. A6.2.4. The upper trace shows the short-term-average (STA) of the optimally filterted (1.5-4.0 Hz) P-beam at the WRA array for the North Korean underground nuclear test of 9 October 2006 (NK event). The filtered and unfiltered P-beams are shown in traces nos. 2 and 3.

5. AKASG, Ukraine

Channel Name	Latitude	Longitude	Distance to NK	**Baz to NK**
AK02	50.6573 N	29.2057 E	64.817 deg 7199.76 km	55.111 deg.

Phase	Arr.-time (th)	Tr.-time (th)	Slow. (th)	Slow. (obs)	Baz (obs)	R. pwr
P	01.46.07.91	640.31	6.52 s/deg. 17.05 km/s	16.12 km/s-	50.99 deg.	0.618

Phase	Arr.time (STA_{max})	Tr.-time (STA_{max})	STA len. (s)	STA_{max}	Filter	Channels	Correction m_b - log(STA_{max})
P	01.46.09.01	641.41	1.0 s	79.91	1.0-3.0Hz	All BHZ Not AK01	2.1974

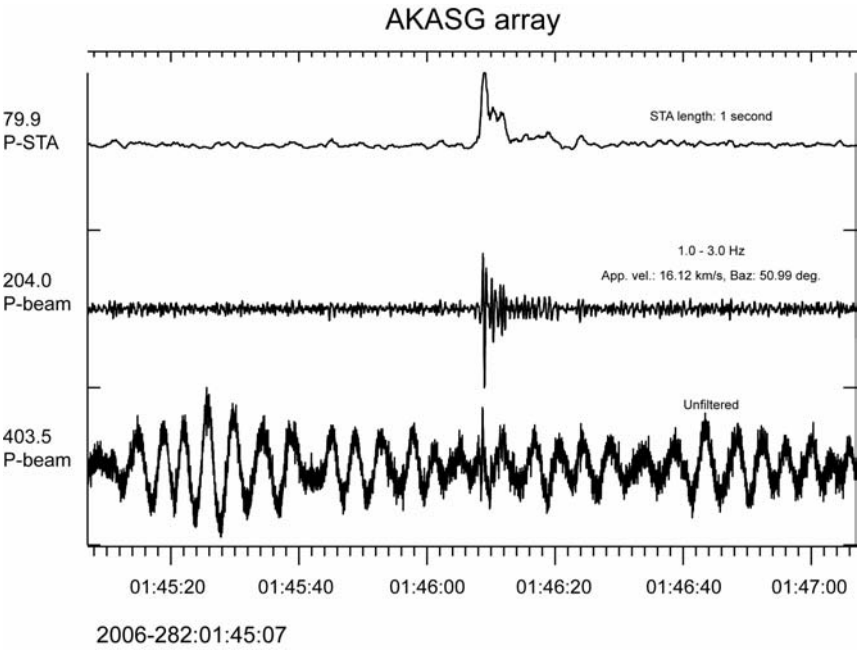

Fig. A6.2.5. The upper trace shows the short-term-average (STA) of the optimally filtered (2-4 Hz) P-beam at the AKASG array for the NK event. The filtered and unfiltered P-beams are shown in traces nos. 2 and 3.

6. NVAR, USA

Channel Name	Latitude	Longitude	Distance to NK	Baz to NK
NV01	38.4296 N	118.3036 W	79.690 deg 8853.49 km	315.050 deg.

Phase	Arr.-time (th)	Tr.-time (th)	Slow. (th)	Slow. (obs)	Baz (obs)	R. pwr
P	01.47.37.06	729.461	5.43s/deg. 20.48 km/s	18.03 km/s-	298.28 deg.	0.838

Phase	Arr.time (STA_{max})	Tr.-time (STA_{max})	STA len. (s)	STA_{max}	Filter	Channels	Correction m_b - log(STA_{max})
P	01.47.39.24	731.64	1.0 s	158.56	1.0-3.0Hz	All SHZ Not NV03 NV04 NV11	1.8998

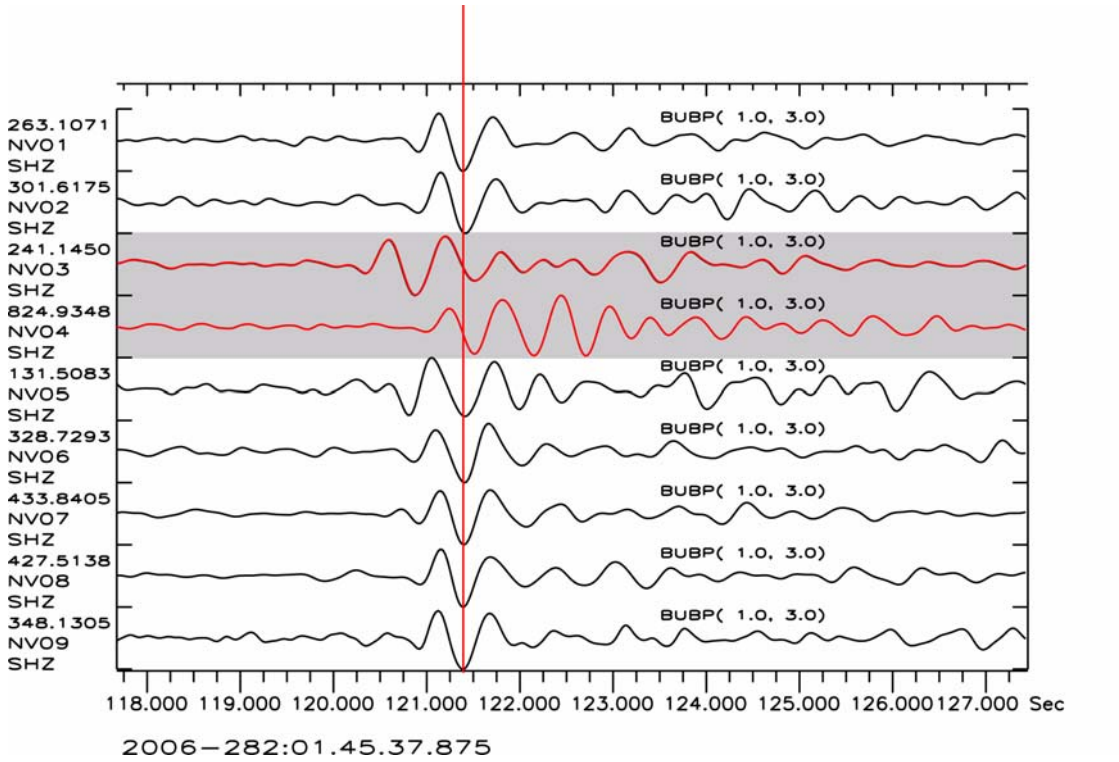

Fig. A6.2.6. Illustration of timing problems discovered at the NVAR array for the P-phase from the North Korean nuclear test. The signals at the different array sensors are aligned according to the estimated back-azimuth and slowness of the incoming phase, but without including the assumed erroneous channels NV03 and NV04 in the estimation. These channels are consequently not included in processing.

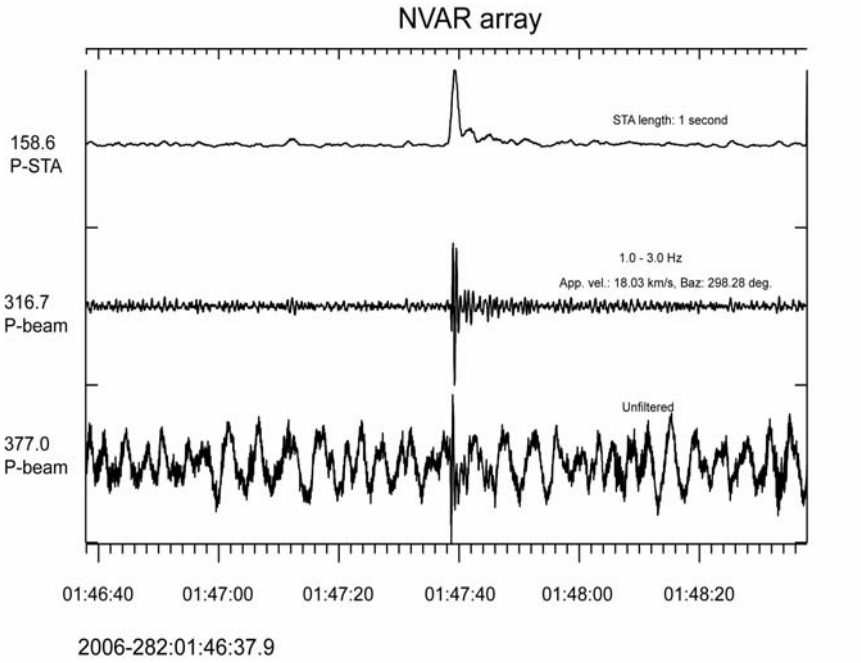

Fig. A6.2.6. T
he upper trace shows the short-term-average (STA) of the optimally filtered (1-3 Hz) P-beam at the NVAR array for the NK event. The filtered and unfiltered P-beams are shown in traces nos. 2 and 3.

7. FINES, Finland

Channel Name	Latitude	Longitude	Distance to NK	Baz to NK
FI01	61.4436 N	26.0771 E	60.285 deg 6694.58 km	57.709 deg.

Phase	Arr.-time (th)	Tr.-time (th)	Slow. (th)	Slow. (obs)	Baz (obs)	R. pwr
P	01.45.37.45	609.85	6.85s/deg. 16.23 km/s	19.47 km/s-	66.30 deg.	0.858

Phase	Arr.time (STA_{max})	Tr.-time (STA_{max})	STA len. (s)	STA_{max}	Filter	Channels	Correction m_b - log(STA_{max})
P	01.45.38.79	611.19	1.0 s	154.91	2.0-4.0 Hz	All sz	1.9099

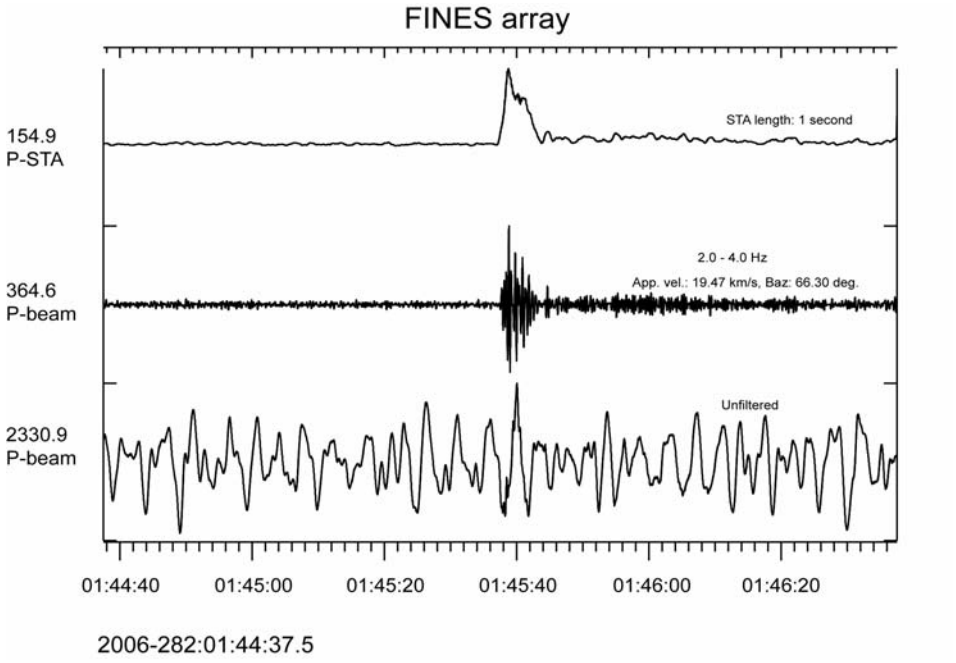

Fig. A6.2.7. The upper trace shows the short-term-average (STA) of the optimally filtered (2-4 Hz) P-beam at the FINES array for the NK event. The filtered and unfiltered P-beams are shown in traces nos. 2 and 3.

8. NOA, Norway

Channel Name	Latitude	Longitude	Distance to NK	Baz to NK
NB200	61.0397 N	11.2148 E	66.204 deg 7351.14 km	46.741 deg.

Phase	Arr.-time (th)	Tr.-time (th)	Slow. (th)	Slow. (obs)	Baz (obs)	R. pwr
P	01.46.16.70	649.10	6.42s/deg. 17.32 km/s	18.13 km/s corr NOA	43.53 deg. corr NOA	-

Phase	Arr.time (STA_{max})	Tr.-time (STA_{max})	STA len. (s)	STA_{max}	Filter	Channels	Correction m_b - log(STA_{max})
P	01.46.17.97	650.37	2.0 s	60.40	2.0-4.0 Hz	All sz	2.3190

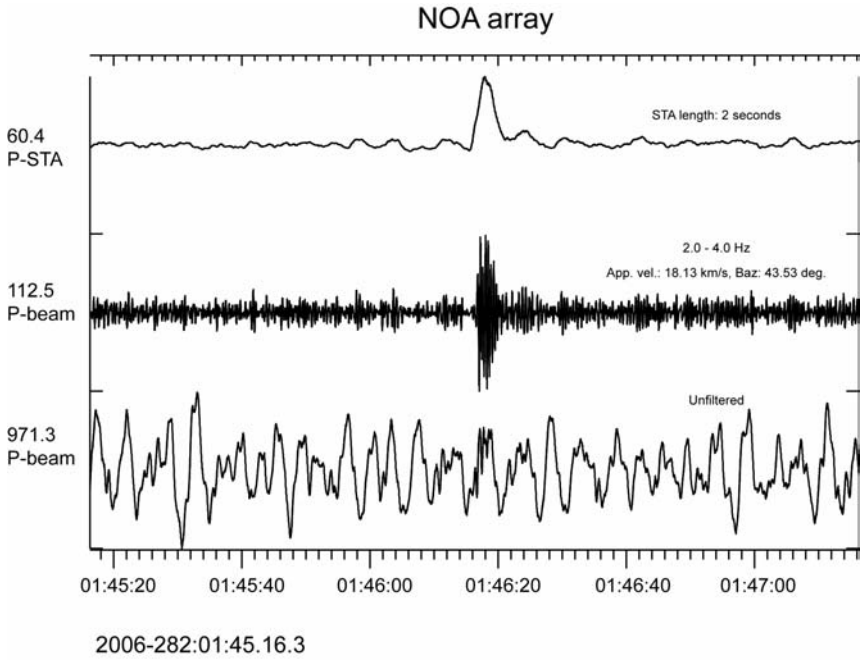

*Fig. A6.2.8. **T**he upper trace shows the short-term-average (STA) of the optimally filtered (2-4 Hz) P-beam at the NOA array for the NK event. The filtered and unfiltered P-beams are shown in traces nos. 2 and 3.*

9. ARCES, Norway

Channel Name	Latitude	Longitude	Distance to NK	Baz to NK
ARA0	69.5349 N	25.5058 E	56.377 deg 6259.74 km	61.598 deg.

Phase	Arr.-time (th)	Tr.-time (th)	Slow. (th)	Slow. (obs)	Baz (obs)	R. pwr
P	01.45.10.04	582.44	7.13s/deg. 15.59 km/s	11.19 km/s	65.27 deg.	0.53

Phase	Arr.time (STA_{max})	Tr.-time (STA_{max})	STA len. (s)	STA_{max}	Filter	Channels	Correction m_b - log(STA_{max})
P	01.45:11.77	584.17	2.0 s	10.40	2.5-4.5 Hz	ARA0 C-ring D-ring	3.0830

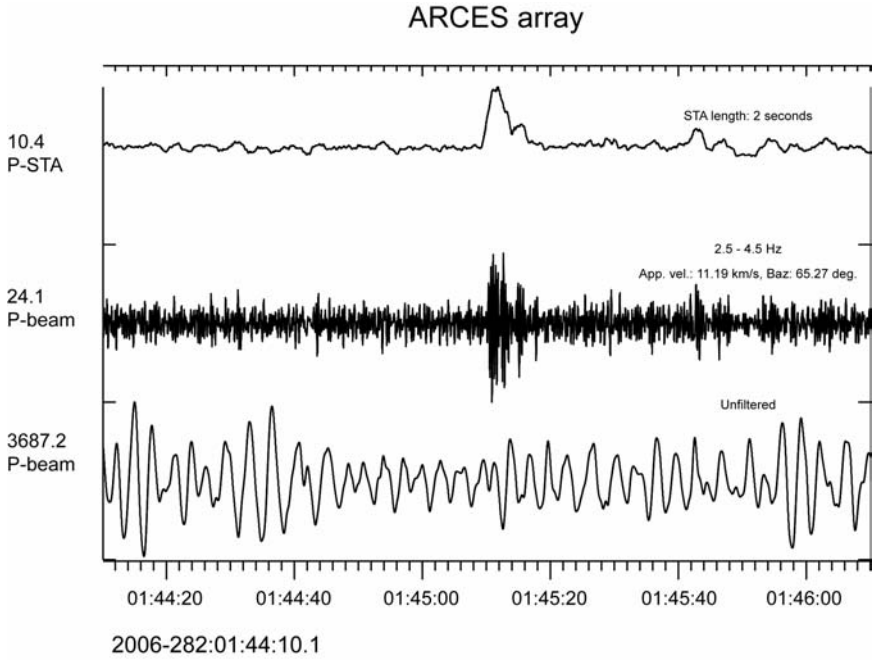

Fig. A6.2.9. The upper trace shows the short-term-average (STA) of the optimally filtered (2.5-4.5 Hz) P-beam at the ARCES array for the NK event. The filtered and unfiltered P-beams are shown in traces nos. 2 and 3.

6.3 A Case Study of Seismic Event Identification: Explosions in NW Russia using the ARCES seismic array

6.3.1 Introduction

There are many instances in which a full overview of seismic events from a given source region is required. In many cases of industrial seismic sources, such as mines and quarries, this may be solely for the purpose of event screening such that successive events from the same site may be associated confidently with the correct source. A description of an algorithm applying traditional regional array processing methods for identifying quarry blasts at regional distances from the ARCES array is provided by Gibbons et al. (2005). This method was extremely effective for blasts at the open-cast Kovdor mine in NW Russia. The events were characterized by very consistent slowness and azimuth measurements for the first Pn-phase arrivals, and events could be identified quite reliably by assessing the slowness and SNR in fixed time-windows following this initial arrival. The success of this case study was largely due to the high SNR of the initial arrival and the repeatability of f-k slowness vector measurements in calibrated fixed-frequency bands. Weaker events will result in a lower SNR which may lead to far poorer slowness estimates in short time-windows and subsequently limit the application of such algorithms.

Waveform correlation methods can be highly successful at identifying seismic sources (e.g. Harris, 1991) and, often matching the entire signal as opposed to a single transient phase arrival, can lower significantly the detection threshold for events from specific sources (e.g. Gibbons and Ringdal, 2006, and references therein). In recent years, several different case studies have demonstrated the advantages of applying waveform correlation to the detection of low-magnitude events. Gibbons and Ringdal (2004), Stevens et al. (2006) demonstrate how signals from cavity-decoupled chemical explosions buried deep in the background seismic noise could be detected with essentially a zero false-alarm rate by correlating against the signals from larger co-located (or almost co-located) explosions. Gibbons and Ringdal (2005) used correlation of SPITS array data to detect small mining-induced events at the Barentsburg mine at a distance of approximately 50 km. Gibbons et al. (2007) used the signals from a magnitude 3.5 earthquake in the Rana region of northern Norway to detect aftershocks and almost co-located earthquakes down to magnitude 0.5 at distances of over 600 km using the Nordic IMS array stations. An important characteristic common to each of these case studies, despite the different source mechanisms, is the similarity of waveforms from one event to the next.

Significant variation between the waveforms from event to event poses a significant difficulty for matched-filter detectors as described by Gibbons and Ringdal (2006). A case of interesting seismic events is described by Ringdal and Schweitzer (2005). The events are located close to the northern coast of the Kola Peninsula in Russia. The coordinates of the site are not known and events are only located to within the uncertainties of the location estimates obtained with the arrays in the region (c.f. Figure 12 of Ringdal and Schweitzer, 2005). The explosions were brought to the attention of researchers at NORSAR by residents of the Varanger region on the northern coast of Norway who felt and heard the events over a large geographical area. They have been of interest due to the generation of infrasound signals recorded both on the microbarograph mini-array at Apatity and on the ARCES seismic array. At the time, only 6 events had been identified and waveforms from these events, recorded at ARCES, are displayed in Figure 6.3.1.

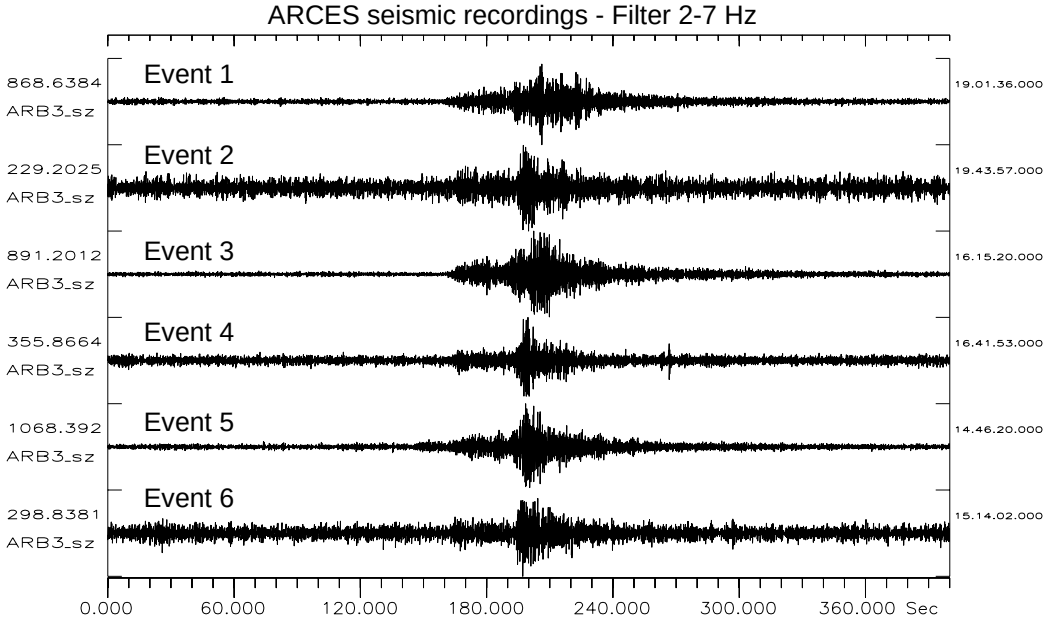

Fig. 6.3.1. Waveforms on a single sensor of the ARCES array for the six NW Russia events identified by Ringdal and Schweitzer (2005). Figure reproduced from Ringdal and Schweitzer (2005).

The six different signals in Figure 6.3.1 bear very little resemblance to each other and the lack of waveform similarity is confirmed by a calculation of correlation coefficients. The waveform dissimilarity is observed in a wide range of frequency bands and it is therefore assumed that (even if the events are closely located geographically) source-time histories are significantly different. How do we best proceed to identify other events related to this source? Using the fully-automatic GBF lists (Ringdal and Kværna, 1989) is not an option since the automatic location estimates for the (many hundreds of) events from the Zapoljarni ore mines (approximately 50 km from the assumed source location) cover an area of many thousands of square kilometers which encompass the region needing to be covered here (see Kværna et al., 2006). Is it possible to use full-waveform methods which take essentially all events from this site with an acceptable false-alarm rate?

6.3.2 A multi-channel correlation detector for the ARCES array

All of the events in Figure 6.3.1 appear to have either a low SNR or a waveform suggesting a complicated source-time function. It was judged that event number 5 appeared to have the best combination of a relatively simple waveform envelope and a reasonable SNR (bearing in mind that a large coda-amplitude is more helpful for correlation detectors than an impulsive initial arrival and a high STA:LTA value). The event is assumed to have an origin time of 2005-076:14.48.24.24 and coordinates 69.5508^{o} N, 31.8589^{o} E with zero depth. An empirical matched filter detector using a 60.0 second long template of ARCES array data, filtered between 3.0 and 8.0 Hz, was initiated and run over three years of continuous data.

The filtered and normalized waveform template was correlated against incoming waveform data segments with a length of approximately 10 minutes. Prior to the main run, the statistics of single-channel and array correlation coefficient traces were examined for different scenarios

(no identified signal, unrelated signal, signal from close to the target area - in this case the Zapoljarni mines in NW Russia, signal from exactly the target area) in a similar way to that displayed in Figure 3 of Gibbons et al. (2006). On the basis of these studies, it was determined that a preliminary detection should be declared whenever a value on the array correlation coefficient beam (ACCB) exceeded by a factor for 10.0 the standard deviation of the most centrally distributed 95% of the values of the ACCB. For every occasion on which a local maximum of the ACCB satisfied these conditions, the 2.5 seconds preceeding and following this detection were associated with the detection in an attempt to preclude the recording of local maxima within the auto-correlation function as detections. Every occurrence of a correlation detection was followed by an f-k measurement of the single-channel correlation coefficient traces as described by Gibbons and Ringdal (2006) with the slowness vector and the relative beam-gain being recorded.

Between January 1, 2002, and December 31, 2005, a total of 17485 detections were made based upon the value of the (scaled) array correlation coefficient beam[1] alone. This is clearly far more detections than is likely to correspond to the actual events being monitored (this is approximately 20 detections per day). Each detection is associated with four measurements:

1. Value of the array correlation coefficient beam (ACCB)
2. Multiple by which the ACCB exceeds the standard deviation of values within the time-segment being investigated
3. The slowness vector pertaining to the maximum beam-gain from the single-channel correlation coefficient traces (using broadband f-k analysis with the assumption of a plane-wave propagation model)
4. The relative f-k power or beam-gain corresponding to this optimal slowness vector

The value of the correlation coefficient should of course be as large as possible to indicate the greatest possible waveform similarity.

The scaled correlation coefficient should also be large to indicate the significance of a detection.

The correlation coefficient slowness vector should be as close as possible to a zero vector to indicate that the detected incoming wavefield and the wavefield represented by the template come from a very similar direction.

The beam-gain parameter should be high to indicate the significance of an “almost zero” slowness vector.

1. Whilst the actual beam of correlation coefficients was used rather than a scaled trace as described by Gibbons and Ringdal (2006), the threshold was always set as a multiple of the standard deviation of the correlation coefficients being considered. This provided an experimental dynamic threshold. It will be the subject of further investigations as to which detection statistics are likely to provide the most sensitive and the most robust correlation detectors.

Selection criteria for detections which are likely to correspond to signals from events in the source region being monitored need to assess this parameter space and determine values for each of the measurements which define a threshold of plausibility. A decision was made to remove all preliminary detections which did not satsify the following three conditions:

- Value of maximum ACCB must exceed 20.0 times the standard deviation of ACCB values in the time segment considered
- The magnitude of the CC-trace slowness vector must not exceed 0.02 s/km
- The beam-gain of the CC-traces must exceed 0.2

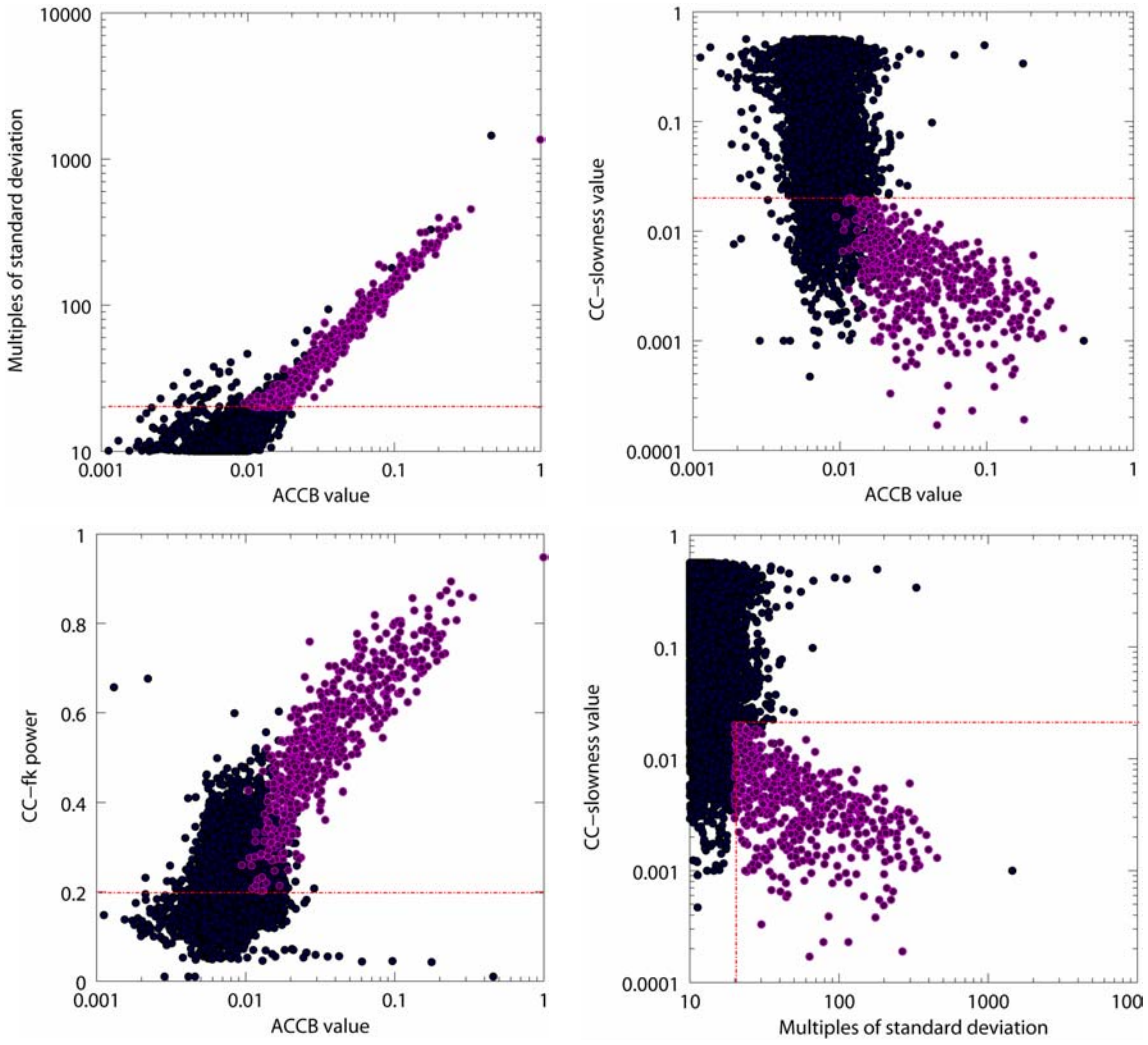

Fig. 6.3.2. Properties of the 17485 preliminary correlation detections for the ARCES Russian Explosion site template. The brighter colored symbols indicate the 557 detections which passed the three conditions listed above. ACCB stands for "Array Correlation Coefficient Beam". The dashed red lines indicate the cut off points in each parameter space for the acceptance of correlation detections.

Figure 6.3.2 displays the listed properties of the full set of preliminary detections together with the detections which passed the subsequent post-processing tests highlighted. The new conditions placed upon the correlation detections have reduced the number of detections under consideration from 17485 to 557.

A closer inspection of the detection lists reveals that almost all of these 557 detections in the reduced list consist of multiple detections in rapid succession. The reason for this becomes apparent when inspecting the waveforms and correlation traces for an example detection (Figure 6.3.3). Instead of a single maximum of the correlation beam, surrounded by diminishing sidelobes, the correlation beam contains approximately 15 seconds of values which are approximately an order of magnitude higher than the background values. Close inspection of the waveforms reveal that signals are not particularly similar. For example, the correlation coefficient traces in this example could not be used to measure relative delay times for double-difference relocation. We cannot yet be certain how far apart the source locations for these two events are. However, the emergence of a high amplitude signal with sound velocity from the same direction at a similar time to that corresponding to the master event is an indication that the source type at least might be similar and that the distance separating the events is probably not very large.

We proceed to attempt to identify which of the 557 detections correspond to seismic events close to the source of our master event.

The first step is to separate out multiple detections. This was performed using a simple association algorithm by which detections were eliminated if they occurred within 60.0 seconds of a detection with a higher value of the scaled correlation coefficient. Given a sequence of associated detections, the one corresponding to the highest scaled correlation coefficient often occurs later in the sequence. The resulting list of detections contained 244 hypothetical events.

The second step is to attempt to associate these hypothetical events with events in the automatic GBF event bulletin. Out of the 244 event hypotheses, 220 were associated uniquely with an automatic GBF event solution. These event location estimates are displayed in Figure 6.3.4. These estimates cover an area of many thousands of square kilometers and GBF estimates for events from many other sites in this part of the world show a similar distribution (see, for example, Kværna et al. 2006). Comparing the times of detections with times of confirmed events at mines in Zapoljarni confirms that none of the event hypotheses resulting from the current detector coincided with known mining events from this region. We conclude that, despite the waveform dissimilarity between the different signals from these events, the waveform correlation procedure described provides a highly effective method for identifying the source region.

Three of the 244 event hypotheses corresponded to multiple GBF solutions falling within the region displayed in Figure 6.3.4. Only 21 of the event hypotheses did not correspond to events in the GBF. These are summarised in Table 1. Four of these appear to be convincing correlation detections but for which the signal is too weak to be detected by the online system. Vespagram analysis of the waveforms did provide indications of coherent energy with the appropriate apparent velocity and azimuth at the appropriate times, although the weak signal made it impossible to estimate arrival times for the primary and secondary phases. A further three were convincing correlation detections which did not appear on the GBF due to interfering signals or other exceptional reasons.

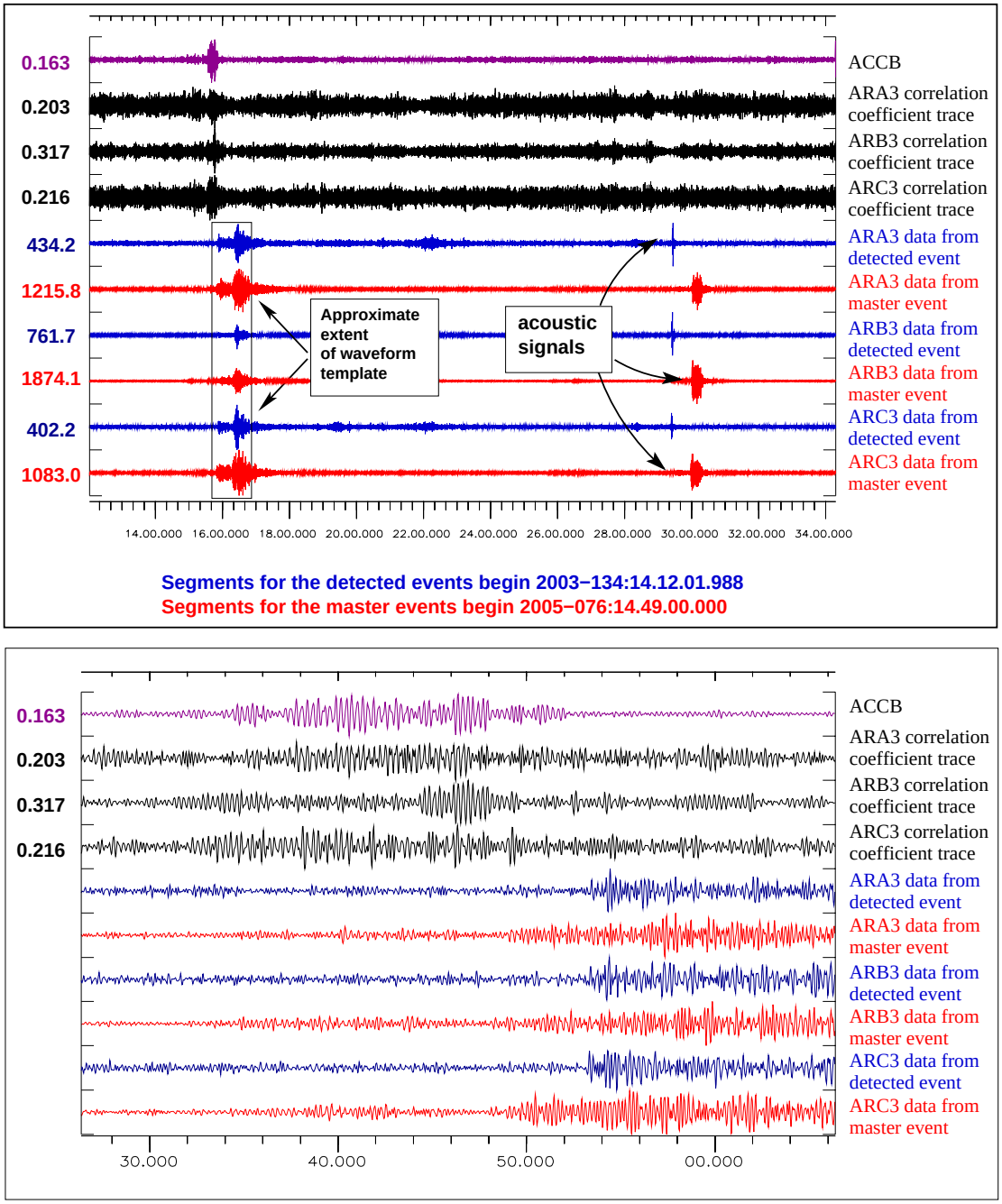

Fig. 6.3.3. A typical correlation detection on the ARCES array for the Russian surface explosions. Whilst there is no single correlation maximum (as was the case for the examples provided in Gibbons and Ringdal, 2006, and Gibbons et al., 2006) the alignment of the single site correlation coefficient traces reduces the suppression of the single channel values under the stacking operation. This alignment becomes clear when the broadband f-k analysis is performed upon the single channel values. Under the detection reduction algorithm presented, this event appears as two distinct detections.

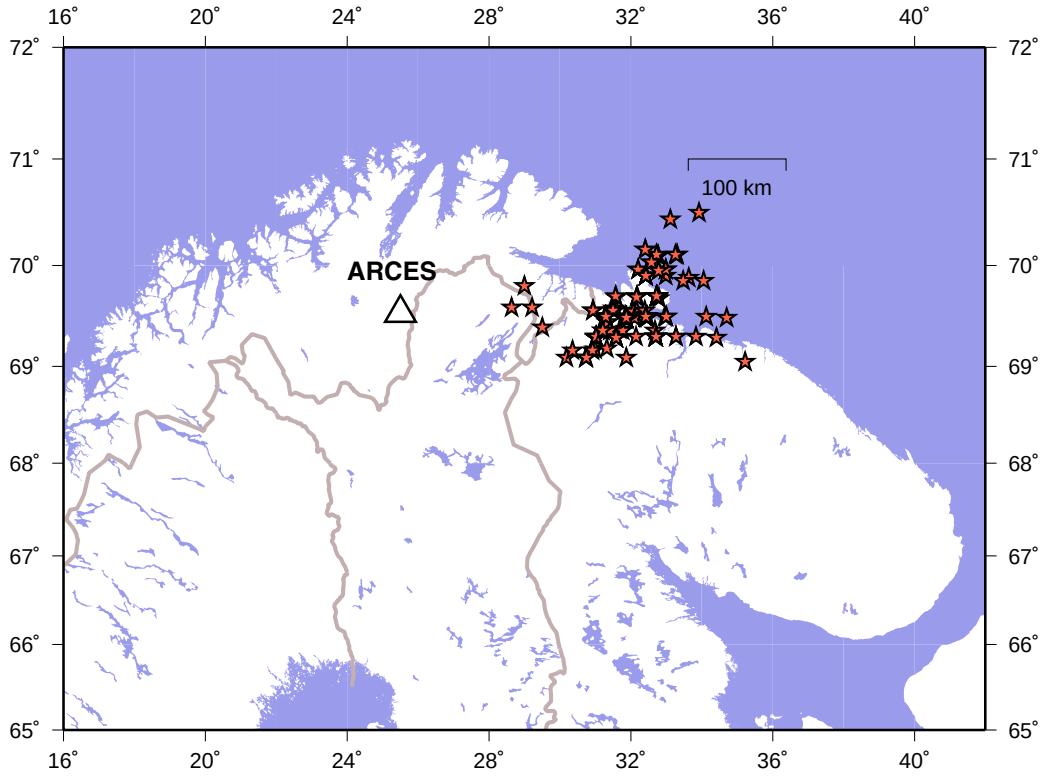

Fig. 6.3.4. Fully automatic GBF location estimates for events corresponding to 220 of 244 event hypotheses for Russian explosions resulting from the correlation detector described.

All times in Table 6.3.1 labelled "False alarm" were followed by a high amplitude Rg phase in the ARCES data some 70 seconds later. Visual inspection of the f-k plots of the correlation traces reveals a very different pattern of side-lobes to those observed for the more convincing detections - this may at a later stage be incorporated into more sophisticated selection criteria. The presence of the high-amplitude Rg phase is a very promising screening criterion due to the consistency of the time at which it occurs in relation to the event hypothesis and the stability of the f-k estimates using this signal.

6.3.3 Summary

We have demonstrated in this study that the rank-1 waveform correlation detector on an array has proved to be a very effective tool for the detection and approximate location of events from a given source region despite the lack of similarity between signals from subsequent events. Of paramount importance is the alignment of the correlation coefficient traces which facilitates a powerful screening criterion.

We do not yet have Ground Truth confirmation of these events and some unrelated events from a similar direction may have been included. However, this procedure has created a shortlist of events for analyst review which has far fewer possible false alarms than any other procedure currently available.

Acknowledgement

This work has been sponsored by National Nuclear Security Administration under Contract No. DE-FC52-05NA26604.

Table 6.3.1. Summary of the 21 event hypotheses for the presumed Kola Peninsula explosions not associated with an automatic GBF event location.

Event time hypothesis	Evaluation
2002-015:10.03.27.813	False alarm
2002-231:14.32.05.388	Convincing signal correlation: signal too weak for STA:LTA detection
2002-254:14.49.16.963	Convincing signal correlation: signal too weak for STA:LTA detection
2002-255:16.25.09.788	Convincing signal correlation: signal too weak for STA:LTA detection
2002-304:05.05.54.688	False alarm
2002-321:14.38.25.013	False alarm
2002-361:08.52.51.488	False alarm
2002-362:23.06.45.138	False alarm
2003-090:02.36.36.463	False alarm
2003-226:15.15.56.213	Convincing signal correlation: signal too weak for STA:LTA detection
2003-313:19.08.51.838	False alarm
2003-322:19.38.47.688	Convincing correlation: strong Sg phase detected by STA;LTA detector but P-phase obscured by strong unrelated Rg signal
2003-328:18.39.06.338	Convincing correlation: Strong signal located by single station process.[a] Presumed absent from GBF list due to a one-off technical fault.
2003-334:00.54.21.225	False alarm
2004-292:02.18.41.750	False alarm
2004-319:04.45.05.300	False alarm
2005-059:04.39.54.700	False alarm
2005-075:08.46.56.875	False alarm
2005-272:16.56.54.325	Convincing correlation: in coda of an unrelated high amplitude regional phase.
2005-310:12.12.35.325	False alarm
2005-328:19.12.14.550	False alarm

a. http://www.norsar.no/NDC/bulletins/dpep/2003/328/ARC/ARC03328.html

References

Gibbons, S. J., Bøttger Sørensen, M., Harris, D. B., and Ringdal, F. (2007). "The detection and location of low magnitude earthquakes in northern Norway using multi-channel waveform correlation at regional distances" Phys. Earth Planet. Inter., **160**, pp. 285-309.

Gibbons, S. J., Kværna, T., and Ringdal, F. (2005). "Monitoring of seismic events from a specific source region using a single regional array: a case study", *J. Seism.*, **9**, pp. 277-294.

Gibbons, S. J. and Ringdal, F. (2004). A waveform correlation procedure for detecting decoupled chemical explosions, NORSAR Scientific Report: Semiannual Technical Summary No. 2 - 2004. NORSAR, Kjeller, Norway. pp. 41-50.

Gibbons, S. J. and Ringdal, F. (2005). The detection of rockbursts at the Barentsburg coal mine, Spitsbergen, using waveform correlation on SPITS array data, NORSAR Scientific Report: Semiannual Technical Summary No. 1 - 2005. NORSAR, Kjeller, Norway. pp. 35-48.

Gibbons, S. J., and Ringdal, F. (2006). "The detection of low magnitude seismic events using array-based waveform correlation" *Geophys. J. Int.*, **165**, pp. 149-165.

Harris, D. B. (1991). A waveform correlation method for identifying quarry explosions, *Bull. seism. Soc. Am.*, **81**, pp. 2395-2418.

Kværna, T., Gibbons, S. J., Ringdal, F. and Harris, D. B. (2006). "Integrated Seismic Event Detection and Location by Advanced Array Processing". In Proceedings of the 28th Seismic Research Review, Orlando, Florida, September 19-21, 2006 ("*Ground-based Nuclear Explosion Monitoring Technologies*") LA-UR-06-5471, pp 997-1006.

Ringdal, F., and Kværna, T. (1989). A multi-channel processing approach to real time network detection, phase association, and threshold monitoring, *Bull. seism. Soc. Am.*, **79**, pp. 1927-1940.

Ringdal, F. and Schweitzer, J. (2005). "Combined seismic/infrasonic processing: A case study of explosions in NW Russia.", In *NORSAR Scientific Report: Semiannual Technical Summary No. 2 - 2005*. NORSAR, Kjeller, Norway. pp. 49-60.

Stevens, J. L., Gibbons, S., Rimer, N., Xu, H., Lindholm, C., Ringdal, F., Kværna, T. and Murphy, J. R. (2006). "Analysis and Simulation of Chemical Explosions in Nonspherical Cavities in Granite" *J. Geophys. Res., Solid Earth*, **111**, B04306, doi:10.1029/2005JB003768.

S. J. Gibbons
F. Ringdal